

Mathematical Basis for Electromagnetic Multiple Scattering in Periodic Structures: An Integral Equation Perspective

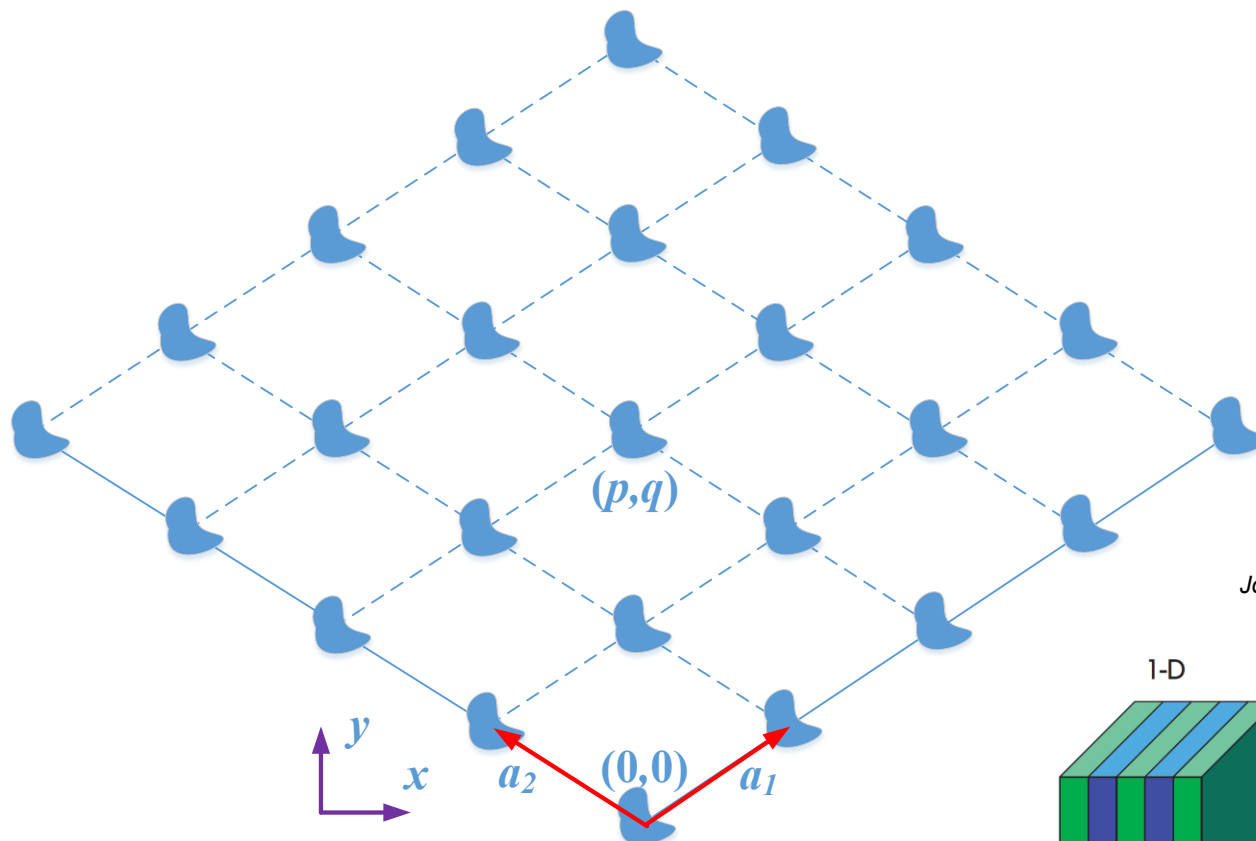
**从积分方程视角看
周期结构中多次电磁散射的数学基础**

Shurun Tan 谭述润

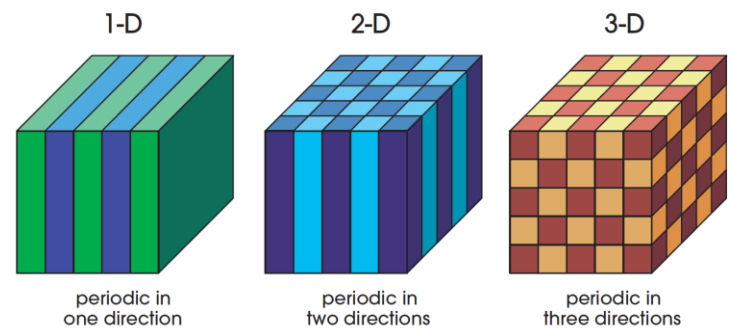
**Zhejiang University/University of Illinois at Urbana-Champaign
Institute, Zhejiang University, Haining, China**

浙江大学伊利诺伊大学厄巴纳香槟校区联合学院，浙江大学

Periodic Structures



Joannopoulos et.al., Photonic Crystals, 2008



Natural Periodic Structures



peacock feathers

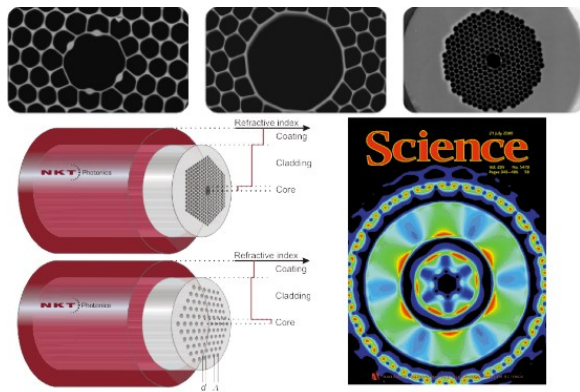


butterfly wings

These beautiful colors are results of light interactions with natural photonic crystals.

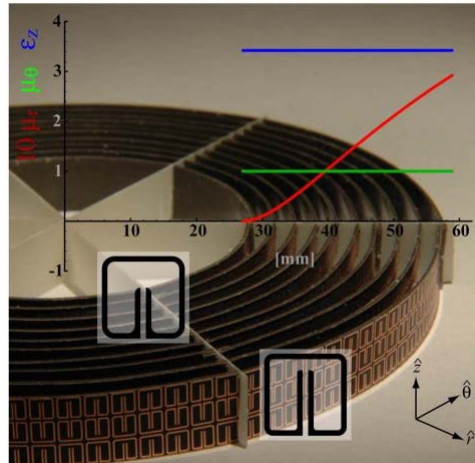
Engineered Periodic Structures

Courtesy: optoelectronics.eecs.berkeley.edu



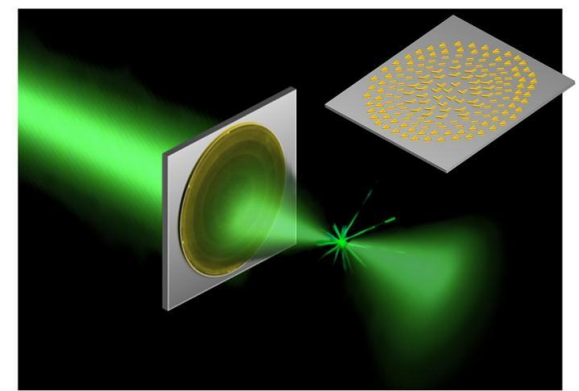
Photonic crystals in optical fibers

Schurig et al., *Science*, 314:977-980, 2006



Metamaterials in cloaking

Meta-surfaces in planar optics



Engineered Electromagnetic Materials controls the propagation of EM Waves in microwave and optical devices.

Keywords

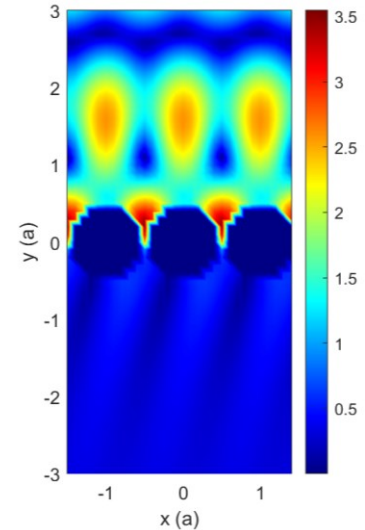
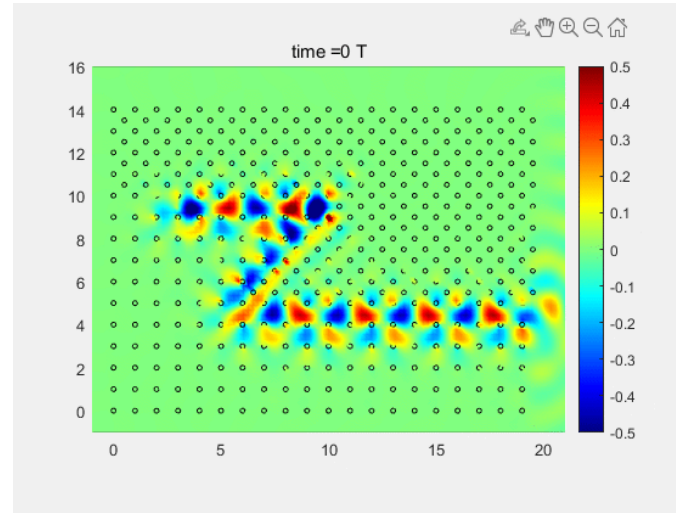
Integral Equation &
Multiple Scattering

Broadband Green's
Function Approach

Foldy-Lax Multiple
Scattering Theory

Topological
Photonics

Periodic
Gratings

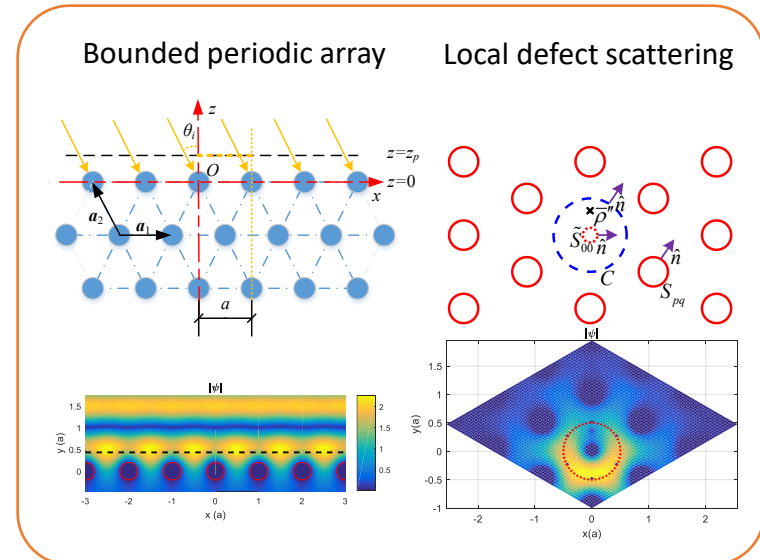
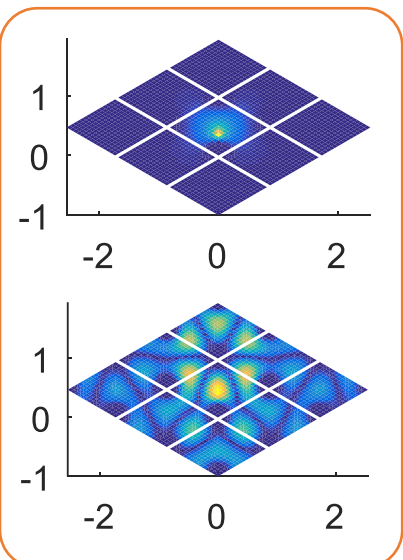
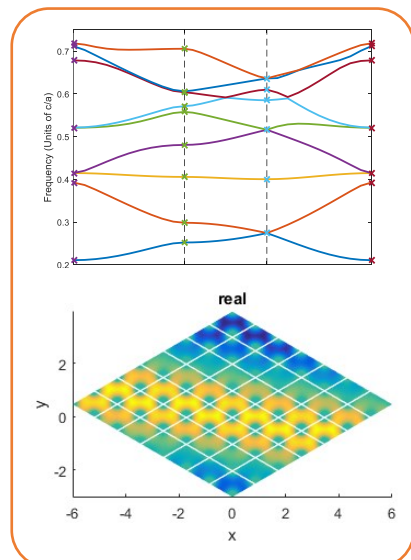
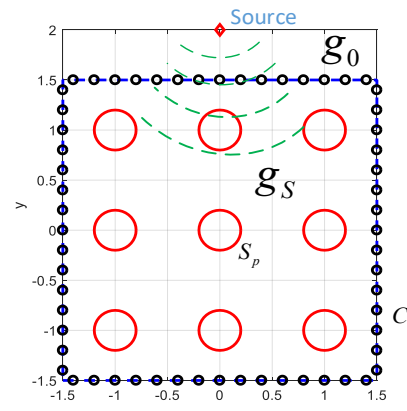
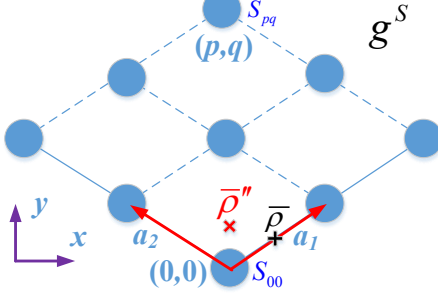
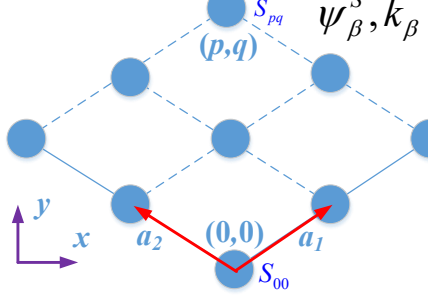


- Band characterization
- Green's function
- Topological edge modes

- Near fields
- Scattering far fields
- Reflection and transmission

The Broadband Green's Function (BGF) Approach

The Broadband Green's Function Approach



**Band & Mode
characterization**



**Broadband
Green's function**



**Scattering from
bounded array**

Band and Mode Characterization



With BGF, we formulate the highly-resonant multiple scattering problem using surface integral equations;



We then convert the SIEs into a tractable linear eigenvalue problem of a moderate size.

The Governing Equations

Wave equation: $\nabla^2 \psi(\bar{\rho}) + k_0^2 \varepsilon_r(\bar{\rho}) \psi(\bar{\rho}) = 0$

Periodicity: $\varepsilon_r(\bar{\rho} + \bar{R}) = \varepsilon_r(\bar{\rho})$

Bloch theorem: $\psi(\bar{\rho} + \bar{R}) = \psi(\bar{\rho}) \exp(i \bar{k}_b \cdot \bar{R})$

Green's function: $\nabla^2 g(\bar{\rho}; \bar{\rho}') + k_0^2 g(\bar{\rho}; \bar{\rho}') = \delta(\bar{\rho} - \bar{\rho}')$

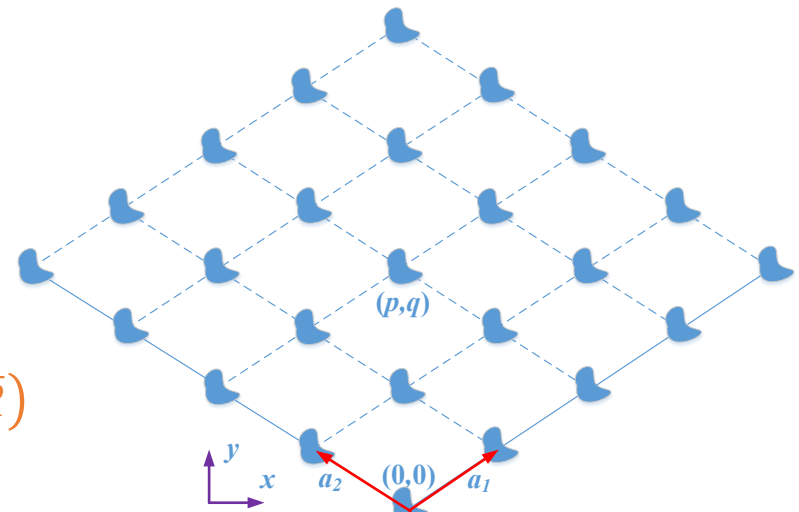
Extinction theorem:

$$\sum_{p,q} \int_{C_{pq}} d\bar{\rho}' [g(\bar{\rho}; \bar{\rho}') \hat{n}' \cdot \nabla \psi(\bar{\rho}') - \psi(\bar{\rho}') \hat{n}' \cdot \nabla g(\bar{\rho}; \bar{\rho}')] = \begin{cases} \psi(\bar{\rho}), & \text{if } \bar{\rho} \text{ outside scatterer} \\ 0, & \text{if } \bar{\rho} \text{ inside scatterer} \end{cases}$$

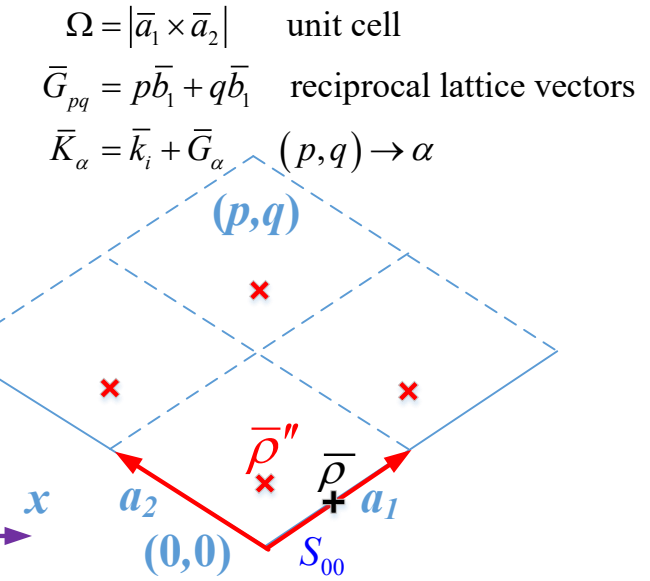
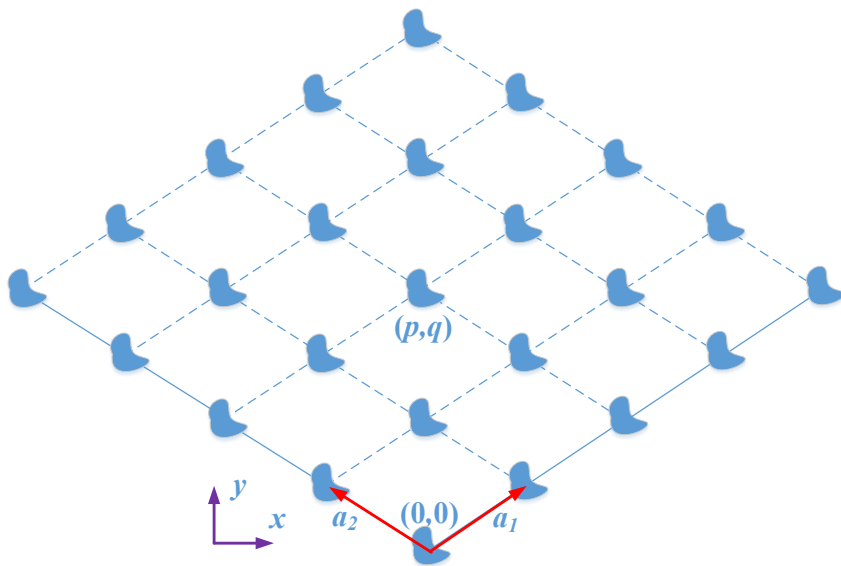
$$= \sum_{p,q} \int_{C_{00}} d\bar{\rho}' [g(\bar{\rho}; \bar{\rho}' + \bar{R}_{pq}) \hat{n}' \cdot \nabla \psi(\bar{\rho}') - \psi(\bar{\rho}') \hat{n}' \cdot \nabla g(\bar{\rho}; \bar{\rho}' + \bar{R}_{pq})] \exp(i \bar{k}_b \cdot \bar{R}_{pq})$$

$$= \int_{C_{00}} d\bar{\rho}' [g_P(\bar{\rho}; \bar{\rho}') \hat{n}' \cdot \nabla \psi(\bar{\rho}') - \psi(\bar{\rho}') \hat{n}' \cdot \nabla g_P(\bar{\rho}; \bar{\rho}')] \quad \text{where}$$

Lattice Green's function: $g_P(\bar{\rho}; \bar{\rho}') = \sum_{p,q} g(\bar{\rho}; \bar{\rho}' + \bar{R}_{pq}) \exp(i \bar{k}_b \cdot \bar{R}_{pq})$



What Makes it Possible? ---- The Hybrid Representation of the Lattice Green's Function



$$g_P^0(k, \bar{k}_i; \bar{\rho}, \bar{\rho}') = \sum_{\bar{R}} g^0(k; \bar{\rho}, \bar{\rho}' + \bar{R}) \exp(i \bar{k}_i \cdot \bar{R}) = \frac{1}{\Omega} \sum_{\bar{K}} \frac{\exp(i \bar{K} \cdot (\bar{\rho} - \bar{\rho}'))}{|\bar{K}|^2 - k^2}$$

$$g_P^0(k, \bar{k}_i; \bar{\rho}, \bar{\rho}') = \sum_{\bar{R}} g^0(i\xi; \bar{\rho}, \bar{\rho}' + \bar{R}) \exp(i \bar{k}_i \cdot \bar{R}) + \sum_{\bar{K}} \frac{1}{\frac{1}{k^2 + \xi^2} - \frac{1}{|\bar{K}|^2 + \xi^2}} \frac{\exp(i \bar{K} \cdot (\bar{\rho} - \bar{\rho}'))}{\left(|\bar{K}|^2 + \xi^2\right)^2 \Omega}$$

Features & Advantages of the Broadband Green's Function

$$g_P^0(k, \bar{k}_i; \bar{\rho}, \bar{\rho}') = \sum_{\bar{R}} g^0(i\xi; \bar{\rho}, \bar{\rho}' + \bar{R}) \exp(i\bar{k}_i \cdot \bar{R}) + \sum_{\bar{K}} \frac{1}{\frac{1}{k^2 + \xi^2} - \frac{1}{|\bar{K}|^2 + \xi^2}} \frac{\exp(i\bar{K} \cdot (\bar{\rho} - \bar{\rho}'))}{\left(|\bar{K}|^2 + \xi^2\right)^2} \Omega$$

Spatial series **Spectral series**

- Exponentially convergent spatial series:
 - No frequency dependence
 - Represents fast decaying near field interactions
 - Diagonal dominant: good condition number in matrix representation
 - Well-studied singularity in free space Green function $g^0(\bar{\rho}, \bar{\rho}')$

Features & Advantages of the Broadband Green's Function

$$g_P^0(k, \bar{k}_i; \bar{\rho}, \bar{\rho}') = \sum_{\bar{R}} g^0(i\xi; \bar{\rho}, \bar{\rho}' + \bar{R}) \exp(i\bar{k}_i \cdot \bar{R}) + \sum_{\bar{K}} \frac{1}{\frac{1}{k^2 + \xi^2} - \frac{1}{|\bar{K}|^2 + \xi^2}} \frac{\exp(i\bar{K} \cdot (\bar{\rho} - \bar{\rho}'))}{\left(|\bar{K}|^2 + \xi^2\right)^2} \Omega$$

Spatial series **Spectral series**

- Fast convergent spectral series:
 - Separable frequency dependence in $1/(k^2 + \xi^2)$
 - Ready to be evaluated in a broad frequency range of interest
 - Represents long range far field interactions: the leading reason for poor conditioning of g_P^0
 - No spatial singularity at any $(\bar{\rho}, \bar{\rho}')$ pair
 - Contains frequency poles when $k = |\bar{K}|$ (light-line dispersions)

Band Characterization Using Surface Integral Equations: PEC, TMz

- Surface Integral Equation (SIE) with g_P^0

$$0 = \int_{S_{00}} d\bar{\rho}' g_P^0(k, \bar{k}_i; \bar{\rho}, \bar{\rho}') \hat{n}' \cdot \nabla' \psi(\bar{\rho}'), \quad \bar{\rho} \rightarrow S_{00}$$

- Discretization of the SIE

$$\bar{\bar{L}}(k)\bar{q} = 0 \quad \text{where} \quad L_{mn}(k) = \frac{1}{\Delta t_n} \int_{S_n} d\bar{\rho}' g_P^0(k, \bar{k}_i; \bar{\rho}, \bar{\rho}')$$

- Apply the broadband hybrid representation of g_P^0

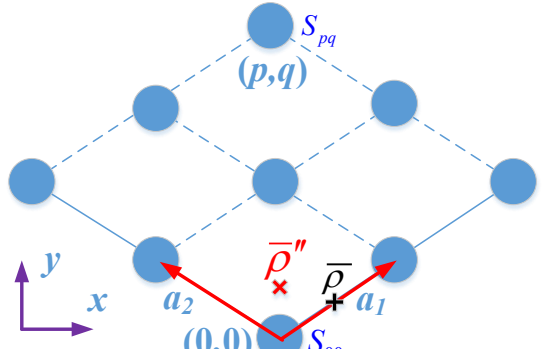
$$\bar{\bar{L}}(\lambda) = \bar{\bar{L}}(i\xi) + \bar{\bar{R}} \left(\lambda \bar{\bar{I}} - \bar{\bar{D}} \right)^{-1} \bar{\bar{R}}^\dagger$$

where $\lambda = \frac{1}{k^2 + \xi^2}$

$$R_\alpha(\bar{\rho}) = D_\alpha \psi_\alpha(\bar{\rho})$$

$$\psi_\alpha(\bar{\rho}) = \frac{1}{\sqrt{\Omega}} \exp(i \bar{K}_\alpha \cdot \bar{\rho})$$

$$D_\alpha = \frac{1}{|\bar{K}_\alpha|^2 + \xi^2}$$



Linear Eigenvalue Problem Formulation of Band Characterization

Instead of solving $\det(\bar{\bar{L}}(\lambda)) = 0$

Consider

$$\bar{\bar{L}}(\lambda)\bar{q} = \bar{\bar{L}}(i\xi)\bar{q} + \bar{\bar{R}}\left(\lambda\bar{\bar{I}} - \bar{\bar{D}}\right)^{-1}\bar{\bar{R}}^\dagger\bar{q} = 0$$

Note the pole singularity

$$(\lambda\bar{\bar{I}} - \bar{\bar{D}})^{-1}$$

Linear Eigenvalue Problem

Define

$$\bar{b} = (\lambda\bar{\bar{I}} - \bar{\bar{D}})^{-1}\bar{\bar{R}}^\dagger\bar{q}$$

$$\bar{\bar{P}}\bar{b} = \lambda\bar{b}$$

Together with

$$\bar{q} = -[\bar{\bar{L}}(i\xi)]^{-1}\bar{\bar{R}}\bar{b}$$

$$\bar{\bar{P}} = \bar{\bar{D}} - \bar{\bar{R}}^\dagger [\bar{\bar{L}}(i\xi)]^{-1}\bar{\bar{R}}$$

Advantage of the Linear Eigenvalue Problem Formulation

$$\bar{\bar{P}}\bar{b} = \lambda \bar{b}$$

$$\bar{\bar{P}} = \bar{\bar{D}} - \bar{\bar{R}}^\dagger \left[\bar{\bar{L}}(i\xi) \right]^{-1} \bar{\bar{R}}$$

- $\bar{\bar{P}}$ independent of frequency, thus get all the eigenvalues (bands) of interest at once
- Size of $\bar{\bar{P}}$ depends on the number of Floquet planewaves in the fast convergent spectral series
- Contrary to $\bar{L}(k)$:
- $\bar{\bar{L}}(i\xi)$ is of small condition number, easy to invert

High-Order Convergence

$$\begin{aligned}
g_P^0(k, \bar{k}_i; \bar{\rho}, \bar{\rho}') &= g_P^0(i\xi, \bar{k}_i; \bar{\rho}, \bar{\rho}') - \frac{\xi^2 + k^2}{2\xi} \frac{d}{d\xi} g_P^0(i\xi, \bar{k}_i; \bar{\rho}, \bar{\rho}') \\
&\quad + \frac{(\xi^2 + k^2)^2}{8\xi} \frac{d}{d\xi} \left[\frac{1}{\xi} \frac{d}{d\xi} g_P^0(i\xi, \bar{k}_i; \bar{\rho}, \bar{\rho}') \right] \\
&\quad + (\xi^2 + k^2)^2 \sum_{\bar{K}} \frac{1}{\frac{1}{k^2 + \xi^2} - \frac{1}{|\bar{K}|^2 + \xi^2}} \frac{\exp(i\bar{K} \cdot (\bar{\rho} - \bar{\rho}'))}{(|\bar{K}|^2 + \xi^2)^4} \Omega
\end{aligned}$$

Spatial series:
exponentially
convergent

Spectral series:
very fast $1/K^8$
convergent

$$\bar{\bar{L}}(\lambda) = \bar{\bar{L}}^{(c)}(i\xi, \lambda) + \frac{1}{\lambda^2} \bar{\bar{R}} \left(\lambda \bar{\bar{I}} - \bar{\bar{D}} \right)^{-1} \bar{\bar{R}}^\dagger \quad R_\alpha(\bar{\rho}) = D_\alpha^2 \psi_\alpha(\bar{\rho})$$

$$\bar{\bar{L}}^{(c)}(i\xi, \lambda) = \bar{\bar{L}}(i\xi) - \frac{1}{\lambda} \frac{1}{2\xi} \bar{\bar{L}}'(i\xi) + \frac{1}{\lambda^2} \frac{1}{8\xi} \bar{\bar{L}}''(i\xi)$$

High-Order Convergence & Nonlinear Problem Formulation

$$\bar{\bar{P}}(\lambda)\bar{b} = \lambda\bar{b}$$

$$\bar{\bar{P}}(\lambda) = \bar{\bar{D}} - \frac{1}{\lambda^2} \bar{\bar{R}}^\dagger \left[\bar{\bar{L}}^{(c)}(i\xi, \lambda) \right]^{-1} \bar{\bar{R}}$$



$$\bar{\bar{L}}^{(c)}(i\xi, \lambda) = \bar{\bar{L}}(i\xi) - \frac{1}{\lambda} \frac{1}{2\xi} \bar{\bar{L}}'(i\xi) + \frac{1}{\lambda^2} \frac{1}{8\xi} \bar{\bar{L}}''(i\xi)$$

$$\det \bar{\bar{H}}(\lambda) = 0$$

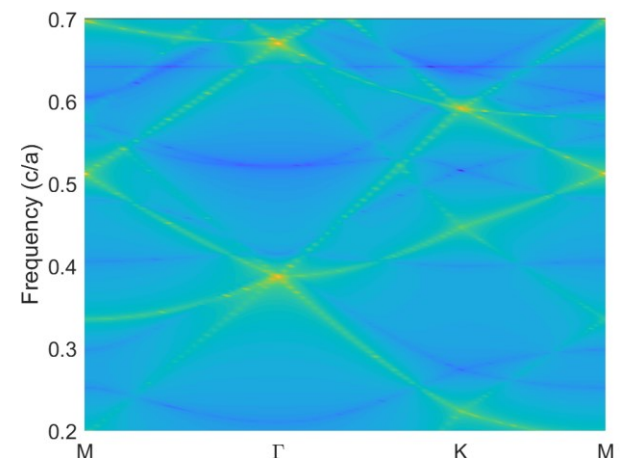
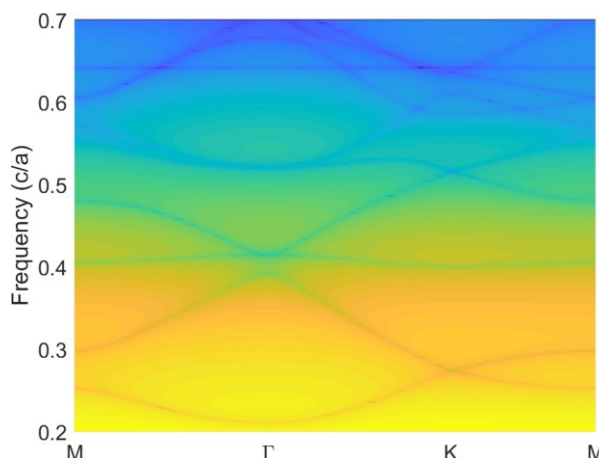
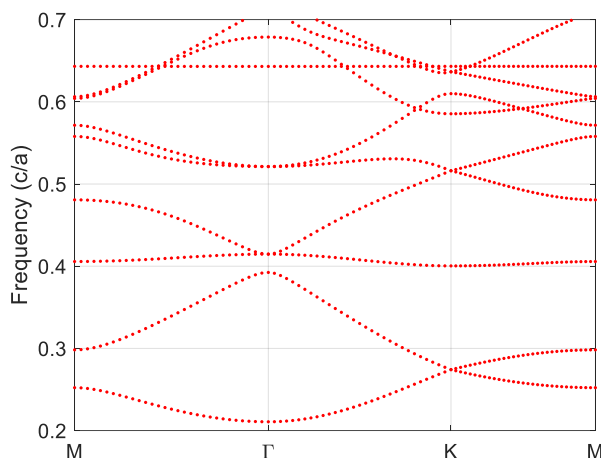
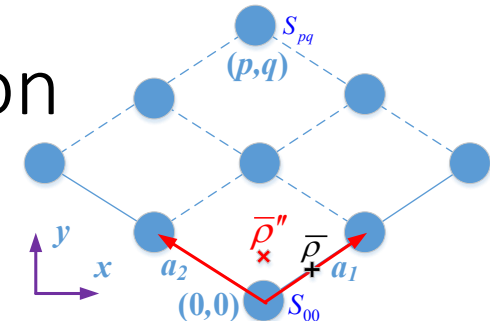
$$\bar{\bar{H}}(\lambda)\bar{b} = 0$$

$$\bar{\bar{H}}(\lambda) = \bar{\bar{I}} - \frac{1}{\lambda} \bar{\bar{P}}(\lambda)$$

- $\bar{\bar{P}}$ and $\bar{\bar{H}}$: **very small** matrix size, simple frequency dependence
- $\bar{\bar{L}}^{(c)}(i\xi, \lambda)$:
 - Easy to evaluate over a broad frequency of interest
 - Smooth function of λ , no poles in inversion
 - Highly diagonal, good conditioning, and easy to invert
- $\bar{\bar{H}}(\lambda)$: highly diagonal with **well-regularized** diagonal elements

PEC Scatterer Array: TMz Polarization

$$\begin{aligned}\varepsilon_b &= 8.9\varepsilon_0 \\ b &= 0.2a\end{aligned}$$



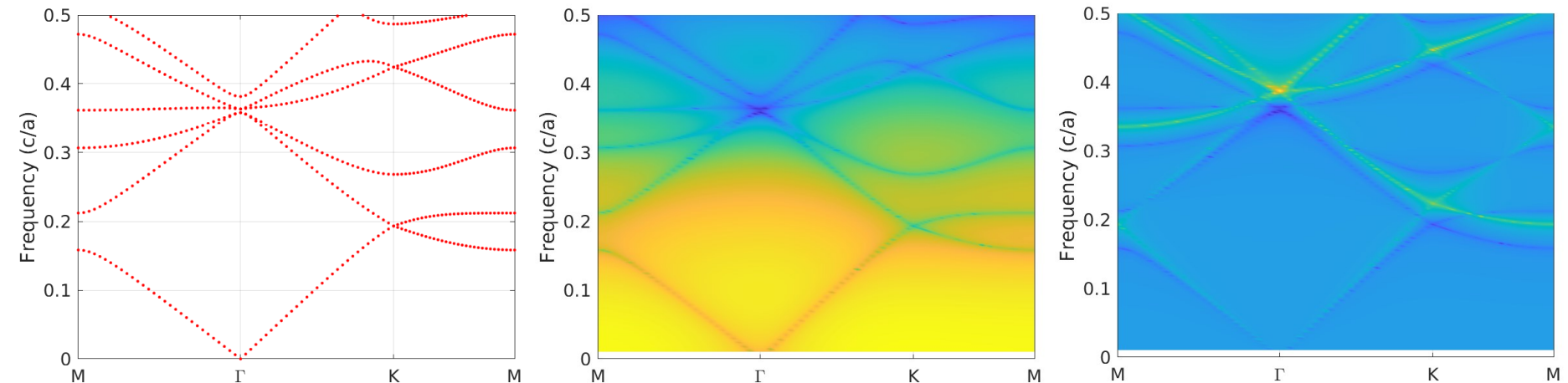
$$\bar{\bar}{P}\bar{b} = \lambda \bar{b}$$

$$\det \bar{\bar}{H}(\lambda) = 0$$

High order $\det \bar{\bar}{L}(\lambda) = 0$

- Very good agreement; constant band: isolated internal resonance
- Linear eigenvalue problem: get all the bands in one shot
- $\det(\bar{\bar}{H})$: yields all the physical bands effectively
- $\det(\bar{\bar}{L})$: difficult to separate zeros and poles when they overlap

PEC Scatterer Array: TEz Polarization



$$\bar{\bar{P}}\bar{C} = \lambda \bar{C}$$

$$\det \bar{\bar{H}}(\lambda) = 0$$

High order $\det \bar{\bar{S}}(\lambda) = 0$

- Very similar formulation, very good agreement, applicable to arbitrarily-shaped non-penetrable scatterers

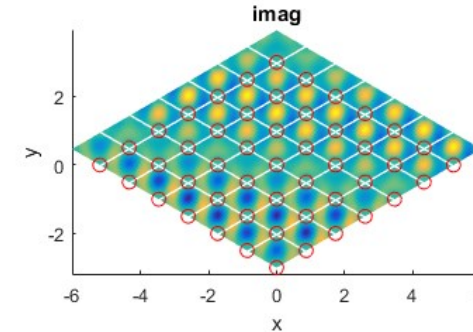
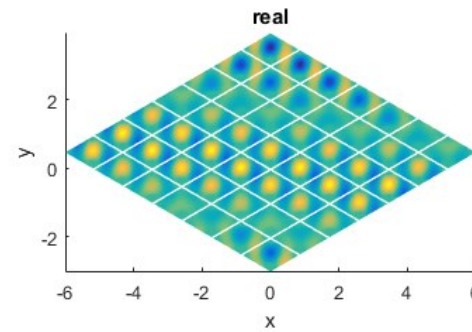
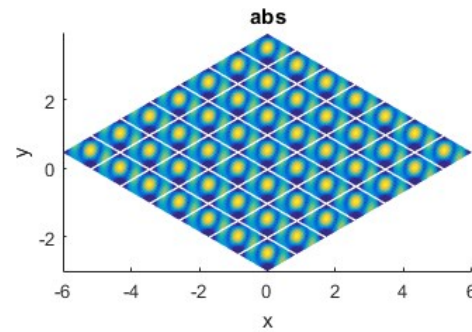
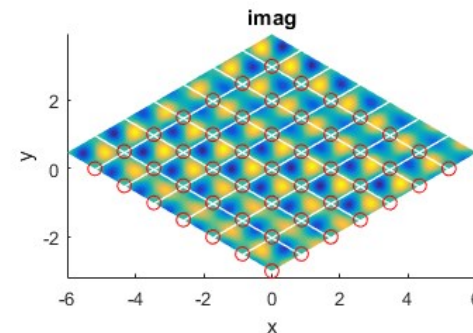
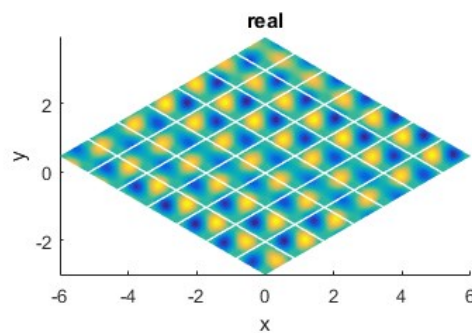
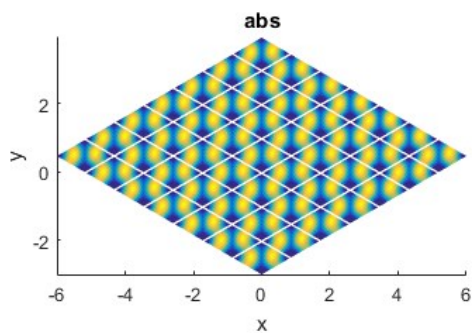
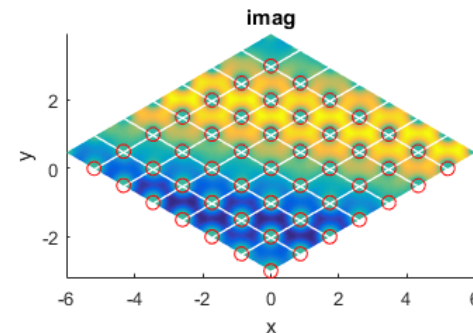
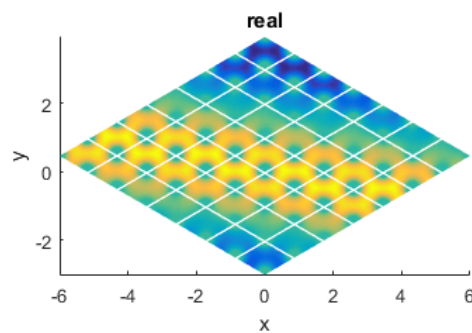
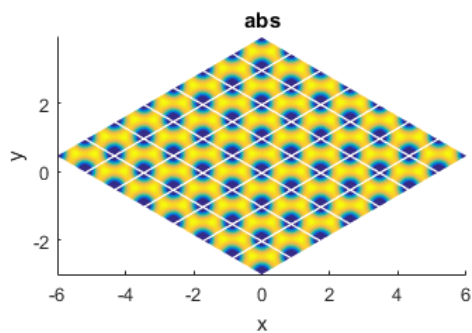
Modal Fields and Normalization

$$\begin{aligned}
 \psi_\beta(\bar{k}_i; \bar{\rho}) = & \int_{S_{00}} d\bar{\rho}' \frac{1}{\Omega_0} \sum_{|\alpha|>M} \frac{\exp(i\bar{k}_{i\alpha} \cdot (\bar{\rho} - \bar{\rho}'))}{|\bar{k}_{i\alpha}|^2 - k_L^2} J(\bar{\rho}') \\
 & + \int_{S_{00}} d\bar{\rho}' \frac{1}{\Omega_0} \sum_{|\alpha|\leq M} \frac{\exp(i\bar{k}_{i\alpha} \cdot (\bar{\rho} - \bar{\rho}'))}{|\bar{k}_{i\alpha}|^2 - k_L^2} J(\bar{\rho}') \\
 & + \int_{S_{00}} d\bar{\rho}' \frac{1}{\Omega_0} \sum_{|\alpha|\leq M} \frac{(k_\beta^2 - k_L^2)}{(|\bar{k}_{i,\alpha}|^2 - k_\beta^2)(|\bar{k}_{i,\alpha}|^2 - k_L^2)} \exp(i\bar{k}_{i,\alpha} \cdot (\bar{\rho} - \bar{\rho}')) J(\bar{\rho}')
 \end{aligned}$$

- First term orthogonal to the rest: efficient normalization
- First term eliminates Gibbs oscillation in plane wave expansion: accurate

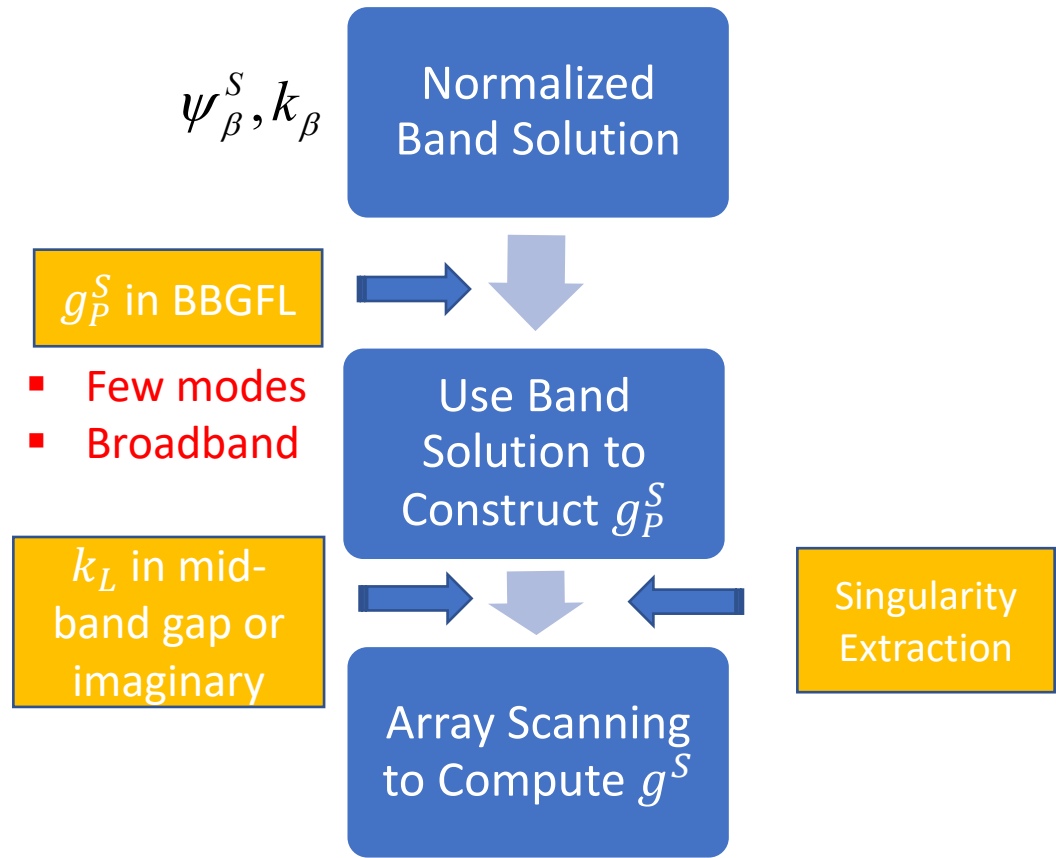
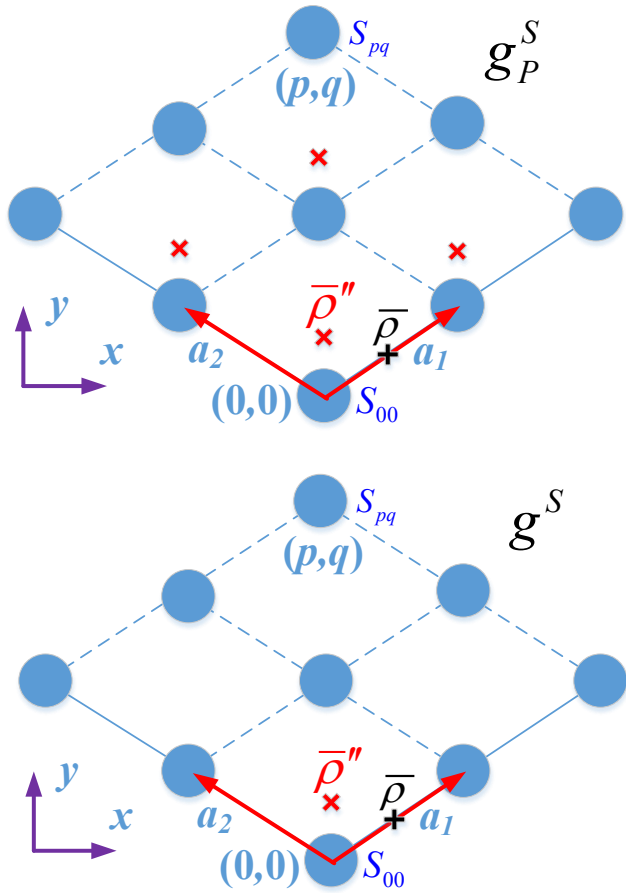
$$\begin{aligned}
 \iint_{\Omega_{00}} d\bar{\rho} |\psi_\beta(\bar{k}_i; \bar{\rho})|^2 = & \text{volume integral once at } k_L \\
 & + \sum_{|\alpha|\leq M} |\text{plane wave expansion coefficients}|^2
 \end{aligned}$$

Modal Fields $\psi_\alpha^S(\bar{k}_i; \bar{\rho})$: TMz



$$b = 0.2a \quad \varepsilon_{rb} = 8.9 \quad \bar{k}_i = 0.1\bar{b}_1 + 0.05\bar{b}_1$$

BBGFL: Modal Method to Construct the Broadband Point Source Green's Function g_S



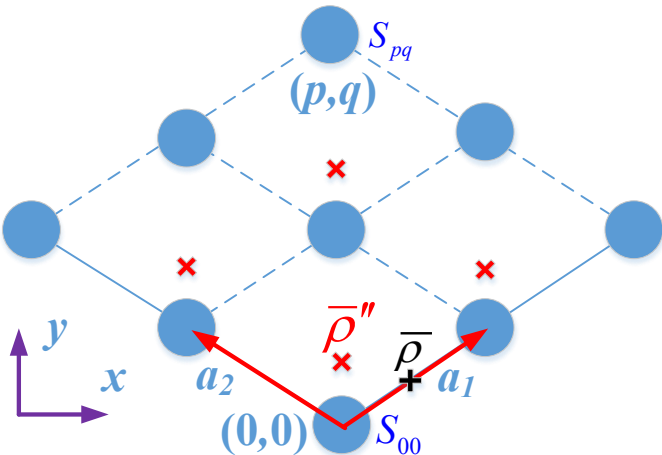
g_P^S in Band Solutions with Improved Convergence

$$g_P^S(k, \bar{k}_i; \bar{\rho}, \bar{\rho}') = \sum_{\beta} \frac{\psi_{\beta}(\bar{k}_i; \bar{\rho}) \psi_{\beta}^*(\bar{k}_i; \bar{\rho}')}{k_{\beta}^2(\bar{k}_i) - k^2}$$

k_{β} : band eigenvalue
 ψ_{β} : band wavefunction

$$g_P^S(k, \bar{k}_i; \bar{\rho}, \bar{\rho}') = g_P^S(k_L, \bar{k}_i; \bar{\rho}, \bar{\rho}') + \sum_{\beta} \frac{(k^2 - k_L^2)}{(k_{\beta}^2(\bar{k}_i) - k^2)(k_{\beta}^2(\bar{k}_i) - k_L^2)} \psi_{\beta}(\bar{\rho}; \bar{k}_i) \psi_{\beta}^*(\bar{\rho}'; \bar{k}_i)$$

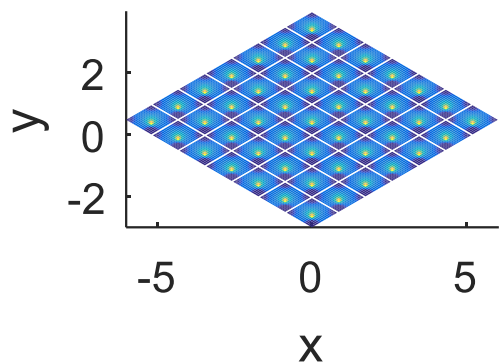
$$g_P^S(k, \bar{k}_i; \bar{\rho}, \bar{\rho}') = g_P^S(k_L, \bar{k}_i; \bar{\rho}, \bar{\rho}') + (k^2 - k_L^2) \left[\frac{1}{2k} \frac{dg_P^S(k, \bar{k}_i; \bar{\rho}, \bar{\rho}')}{dk} \right]_{k=k_L} + \sum_{\beta} \frac{(k^2 - k_L^2)^2 \psi_{\beta}(\bar{\rho}; \bar{k}_i) \psi_{\beta}^*(\bar{\rho}'; \bar{k}_i)}{(k_{\beta}^2(\bar{k}_i) - k^2)(k_{\beta}^2(\bar{k}_i) - k_L^2)^2}$$



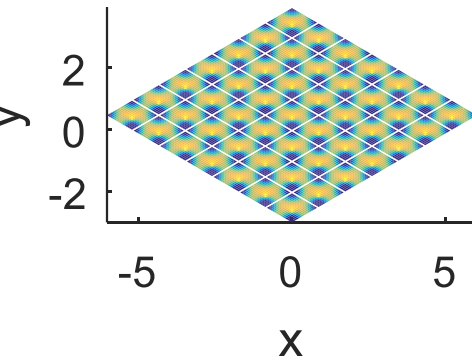
- k_{β} and $\psi_{\beta}(\bar{\rho}; \bar{k}_i)$: function of geometry, independent of k
- Convergence up to $1/k_{\beta}^4$ and $1/k_{\beta}^6$ with 1st and 2nd order extraction, respectively

$g_P^S(k, \bar{k}_i; \bar{\rho}, \bar{\rho}')$: Periodic Sources

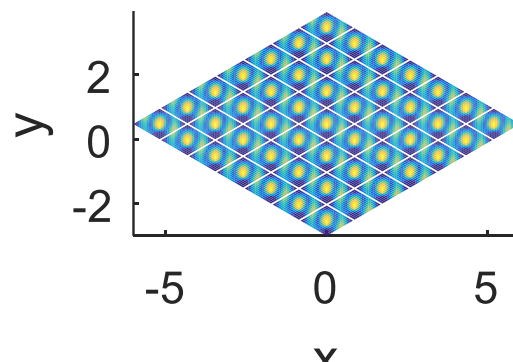
g_P^S at several wavenumbers using determined band solutions



$$f_n = 0.1$$



$$f_n = 0.2$$

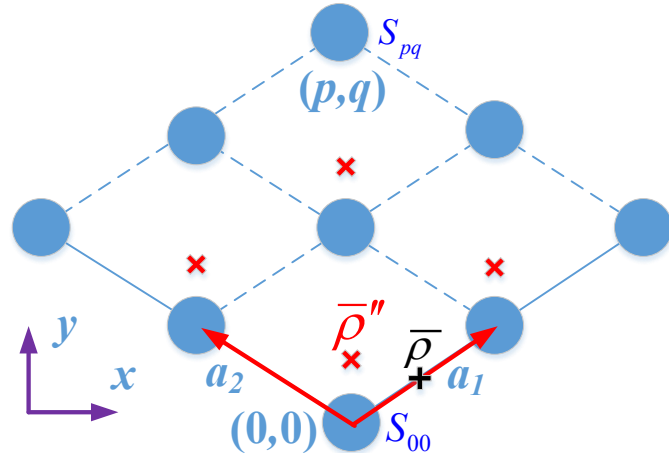
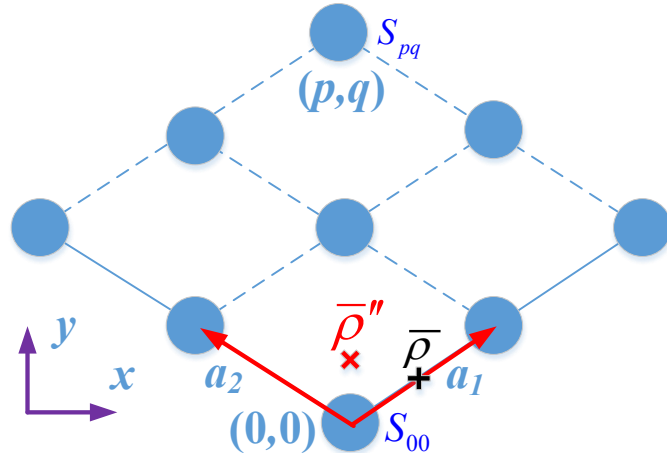


$$f_n = 0.4$$

$$\bar{k}_i = 0.1\bar{b}_1 + 0.05\bar{b}_2$$

- Truncating modal series with $k_\beta \leq 3k$ yields errors less than 1%.

Obtain $g^S(k; \bar{\rho}, \bar{\rho}')$ from $g_P^S(k, \bar{k}_i; \bar{\rho}, \bar{\rho}')$ by Integrating \bar{k}_i over The First Brillouin Zone



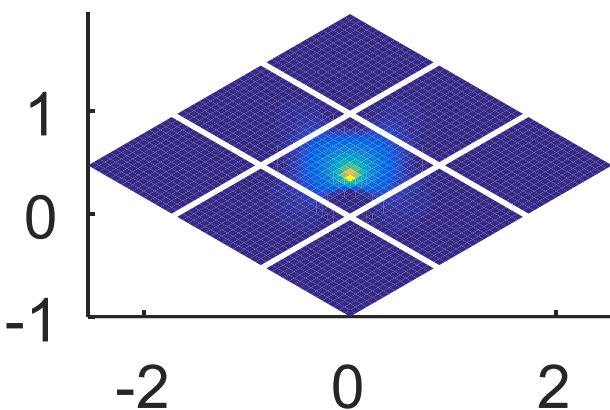
$$g^S(k; \bar{\rho}, \bar{\rho}') = \frac{\Omega_0}{(2\pi)^2} \iint_{BZ_1} d\bar{k}_i g_P^S(k, \bar{k}_i; \bar{\rho}, \bar{\rho}')$$

$$g^S(k; \bar{\rho}, \bar{\rho}') = g^S(k_L; \bar{\rho}, \bar{\rho}') + \frac{\Omega_0}{(2\pi)^2} \iint_{BZ_1} d\bar{k}_i \sum_{\beta} \frac{(k^2 - k_L^2) \psi_{\beta}(\bar{\rho}; \bar{k}_i) \psi_{\beta}^*(\bar{\rho}'; \bar{k}_i)}{(k_{\beta}^2(\bar{k}_i) - k^2)(k_{\beta}^2(\bar{k}_i) - k_L^2)}$$

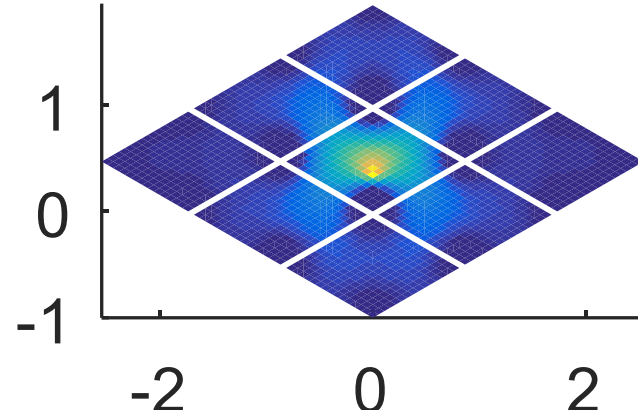
- k_L in mid band-gap or imaginary: $g^S(k_L)$ computed by truncating the arrays around source
- When k in passband, apply singularity extraction, leading to smooth integrand
- Rapid convergence in band summation
- One $g^S(k_L)$, many $g^S(k)$

Green's Function g^S : Point Source, Broadband Calculations

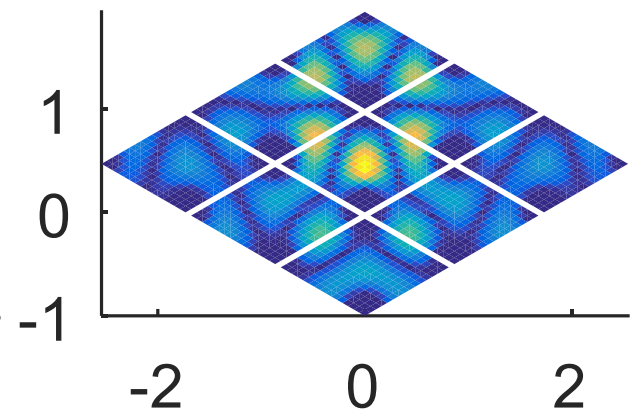
$f_n = 0.1$ (stop)



$f_n = 0.2$ (stop, close to edge)



$f_n = 0.4$ (stop, edge)

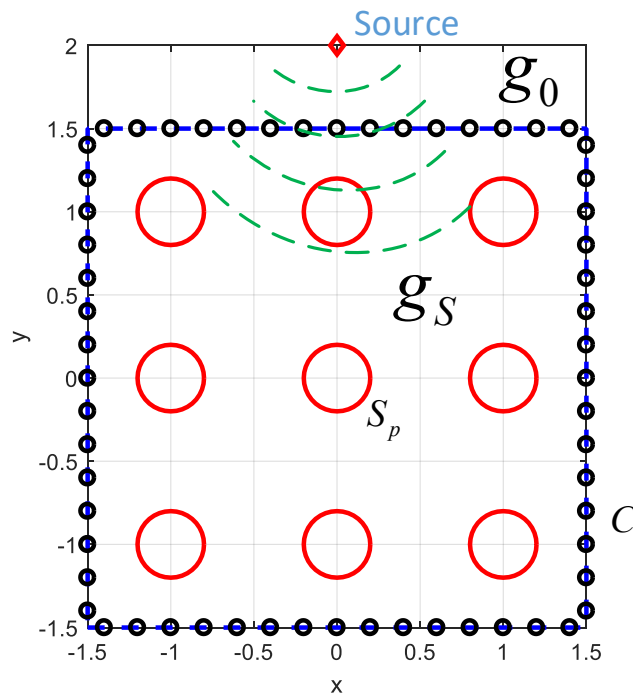


- Fields localized: in stop-band
- Fields extended: close to the band-edge
- Passband: modal method to be worked out

The Critical Role of Green's Function

- Green's functions are **impulse responses**. Once the Green's functions that satisfy **boundary conditions** are obtained, the electromagnetic boundary value problem is solved.
- We consider Green's function of **periodic scatterers** where there are **infinite boundaries**.

Apply g_S to Solve Scattering from Bounded Periodic Structures



□ External: use g_0

$$\psi_{inc}(\bar{\rho}) - \int_C dl' \left[g^0 \frac{\partial \psi}{\partial n'} - \psi \frac{\partial g^0}{\partial n'} \right] = 0, \bar{\rho} \rightarrow C^-$$

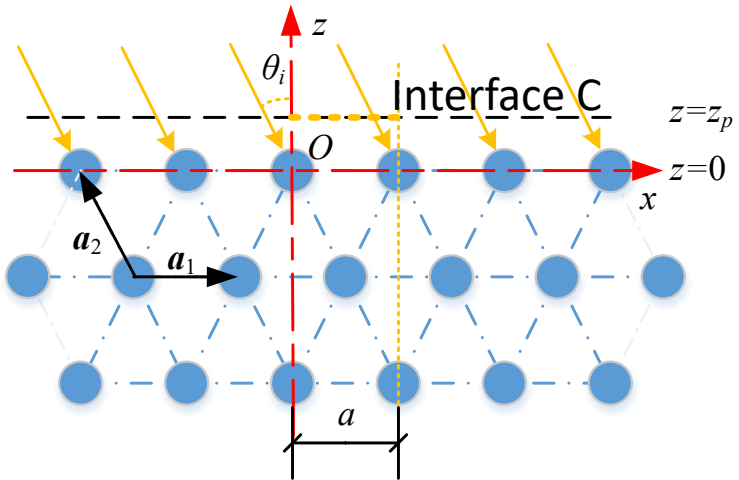
□ Internal: use g_S

$$\int_C dl' \left[g^S \frac{\partial \psi}{\partial n'} - \psi \frac{\partial g^S}{\partial n'} \right] = 0, \bar{\rho} \rightarrow C^+$$

$$g_S(\bar{\rho}, \bar{\rho}') = 0, \bar{\rho} \rightarrow S_p, \forall p$$

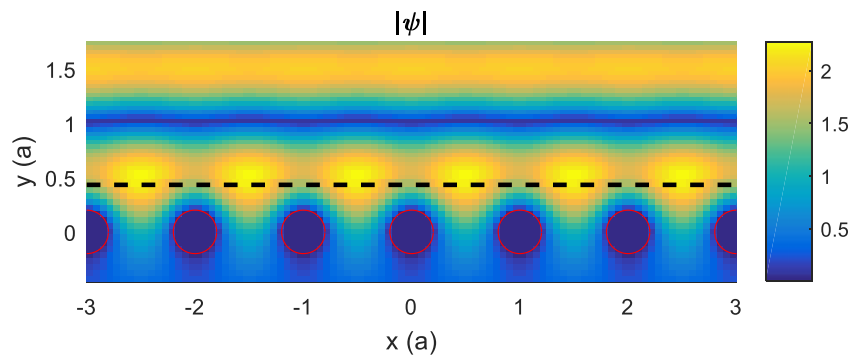
- g_S satisfy boundary conditions on S_p
- Only discretize and solve the equivalent currents on the enclosing boundary
- Accurate and low cost

Scattering from a Half-Space of Periodic Scatterers with g^S : SIE only on Interface



$$\int_0^a dx' \left[g_{Px}^0 \frac{\partial \psi}{\partial z'} - \psi \frac{\partial g_{Px}^0}{\partial z'} \right]_{z'=z_p^-} = \psi_{inc}(\bar{r}), \quad z \rightarrow z_p^-$$

$$\int_0^a dx' \left[g_{Px}^S \frac{\partial \psi}{\partial z'} - \psi \frac{\partial g_{Px}^S}{\partial z'} \right]_{z'=z_p^+} = 0, \quad z \rightarrow z_p^+$$



- Results successfully capture near field patterns around the interface

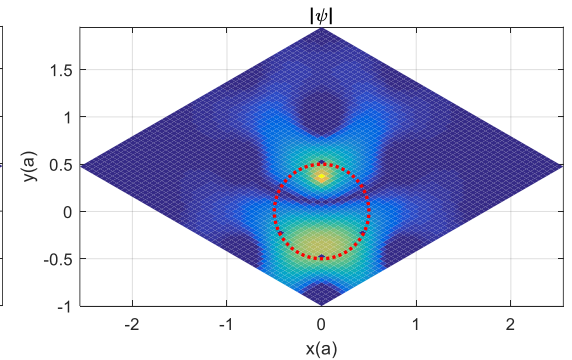
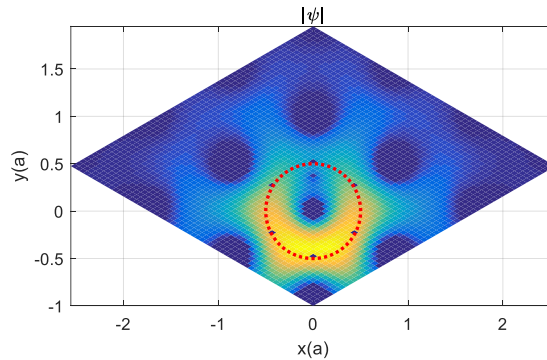
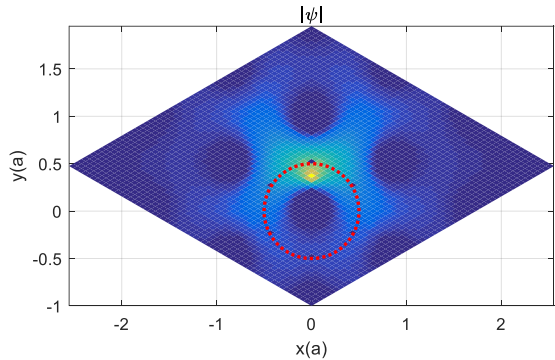
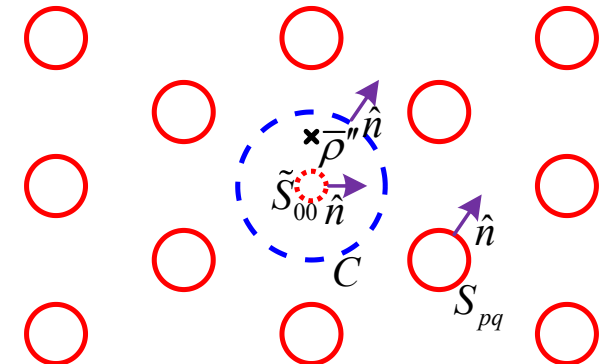
Localized Defect in a Periodic Lattice: SIE only on Boundary Enclosing Impurity

□ External: use g_s

$$-\int_c d\bar{\rho}' \left[g_s \frac{\partial \psi}{\partial n'} - \psi \frac{\partial g_s}{\partial n'} \right] = 0, \bar{\rho} \rightarrow C^-$$

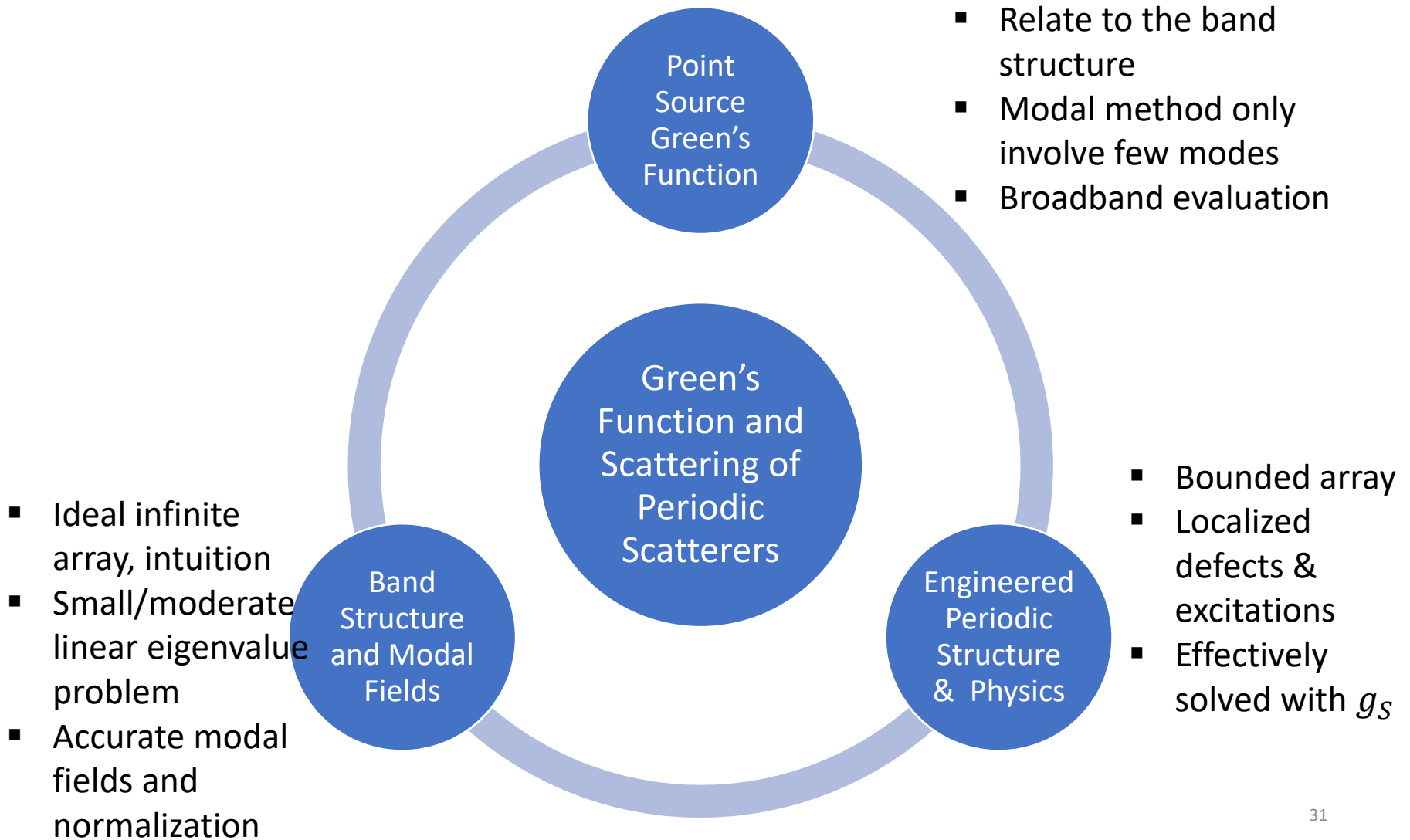
□ Internal: use g_0

$$g_0(\bar{\rho}, \bar{\rho}'') + \int_c d\bar{\rho}' \left[g_0 \frac{\partial \psi}{\partial n'} - \psi \frac{\partial g_0}{\partial n'} \right] - \int_{\tilde{S}_{00}} d\bar{\rho}' g_0 \frac{\partial \psi}{\partial n'} = 0, \bar{\rho} \rightarrow C^+ \text{ or } \tilde{S}_{00}^-$$



- Impurities alter field localization patterns around excitations

The Broadband Green's Function technique : A Solution to Three Challenging Problems



Referred Publications for the Previous Discussion

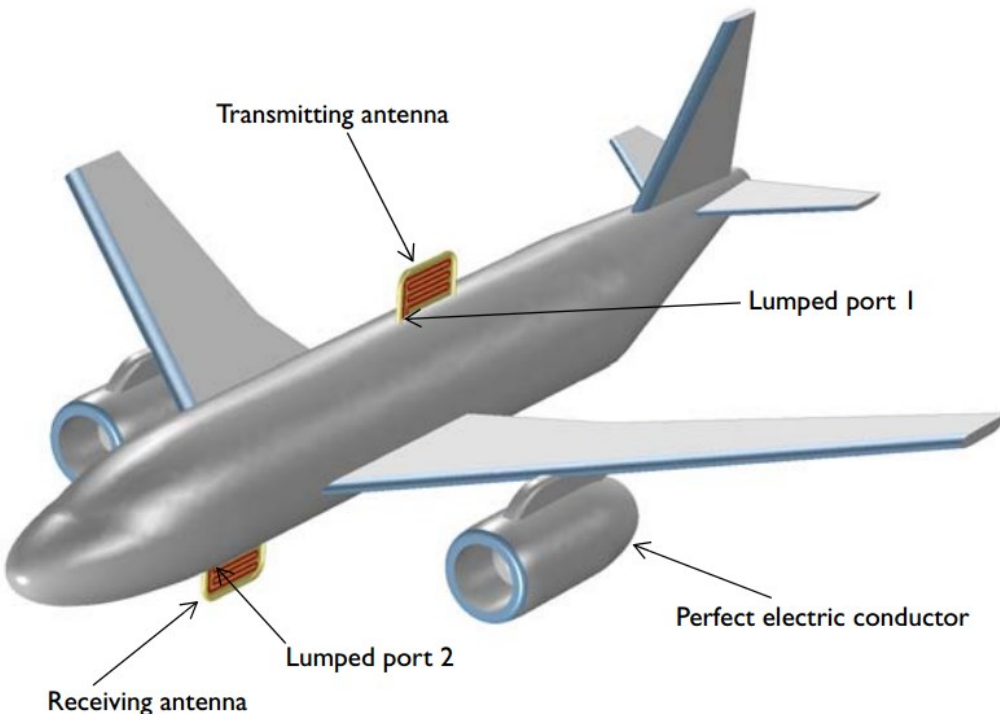
- [12] Feng, Z., Gao, R., Tan, S. & Tsang, L. (2020). Calculation of band diagram and modal Fields of photonic crystals using hybrid representations of the lattice Green's function. ICCEM 2020 Singapore.
- [11] Tan, S., & Tsang, L. (2019). The broadband Green's function technique and its applications in periodic scatterer scattering. PIERS 2019 Xiamen.
- [10] Tan, S., and Tsang, L. (2019). Efficient evaluations of periodic Green's functions through imaginary wavenumber cancellations. ICCEM 2019 Shanghai. (*Paper*)
- [9] Tan, S., & Tsang, L. (2019). Efficient broadband evaluations of lattice Green's functions via imaginary wavenumber components extractions. *Prog. Electromagn. Res.*, 164, 63-74, 2019.
- [8] Tsang, L., Ding, K.-H., & Tan, S. (2018). Broadband Point Source Green's Function in A One-Dimensional Infinite Periodic Lossless Medium Based on BBGFL with Modal Method. *Prog. Electromagn. Res.*, 163, 51-77, 2018.
- [7] Tan, S., & Tsang, L. (2018). Effects of Localized Defects / Sources in a Periodic Lattice Using Green's Function of Periodic Scatterers. APS/URSI 2018 Boston. (*Paper*)
- [6] Tan, S., & Tsang, L. (2017). Green's Functions, Including Scatterers, for Photonic Crystals and Metamaterials with Applications to Wideband Wave Interactions with Finite Periodic Structures. Metamaterials 2017 Marseille. (*Paper*)
- [5] Tan, S., & Tsang, L. (2017). Scattering of Waves by A Halfspace of Periodic Scatterers Using Broadband Green's Function. *Opt. Lett.*, 42(22), 4667-4670.
- [4] Tan, S., & Tsang, L. (2017). Green's functions, including scatterers, for photonic crystals and metamaterials. *J. Opt. Soc. Am. B*, 34(7), 1450-1458.
- [3] Tan, S. (2016). Multiple Volume Scattering in Random Media and Periodic Structures with Applications in Microwave Remote Sensing and Wave Functional Materials. *Ph.D. Dissertation, University of Michigan*.
- [2] Tsang, L., & Tan, S. (2016). Calculations of band diagrams and low frequency dispersion relations of 2D periodic dielectric scatterers using broadband Green's function with low wavenumber extraction (BBGFL). *Opt. Express*, 24(2), 945-965.
- [1] Tsang, L. (2015). Broadband calculations of band diagrams in periodic structures using the broadband Green's function with low wavenumber extraction (BBGFL). *Prog. Electromagn. Res.*, 135, 57-68, 2015.

Tan, S., & Tsang, L. (2018). Efficient Electromagnetic Scattering Analysis for Multiscale Problems Using Green's Functions of Arbitrary Scatterers. PIERS 2018 Toyama. (*Paper*)

Tan, S., & Tsang, L. (2018). An Efficient Electromagnetic Scattering Optimization Scheme for Multiscale Problems Using Green's Functions of Arbitrary Scatterers. *IEEE J. Multiscale and Multiphys. Comput. Techn.*, 3(1), 97-107.

Open and Multi-Scale Scattering Problems

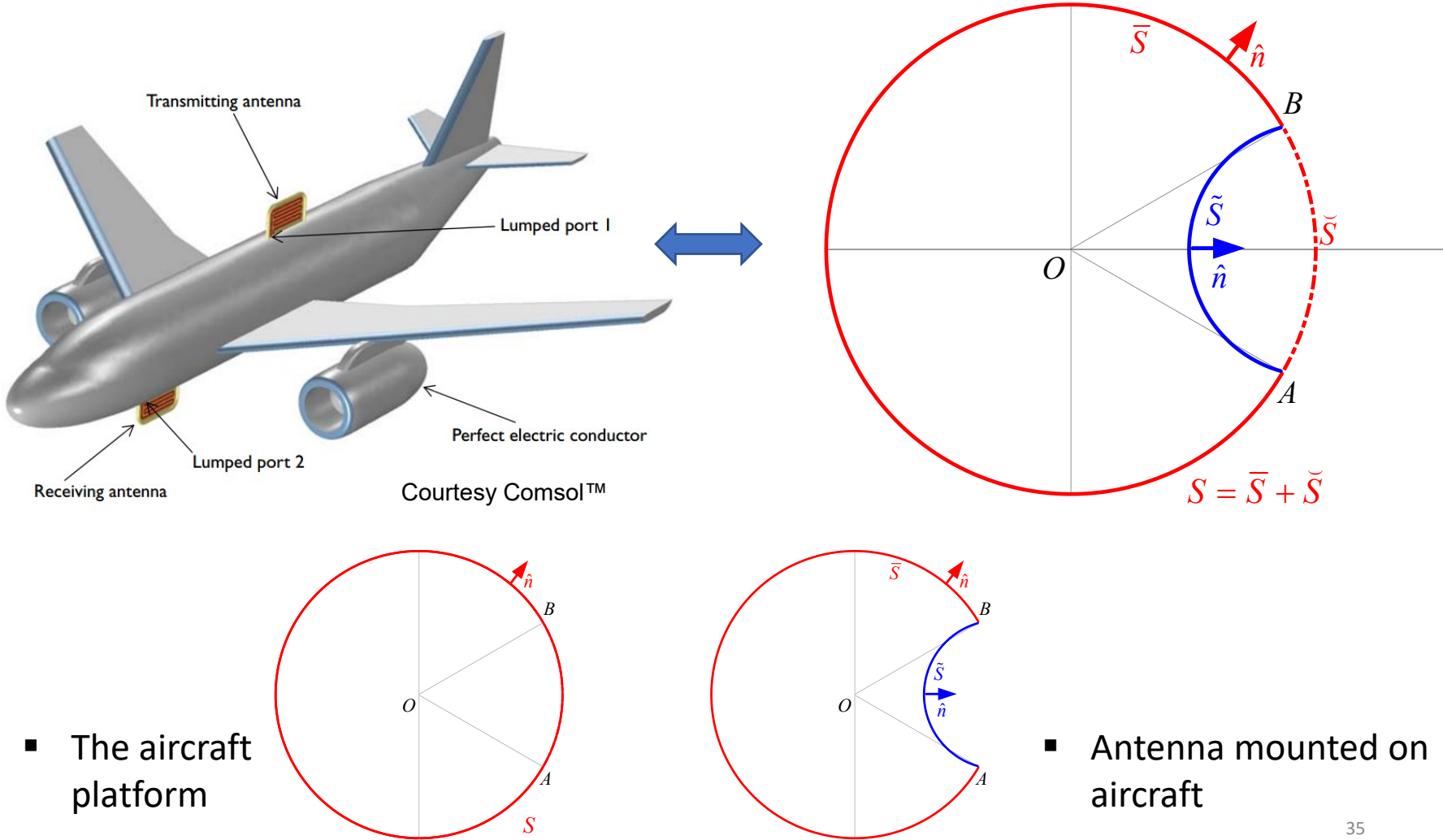
Multi-scale Scattering Problem and Optimization: An Example



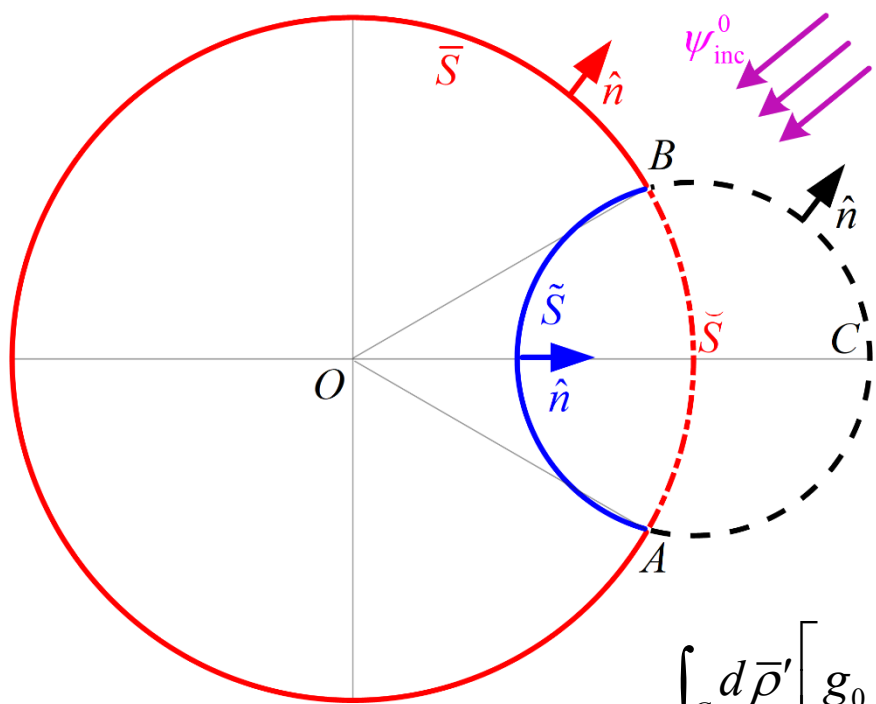
Courtesy Comsol™

- Aircraft platform: large scale
- Antenna: fine scale
- Optimization of antenna for best performance on aircraft platform
- Requires multiple iterations and EM simulations
- Our approach: solve platform scattering **once**, immediately get coupled scattering solution of antenna on platform for **any configurations**

The Multi-scale Scattering Problem: An Analogue



g_s of an Open Scatter Applied to Scattering Problems of Locally Modified Scatterers



$$(\nabla^2 + k^2) g^s(k; \bar{\rho}, \bar{\rho}') = -\delta(\bar{\rho} - \bar{\rho}')$$

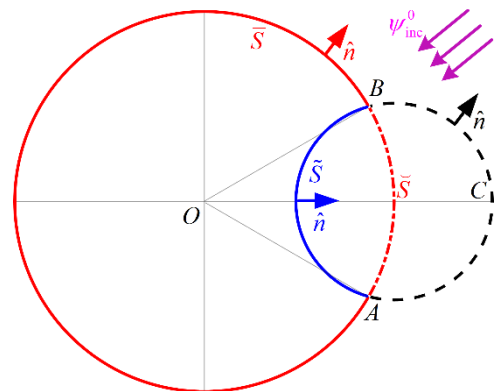
$$\text{s.t. } g^s(k; \bar{\rho}, \bar{\rho}') = 0, \bar{\rho} \text{ on } S$$

$$\int_C d\bar{\rho}' \left[g_s \frac{\partial \psi}{\partial n'} - \psi \frac{\partial g_s}{\partial n'} \right] = \psi_{\text{inc}}^s, \bar{\rho} \rightarrow C^-$$

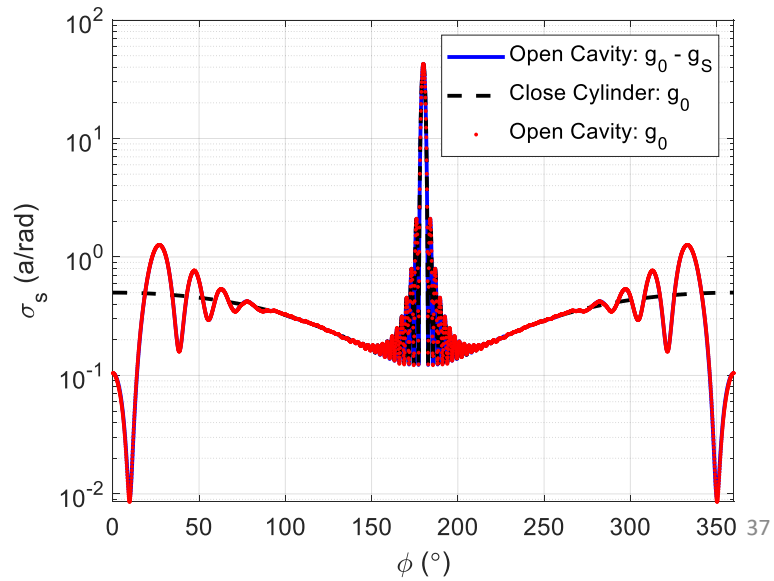
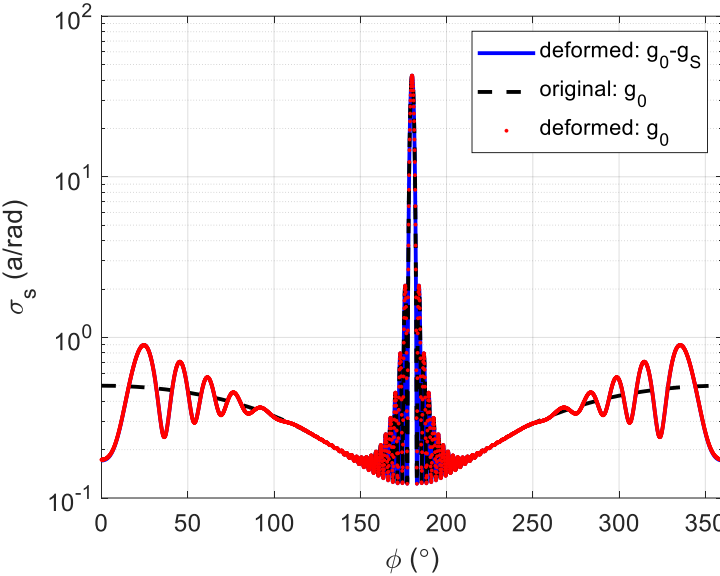
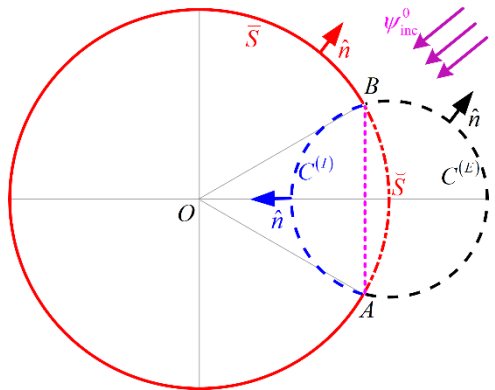
$$\int_C d\bar{\rho}' \left[g_0 \frac{\partial \psi}{\partial n'} - \psi \frac{\partial g_0}{\partial n'} \right] - \int_{\tilde{S}} d\bar{\rho}' g_0 \frac{\partial \psi}{\partial n'} = 0, \bar{\rho} \rightarrow C^+ \text{ or } \tilde{S}^-$$

Scattering of Deformed Scatterers and Open Cavities Using g_S

Deformed scatter



Open cavity

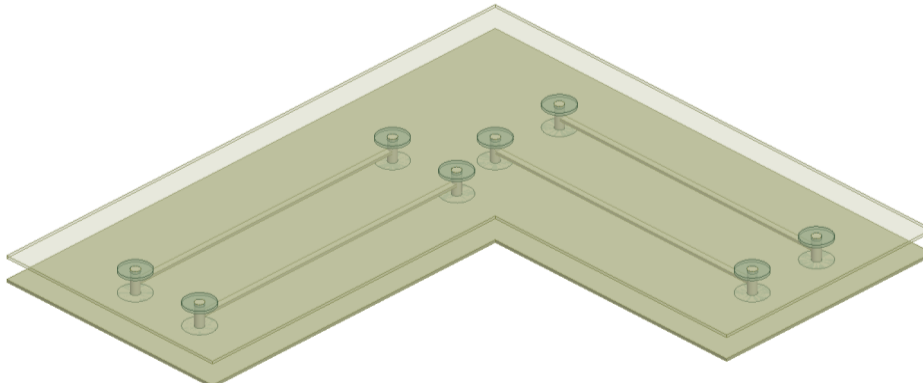


Other Potential Applications of the Broadband Green's Function Theory

Cavity problem and signal/electromagnetic integrity

Casimir forces in nanotechnology

Signal/Electromagnetic Integrity for High-Speed Interconnection and Integration



PCB structure with traces and vias

Waveguide Green's Function

$$g^{\textcolor{blue}{S}}(\textcolor{red}{k}; \bar{\rho}, \bar{\rho}') = \sum_{\beta} \frac{\psi_{\beta}(\bar{\rho}) \psi_{\beta}(\bar{\rho}')}{k_{\beta}^2 - k^2}$$

- Signal and Power Integrity, Packaging, EMC, EMI
- Broadband simulations

Casimir Forces in Nanotechnology

Maxwell Stress Tensor in terms of correlation function

$$\langle 0 | \hat{E}_l(\bar{r}) \hat{E}_m(\bar{r}') | 0 \rangle = \sum_k \omega_k^2 A_k^l(\bar{r}) A_k^{m*}(\bar{r}')$$

Green's function in terms of modes

$$G_{lm}(\bar{r}, \bar{r}'; \omega) = \sum_k \frac{\omega_k}{\omega_k^2 - \omega^2} \frac{2\epsilon_0 c^2}{\hbar} A_k^l(\bar{r}) A_k^{m*}(\bar{r}')$$

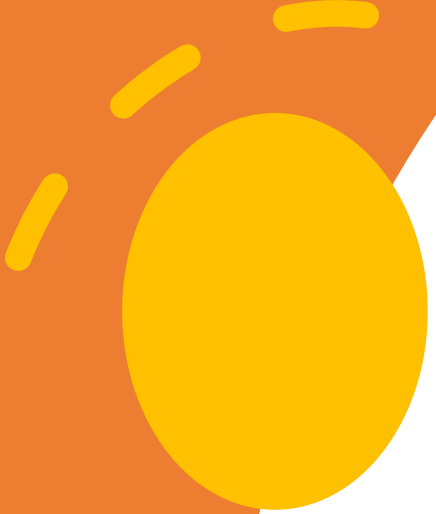
Correlation function in terms of Green's function

$$\langle 0 | \hat{E}_l(\bar{r}) \hat{E}_m(\bar{r}') | 0 \rangle = \frac{\hbar}{2\pi i \epsilon_0 c^2} \int_{-\infty}^{\infty} G_{lm}(\bar{r}, \bar{r}'; \omega) \omega^2 d\omega$$

BBGFL representation of $G_{lm}(\bar{r}, \bar{r}'; \omega)$

Tan, S., & Tsang, L. (2016). The broadband Green's function applied to band diagram simulation of 2D periodic noncircular dielectric scatterers. APS/URSI 2016 Puerto Rico. (*Paper*)

Tsang, L., & Tan, S. (2016). Calculations of band diagrams and low frequency dispersion relations of 2D periodic dielectric scatterers using broadband Green's function with low wavenumber extraction (BBGFL). *Opt. Express*, 24(2), 945-965.



More on The Band Characterization Problem with The BGF Approach

Dielectric scatterer and orientation freedom (link to valley transport)

Topological photonics

Topological acoustics

Spurious mode and cavity mode

3D problem: line media and A-Φ formulation

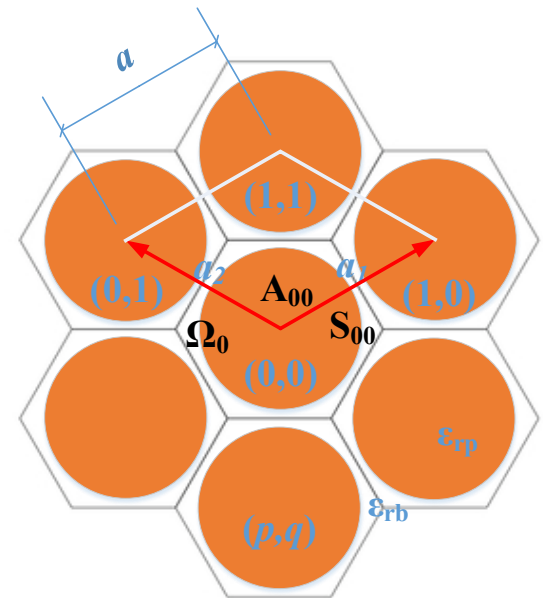
The Surface Integral Equation Formulation for Dielectric Scatterers

Extinction Theorem for region outside the scatterer:

$$\int_{S_{00}} dl' [\psi(\bar{\rho}') \hat{n}' \cdot \nabla' g_P(k, \bar{k}_i; \bar{\rho}, \bar{\rho}') - g_P(k, \bar{k}_i; \bar{\rho}, \bar{\rho}') \hat{n}' \cdot \nabla' \psi(\bar{\rho}')] = 0$$

$\bar{\rho}$ inside scatterer

$$g_P(k, \bar{k}_i; \bar{\rho}, \bar{\rho}') = \frac{1}{\Omega_0} \sum_{mn} \frac{\exp(i\bar{k}_{imn} \cdot (\bar{\rho} - \bar{\rho}'))}{|\bar{k}_{imn}|^2 - k^2}$$



Extinction Theorem inside Scatterer: g_{1P} or g_1 ?

Both are valid extinction theorems

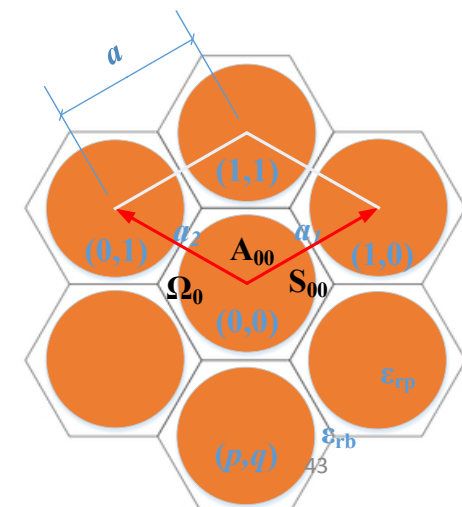
$$-\int_{S_{pq}} dl' [\psi_1(\bar{\rho}') \hat{n}' \cdot \nabla' g_1(\bar{\rho}, \bar{\rho}') - g_1(\bar{\rho}, \bar{\rho}') \hat{n}' \cdot \nabla' \psi_1(\bar{\rho}')] = 0 \quad \bar{\rho} \text{ outside scatterer}$$

$$-\int_{S_{00}} dl' [\psi_1(\bar{\rho}') \hat{n}' \cdot \nabla' g_{1P}(k_1, \bar{k}_i; \bar{\rho}, \bar{\rho}') - g_{1P}(k_1, \bar{k}_i; \bar{\rho}, \bar{\rho}') \hat{n}' \cdot \nabla' \psi_1(\bar{\rho}')] = 0$$

$$g_1(\bar{\rho}, \bar{\rho}') = \frac{i}{4} H_0^{(1)}(k_1 |\bar{\rho} - \bar{\rho}'|)$$

$$g_{1P}(k_1, \bar{k}_i; \bar{\rho}, \bar{\rho}') = \frac{1}{\Omega_0} \sum_{mn} \frac{\exp(i \bar{k}_{imm} \cdot (\bar{\rho} - \bar{\rho}'))}{|\bar{k}_{imm}|^2 - k_1^2}$$

- In KKR (Korringa-Kohn-Rostoker): choose g_P and wave representation of ψ_1 , \rightarrow a non-linear eigenvalue problem
- In BBGFL: choose g_P and g_{1P} , \rightarrow a linear eigenvalue problem, applies to arbitrary geometry
- If we choose g_P and g_1 , \rightarrow a nonlinear eigenvalue problem



g_B and g_{1B} In Surface Integral Equations

$$g_P(k, \bar{k}_i, \bar{\rho}, \bar{\rho}') = g_P(k_L, \bar{k}_i, \bar{\rho}, \bar{\rho}') + g_B(k, k_L, \bar{k}_i, \bar{\rho}, \bar{\rho}')$$

$$g_{1P}(k_1, \bar{k}_i, \bar{\rho}, \bar{\rho}') = g_{1P}(k_{1L}, \bar{k}_i, \bar{\rho}, \bar{\rho}') + g_{1B}(k_1, k_{1L}, \bar{k}_i, \bar{\rho}, \bar{\rho}')$$

$$g_B(k, k_L, \bar{k}_i, \bar{\rho}, \bar{\rho}') = \frac{k^2 - k_L^2}{\Omega_0} \sum_{\alpha} \frac{\exp(i\bar{k}_{i\alpha} \cdot (\bar{\rho} - \bar{\rho}'))}{(|k_{i\alpha}|^2 - k^2)(|k_{i\alpha}|^2 - k_L^2)}$$

$$g_{1B}(k_1, k_{1L}, \bar{k}_i, \bar{\rho}, \bar{\rho}') = \frac{k_1^2 - k_{1L}^2}{\Omega_0} \sum_{\alpha} \frac{\exp(i\bar{k}_{i\alpha} \cdot (\bar{\rho} - \bar{\rho}'))}{(|\bar{k}_{i\alpha}|^2 - k_1^2)(|\bar{k}_{i\alpha}|^2 - k_{1L}^2)}$$

- Only need **a few terms** in g_B and g_{1B} : $1/|\bar{k}_{i\alpha}|^4$
- Size of the eigenvalue problem: small

Dielectric Scatterer Array: Formulation

Coupled SIEs with $g_P(k)$ and $g_P(k_1)$

$$\int_{S_{00}} d\bar{\rho}' \psi(\bar{\rho}') \hat{n}' \cdot \nabla' g_P(k, \bar{k}_i; \bar{\rho}, \bar{\rho}') - \int_{S_{00}} d\bar{\rho}' g_P(k, \bar{k}_i; \bar{\rho}, \bar{\rho}') \hat{n}' \cdot \nabla' \psi(\bar{\rho}') = 0, \quad \bar{\rho} \rightarrow S_{00}^-$$

$$-\int_{S_{00}} d\bar{\rho}' \psi_1(\bar{\rho}') \hat{n}' \cdot \nabla' g_P(k_1, \bar{k}_i; \bar{\rho}, \bar{\rho}') - \int_{S_{00}} d\bar{\rho}' g_P(k_1, \bar{k}_i; \bar{\rho}, \bar{\rho}') \hat{n}' \cdot \nabla' \psi_1(\bar{\rho}') = 0, \quad \bar{\rho} \rightarrow S_{00}^+$$

Boundary conditions

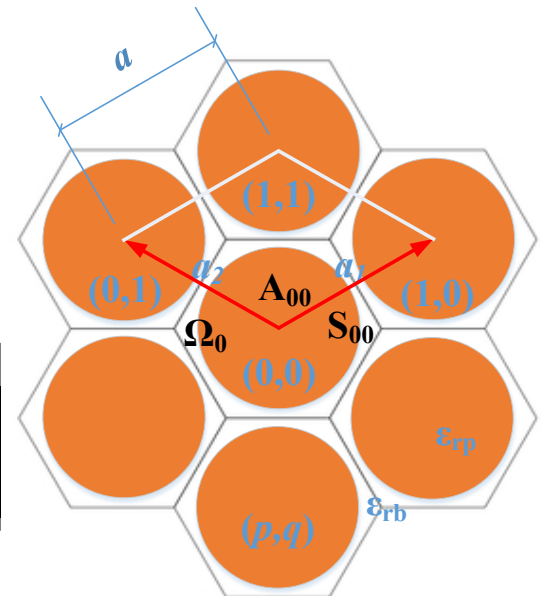
$$\psi_1(\bar{\rho}') = \psi(\bar{\rho}')$$

$$\hat{n}' \cdot \nabla' \psi_1(\bar{\rho}') = \frac{1}{s} \hat{n}' \cdot \nabla' \psi(\bar{\rho}')$$

$$s = \begin{cases} 1 & \text{TMz} \\ \frac{\epsilon_b}{\epsilon_p} & \text{TEz} \end{cases}$$

Matrix representation

$$\bar{Z}(k, k_1) \begin{bmatrix} \bar{p} \\ \bar{q} \end{bmatrix} = 0 \quad \bar{Z}(k, k_1) = \begin{bmatrix} \bar{S}(k) & -\bar{L}(k) \\ \bar{S}_1(k_1) & -\frac{1}{s} \bar{L}_1(k_1) \end{bmatrix}$$



Band diagram: to find the supporting k 's at each \bar{k}_i : $|\bar{Z}(k, k_1; \bar{k}_i)| = 0$

Dielectric Scatterer Array: Linear Eigenvalue Problem Formulation

Invoking the hybrid representation of $g_P(k)$ and $g_P(k_1)$

$$\bar{Z}(\lambda) = \bar{Z}(i\xi) + \begin{bmatrix} \bar{\bar{R}} & \\ & \bar{\bar{R}}_1 \end{bmatrix} \left(\lambda \bar{\bar{I}} - \begin{bmatrix} \bar{\bar{D}} & \\ & \frac{\varepsilon_p}{\varepsilon_b} \bar{\bar{D}}_1 \end{bmatrix} \right)^{-1} \begin{bmatrix} \bar{\bar{Q}}^\dagger & -\bar{\bar{R}}^\dagger \\ \frac{\varepsilon_p}{\varepsilon_b} \bar{\bar{Q}}_1^\dagger & -\frac{1}{s} \frac{\varepsilon_p}{\varepsilon_b} \bar{\bar{R}}_1^\dagger \end{bmatrix}$$

Note the pole singularity k or $k_1 = |\bar{K}_\alpha|$

Define

$$\bar{d} = \left(\lambda \bar{\bar{I}} - \begin{bmatrix} \bar{\bar{D}} & \\ & \frac{\varepsilon_p}{\varepsilon_b} \bar{\bar{D}}_1 \end{bmatrix} \right)^{-1} \begin{bmatrix} \bar{\bar{Q}}^\dagger & -\bar{\bar{R}}^\dagger \\ \frac{\varepsilon_p}{\varepsilon_b} \bar{\bar{Q}}_1^\dagger & -\frac{1}{s} \frac{\varepsilon_p}{\varepsilon_b} \bar{\bar{R}}_1^\dagger \end{bmatrix} \begin{bmatrix} \bar{p} \\ \bar{q} \end{bmatrix}$$

Together with

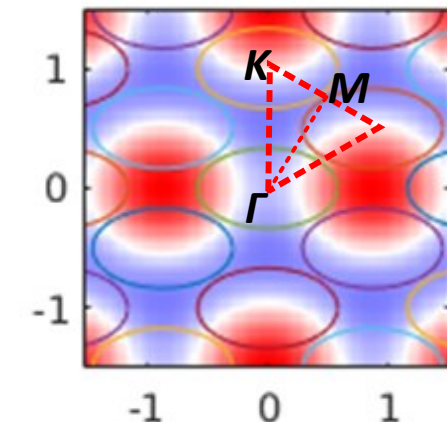
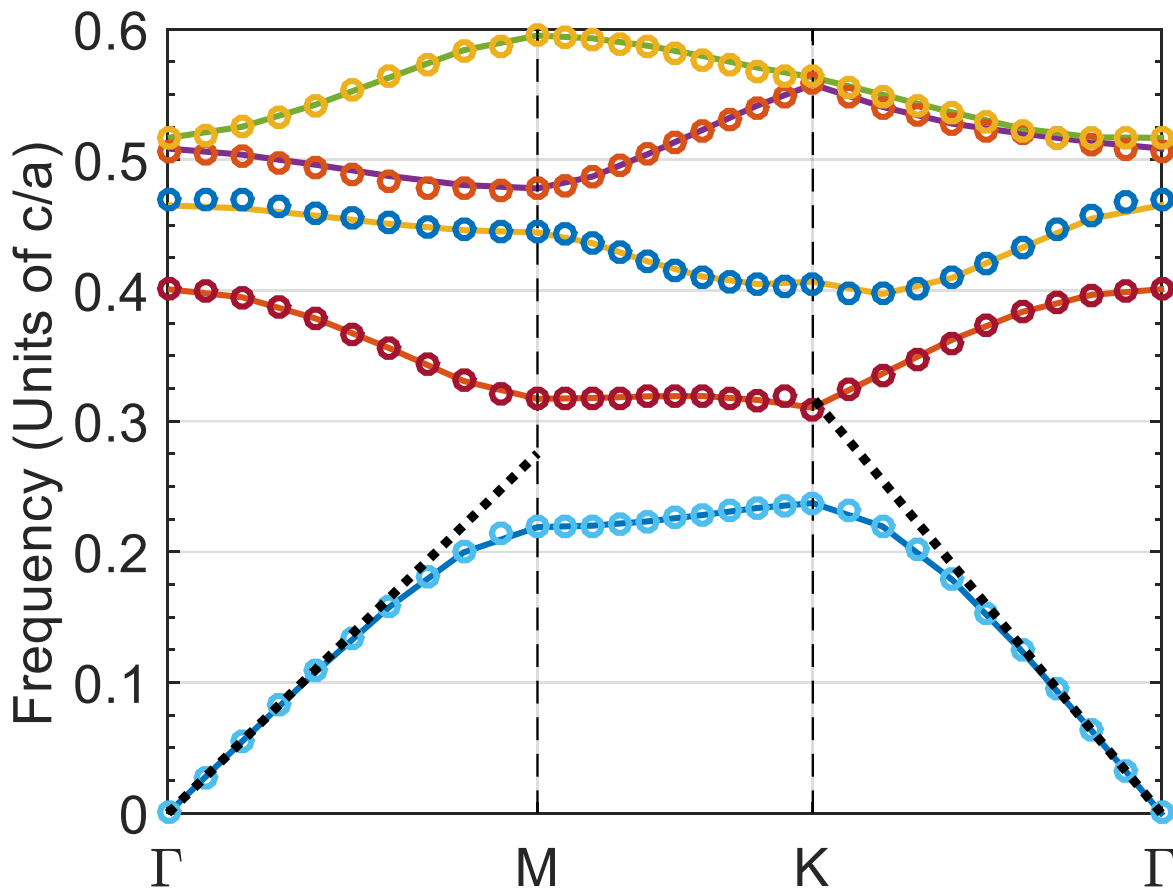
$$\begin{bmatrix} \bar{p} \\ \bar{q} \end{bmatrix} = - \left[\bar{Z}(i\xi) \right]^{-1} \begin{bmatrix} \bar{\bar{R}} & \\ & \bar{\bar{R}}_1 \end{bmatrix} \bar{d}$$

Linear Eigenvalue Problem

$$\bar{\bar{P}} \bar{d} = \lambda \bar{d}$$

$$\bar{\bar{P}} = \begin{bmatrix} \bar{\bar{D}} & \\ & \frac{\varepsilon_p}{\varepsilon_b} \bar{\bar{D}}_1 \end{bmatrix} - \begin{bmatrix} \bar{\bar{Q}}^\dagger & -\bar{\bar{R}}^\dagger \\ \frac{\varepsilon_p}{\varepsilon_b} \bar{\bar{Q}}_1^\dagger & -\frac{1}{s} \frac{\varepsilon_p}{\varepsilon_b} \bar{\bar{R}}_1^\dagger \end{bmatrix} \left[\bar{Z}(i\xi) \right]^{-1} \begin{bmatrix} \bar{\bar{R}} & \\ & \bar{\bar{R}}_1 \end{bmatrix}$$

Band Diagrams of Periodic Elliptical Air Voids: TMz



$$\text{Semi-long radius} = a/\sqrt{3}$$

$$\text{Semi-short radius} = a/3$$

$$\varepsilon_{rb} = 12.25$$

$$\varepsilon_{rp} = 1$$

Maxwell Garnett:

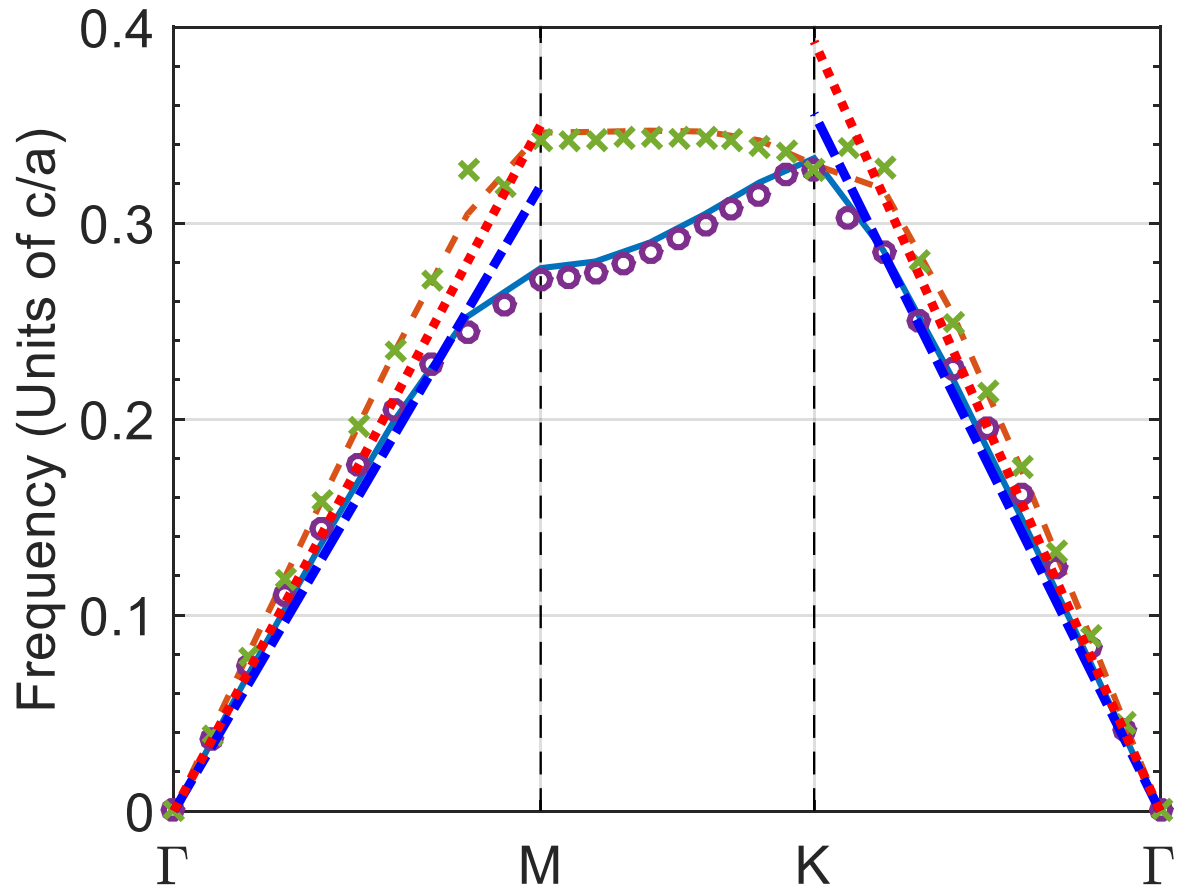
$$\varepsilon_z = (1 - f_v)\varepsilon + f_v\varepsilon_p$$

Low frequency dispersion:

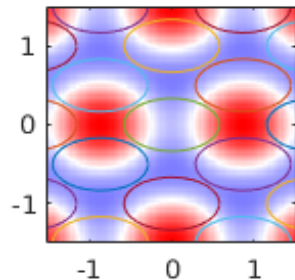
$$k = \omega\sqrt{\varepsilon_z\mu}$$

Plane wave: a linear eigenvalue problem by expanding both field and dielectric constants into Bloch modes. Converge slowly for large permittivity contrast and filling ratio.

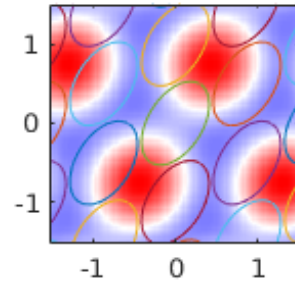
Band Diagrams of Periodic Elliptical Air Voids: TEz



Lower band:
semi-long
axis along \hat{x}



higher band:
semi-long axis
 60° off \hat{x}



Maxwell Garnett:

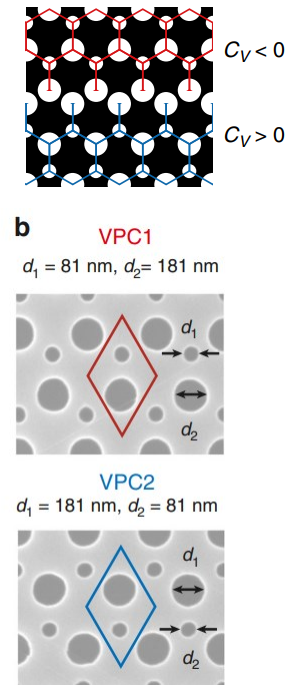
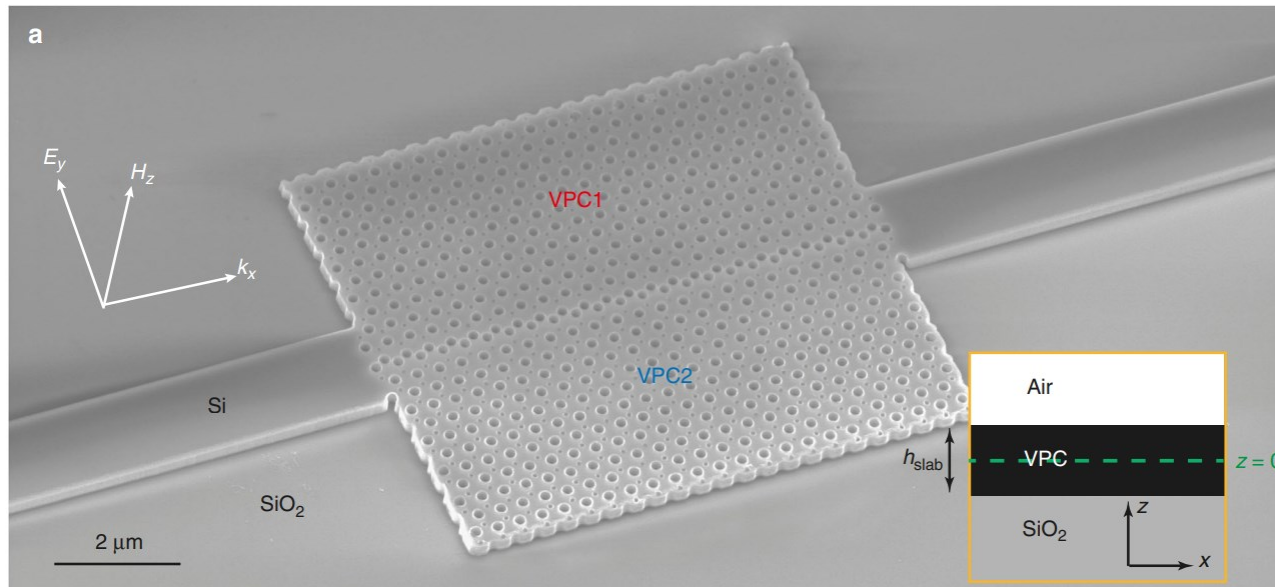
$$\varepsilon_{x,y} = \varepsilon \frac{1 + n_0 \alpha_{x,y} (1 - \chi_{x,y}) / \varepsilon}{1 - n_0 \alpha_{x,y} \chi_{x,y} / \varepsilon}$$

Low frequency dispersion:

$$k = \omega \sqrt{\varepsilon_{\text{eff}}(\theta) \mu} \\ \varepsilon_{\text{eff}}(\theta) = \frac{\varepsilon_x \varepsilon_y}{\varepsilon_x \cos^2 \theta + \varepsilon_y \sin^2 \theta}$$

θ : angle between \hat{k} and semi-long axis

Orientation Freedom of Arbitrarily Shaped Scatterer Links to Topological Valley Transport



Figures courtesy He et al., NATURE COMMUNICATIONS | (2019) 10:872.

Feng, Z., Tan, S., Tsang, L., & Li, E. P. (2019). Efficient characterization of topological photonics using the broadband Green's function. PIERS 2019 Xiamen. (*Paper*)

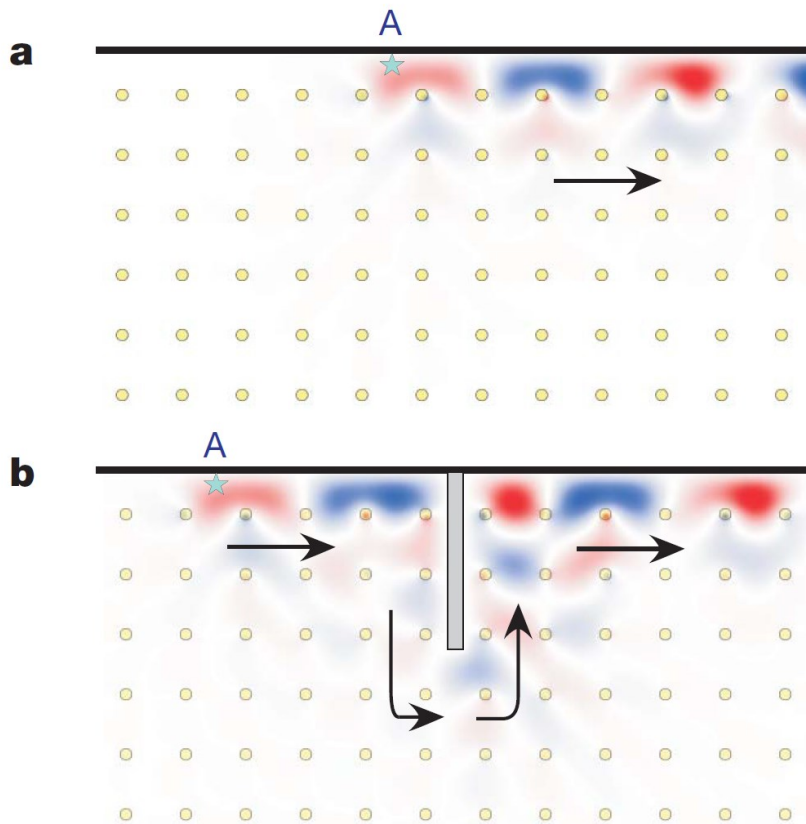
Feng, Z., Tan, S., Tsang, L., & Li, E. (2020). Band characterization of topological photonic crystals using the broadband Green's function technique. Optics Express, 28(19), 27223-27237.

Topological Photonics

Versatility of the BGF approach

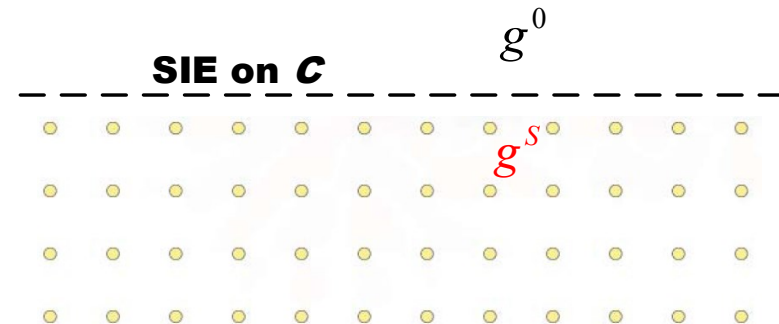
Spurious mode issue

Topological Photonics and Edge States



- Unidirectional backscattering immune topological edge states

- SIE using g^S and g^0 on C



TMz Modes in a Gyromagnetic Photonic Crystal

Inside gyromagnetic scatterers

ε : scalar

$$\bar{\mu} = \begin{bmatrix} \mu & i\kappa & 0 \\ -i\kappa & \mu & 0 \\ 0 & 0 & \mu_0 \end{bmatrix} \quad \bar{\mu}^{-1} = \begin{bmatrix} \tilde{\mu}^{-1} & i\eta & 0 \\ -i\eta & \tilde{\mu}^{-1} & 0 \\ 0 & 0 & \mu_0^{-1} \end{bmatrix}$$

$$\nabla \times \bar{E} = i\omega \bar{\mu} \bar{H}$$

$$\nabla \times \bar{H} = -i\omega \varepsilon \bar{E}$$

$$\nabla^2 E_z + \omega^2 \varepsilon \mu \left(1 - \frac{\kappa^2}{\mu^2} \right) E_z = 0$$

Outside, in background

ε_0, μ_0 : scalar

$$\nabla \times \bar{E} = i\omega \mu_0 \bar{H}$$

$$\nabla \times \bar{H} = -i\omega \varepsilon_0 \bar{E}$$

$$\nabla^2 E_{0z} + \omega^2 \varepsilon_0 \mu_0 E_{0z} = 0$$

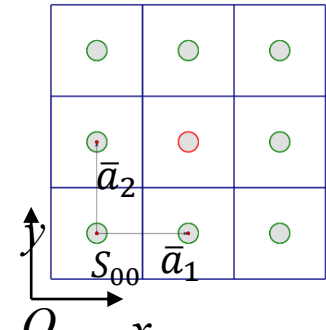
Boundary conditions

$$\hat{n} \times (\bar{E}_0 - \bar{E}) = 0$$

$$E_{0z} = E_z$$

$$\hat{n} \times (\bar{H}_0 - \bar{H}) = 0$$

$$\hat{n} \cdot \nabla E_{0z} = \frac{\mu_0}{\tilde{\mu}} \hat{n} \cdot \nabla E_z + i\eta \mu_0 \hat{t} \cdot \nabla E_z$$



Geometry of
the 2D lattice

An Integral Formulation of the Eigen-Modes

- Inside gyromagnetic scatterers

$$\nabla^2 E_z + \omega^2 \epsilon \mu \left(1 - \frac{\kappa^2}{\mu^2} \right) E_z = 0$$

$$\nabla^2 g(\bar{\rho}, \bar{\rho}') + \omega^2 \epsilon \mu \left(1 - \frac{\kappa^2}{\mu^2} \right) g(\bar{\rho}, \bar{\rho}') = -\delta(\bar{\rho} - \bar{\rho}') \\ g_P(\bar{k}_b; \bar{\rho}, \bar{\rho}') = \sum_{m,n} g(\bar{\rho}, \bar{\rho}' + \bar{R}_{mn}) \exp(i \bar{k}_b \cdot \bar{R}_{mn})$$

- Outside, in background

$$\nabla^2 E_{0z} + \omega^2 \epsilon_0 \mu_0 E_{0z} = 0$$

$$g_{P0}(\bar{k}_b; \bar{\rho}, \bar{\rho}') = \sum_{m,n} g_0(\bar{\rho}, \bar{\rho}' + \bar{R}_{mn}) \exp(i \bar{k}_b \cdot \bar{R}_{mn})$$

$$\int_{C_{00}} d\bar{\rho}' [g_P \hat{n}' \cdot \nabla' E_z - E_z \hat{n}' \cdot \nabla' g_P] = \begin{cases} E_z(\bar{\rho}) & \text{if } \bar{\rho} \text{ inside scatterer} \\ 0 & \text{if } \bar{\rho} \text{ outside scatterer} \end{cases}$$

$$-\int_{C_{00}} d\bar{\rho}' [g_{P0} \hat{n}' \cdot \nabla' E_{0z} - E_{0z} \hat{n}' \cdot \nabla' g_{P0}] = \begin{cases} 0 & \text{if } \bar{\rho} \text{ inside scatterer} \\ E_{0z}(\bar{\rho}) & \text{if } \bar{\rho} \text{ outside scatterer} \end{cases}$$

Coupled Integral Equations

- Let $\bar{\rho}$ approach the boundary in the extinction theorem
- Apply boundary conditions on the scatterers
- Obtain coupled surface integral equations

$$\int_{C_{00}} d\bar{\rho}' [g_P \hat{n}' \cdot \nabla' E_z - E_z \hat{n}' \cdot \nabla' g_P] = 0, \quad \bar{\rho} \rightarrow S_{00}^+$$

$$-\int_{C_{00}} d\bar{\rho}' \left[g_{P0} \left(\frac{\mu_0}{\tilde{\mu}} \hat{n}' \cdot \nabla' E_z + i\eta\mu_0 \hat{t}' \cdot \nabla' E_z \right) - E_z \hat{n}' \cdot \nabla' g_{P0} \right] = 0, \quad \bar{\rho} \rightarrow S_{00}^-$$

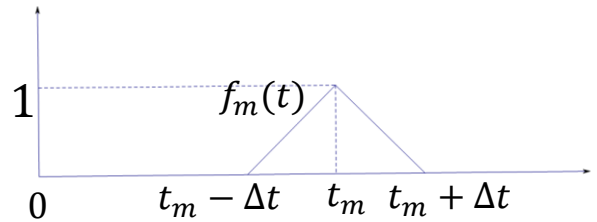
- To construct a linear eigenvalue problem
 - apply the broadband representations of g_P and g_{P0} ,
 - and apply Method of Moments with **roof-top basis function** to discretize the integral equation

Galerkin Method with Roof-Top Basis

Apply Galerkin's method and use roof-top basis function

$$\int_{S_m} dt f_m(t) \int_{S_n} dt' \left[\psi_{1n} \hat{n}' \cdot \nabla' g_P^1(k_1, \bar{k}_i; \bar{\rho}(t), \bar{\rho}'(t')) - g_P^1(k_1, \bar{k}_i; \bar{\rho}(t), \bar{\rho}'(t')) u_{1n} \right] f_n(t') = 0 \quad (\bar{\rho}) \rightarrow S_{00}^+$$

$$\int_{S_m} dt f_m(t) \int_{S_n} dt' \left[\psi_{1n} \hat{n}' \cdot \nabla' g_P^0(k_0, \bar{k}_i; \bar{\rho}(t), \bar{\rho}'(t)) - g_P^0(k_0, \bar{k}_i; \bar{\rho}(t), \bar{\rho}'(t)) \mu_0 \left(\frac{1}{\tilde{\mu}} u_{1n} + \psi_{1n} i \eta \hat{t}' \cdot \nabla' \right) \right] f_n(t') = 0 \quad (\bar{\rho}) \rightarrow S_{00}^-$$



Roof-top basis function and it's derivation

$$f_m(t) = \begin{cases} \frac{1}{\Delta t} (t - t_m + \Delta t); & t_m - \Delta t < t < t_m \\ -\frac{1}{\Delta t} (t - t_m - \Delta t); & t_m < t < t_m + \Delta t \\ 0; & \text{otherwise} \end{cases}$$

$$\hat{t} \cdot \nabla f_m(t) = \begin{cases} \frac{1}{\Delta t}; & t_m - \Delta t < t < t_m \\ -\frac{1}{\Delta t}; & t_m < t < t_m + \Delta t \\ 0; & \text{otherwise} \end{cases}$$

Matrix form

$$\bar{\bar{A}}_1 \bar{\psi}_1 - \bar{\bar{B}}_1 \bar{u}_1 = 0$$

$$(\bar{\bar{A}}_0 - i \mu_0 \eta \bar{\bar{C}}) \bar{\psi}_1 - \frac{\mu_0}{\tilde{\mu}} \bar{\bar{B}}_0 \bar{u}_1 = 0$$

BGF and Linear Eigenvalue Problem

$$[g_P]_{Spe} = \sum_{\bar{K}} R(i\xi, \bar{\rho}) W(k, i\xi) R^*(i\xi, \bar{\rho})$$

$$R(i\xi, \bar{\rho}) = \frac{1}{\sqrt{\Omega}} \frac{\exp(i\bar{K} \cdot \bar{\rho})}{(|\bar{K}|^2 + \xi^2)}$$

$$W(k, i\xi) = \frac{1}{\lambda(i\xi, k) - D(i\xi)} \quad \lambda(i\xi, k) = \frac{1}{k^2 + \xi^2}$$

$$D(i\xi) = \frac{1}{|\bar{K}|^2 + \xi^2}$$

SIE becomes

$$0 = (\bar{\bar{A}}_0(i\xi_0) - i\mu_0\eta\bar{\bar{C}}(i\xi_0))\bar{\psi}_1 - \frac{\mu_0}{\tilde{\mu}}\bar{\bar{B}}_0(i\xi_0)\bar{u}_1$$

Related to $[g_P^0]_{Spa}$

$$+ (\bar{\bar{R}}(i\xi_0)\bar{\bar{W}}(k, i\xi_0)\bar{\bar{Q}}^\dagger(i\xi_0, \bar{\rho}') - i\mu_0\eta\bar{\bar{R}}(i\xi_0)\bar{\bar{W}}(k, i\xi_0)\bar{\bar{R}}_C^\dagger(i\xi_0, \bar{\rho}'))\bar{\psi}_1 - \bar{\bar{R}}(i\xi_0)\bar{\bar{W}}(k, i\xi_0)\bar{\bar{R}}^\dagger(i\xi_0, \bar{\rho}')\bar{u}_1$$

Related to $[g_P^0]_{Spe}$

$$0 = \bar{\bar{A}}_1(i\xi_1, \bar{k}_i; \bar{\rho}, \bar{\rho}')\bar{\psi}_1 - \bar{\bar{B}}_1(i\xi_1, \bar{k}_i; \bar{\rho}, \bar{\rho}')\bar{u}_1$$

Related to $[g_P^1]_{Spa}$

$$+ \bar{\bar{R}}(i\xi_1, \bar{\rho})\bar{\bar{W}}(k, i\xi_1)\bar{\bar{Q}}^\dagger(i\xi_1, \bar{\rho})\bar{\psi}_1 - \bar{\bar{R}}(i\xi_1, \bar{\rho})\bar{\bar{W}}(k, i\xi_1)\bar{\bar{R}}^\dagger(i\xi_1, \bar{\rho})\bar{u}_1$$

Related to $[g_P^1]_{Spe}$

BGF and Linear Eigenvalue Problem (Cont'd)

Define

$$\bar{b} = W(k, i\xi_0)[(\bar{\bar{Q}}^\dagger(i\xi_0, \bar{\rho}') - i\mu_0\eta\bar{\bar{R}}_C^\dagger(i\xi_0, \bar{\rho}'))\bar{\psi}_1 - \bar{\bar{R}}^\dagger(i\xi_0, \bar{\rho}')\bar{u}_1]$$

$$\bar{c} = W(k, i\xi_1)[(\bar{\bar{Q}}^\dagger(i\xi_1, \bar{\rho}')\bar{\psi}_1 - \bar{\bar{R}}^\dagger(i\xi_1, \bar{\rho}')\bar{u}_1]$$

$$\begin{bmatrix} \bar{\psi}_1 \\ \bar{u}_1 \end{bmatrix} = -[Z(i\xi_0, \bar{k}_i)]^{-1} \begin{bmatrix} \bar{\bar{R}}(i\xi_0) & \bar{\bar{0}} \\ \bar{\bar{0}} & \bar{\bar{R}}(i\xi_1) \end{bmatrix} \begin{bmatrix} \bar{b} \\ \bar{c} \end{bmatrix}$$

Eigenvalue problem

$$\bar{\bar{P}} \begin{bmatrix} \bar{b} \\ \bar{c} \end{bmatrix} = \lambda_0 \begin{bmatrix} \bar{b} \\ \bar{c} \end{bmatrix}$$

$$\bar{\bar{P}} = \begin{bmatrix} \bar{\bar{D}}(i\xi_0) & \bar{\bar{0}} \\ \bar{\bar{0}} & \bar{\bar{D}}(i\xi_1) \end{bmatrix} - \begin{bmatrix} \bar{\bar{R}}^\dagger(i\xi_0, \bar{\rho}') - i\mu_0\eta\bar{\bar{R}}_C^\dagger(i\xi_0, \bar{\rho}') & -\frac{\mu_0}{\tilde{\mu}}\bar{\bar{Q}}^\dagger(i\xi_0, \bar{\rho}') \\ \varepsilon_r\mu_r\bar{\bar{R}}^\dagger(i\xi_1, \bar{\rho}') & -\varepsilon_r\mu_r\bar{\bar{Q}}^\dagger(i\xi_1, \bar{\rho}') \end{bmatrix} [Z(i\xi_0, \bar{k}_i)]^{-1} \begin{bmatrix} \bar{\bar{R}}(i\xi_0) & \bar{\bar{0}} \\ \bar{\bar{0}} & \bar{\bar{R}}(i\xi_1) \end{bmatrix}$$

$$[Z(i\xi_0, \bar{k}_i)] = \begin{bmatrix} \bar{\bar{A}}(i\xi_0, \bar{k}_i) - i\mu_0\eta\bar{\bar{C}}(i\xi_0, \bar{k}_i) & -\frac{\mu_0}{\tilde{\mu}}\bar{\bar{B}}(i\xi_0, \bar{k}_i) \\ \varepsilon_r\mu_r\bar{\bar{A}}(i\xi_1, \bar{k}_i) & -\varepsilon_r\mu_r\bar{\bar{B}}(i\xi_1, \bar{k}_i) \end{bmatrix}$$

Advantage of The Linear Eigenvalue Problem Formulation

Eigenvalue problem:

$$\bar{\bar{P}} \begin{bmatrix} \bar{b} \\ \bar{c} \end{bmatrix} = \lambda_0 \begin{bmatrix} \bar{b} \\ \bar{c} \end{bmatrix}$$

Eigenvalue:

$$\lambda_0 = \frac{1}{\xi_0^2 + k_0^2}$$

Surface fields from eigenvector:

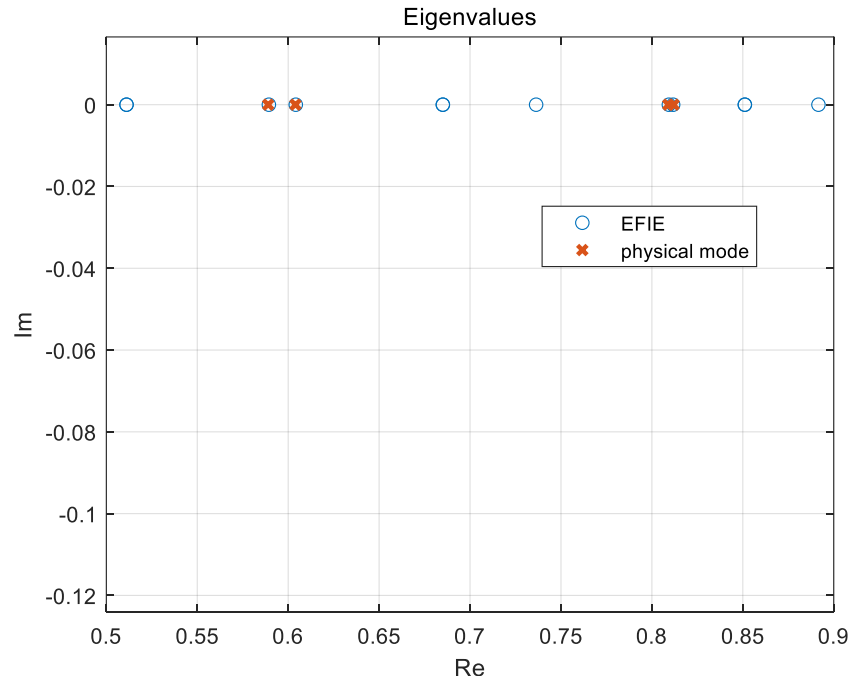
$$\begin{bmatrix} \bar{\psi}_1 \\ \bar{u}_1 \end{bmatrix} = -[Z(i\xi_0, \bar{k}_i)]^{-1} \begin{bmatrix} \bar{\bar{R}}(i\xi_0) & \bar{0} \\ \bar{0} & \bar{\bar{R}}(i\xi_1) \end{bmatrix} \begin{bmatrix} \bar{b} \\ \bar{c} \end{bmatrix}$$

The modal fields are directly related to the surface fields.

- Advantage:
 - $\bar{\bar{P}}$: frequency independent
 - $\bar{\bar{P}}$: small size
 - Get all the eigenvalues simultaneously

Physical Modes and Spurious Modes

Check extinction theorem
to reject spurious mode



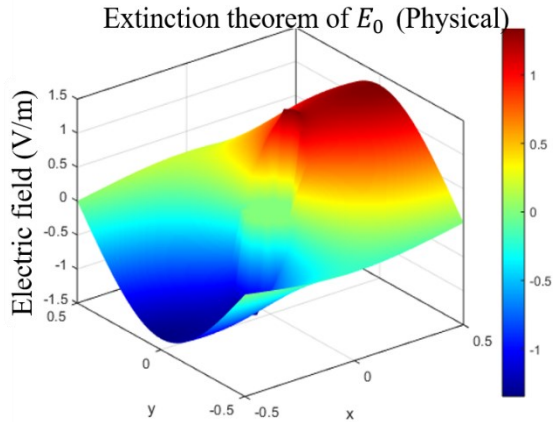
$$\int_{C_{00}} d\bar{\rho}' [g_P \hat{n}' \cdot \nabla' E_z - E_z \hat{n}' \cdot \nabla' g_P] = \begin{cases} E_z(\bar{\rho}) & \text{if } \bar{\rho} \text{ inside scatterer} \\ 0 & \text{if } \bar{\rho} \text{ outside scatterer} \end{cases}$$

$$-\int_{C_{00}} d\bar{\rho}' [g_{P0} \hat{n}' \cdot \nabla' E_{0z} - E_{0z} \hat{n}' \cdot \nabla' g_{P0}] = \begin{cases} 0 & \text{if } \bar{\rho} \text{ inside scatterer} \\ E_{0z}(\bar{\rho}) & \text{if } \bar{\rho} \text{ outside scatterer} \end{cases}$$

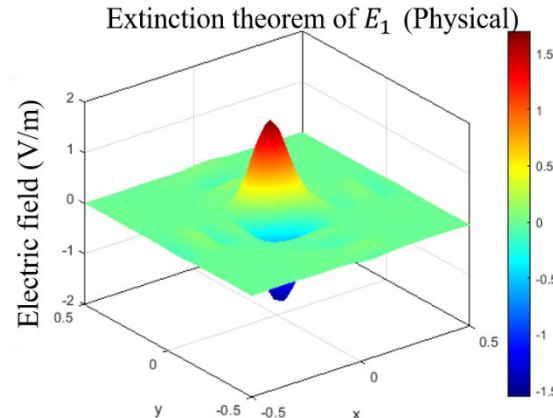
Extinction Theorem Distinguishes Physical Modes versus Spurious Modes

Physical

Extinction theorem of outside region

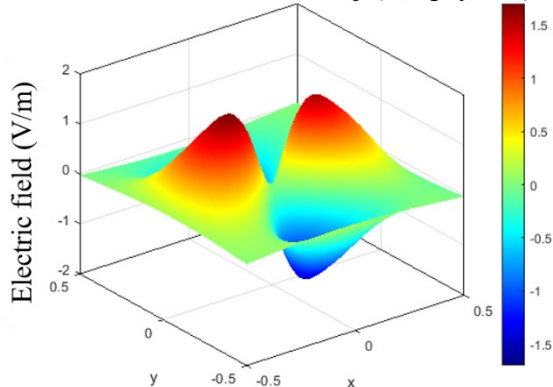


Extinction theorem of inside region

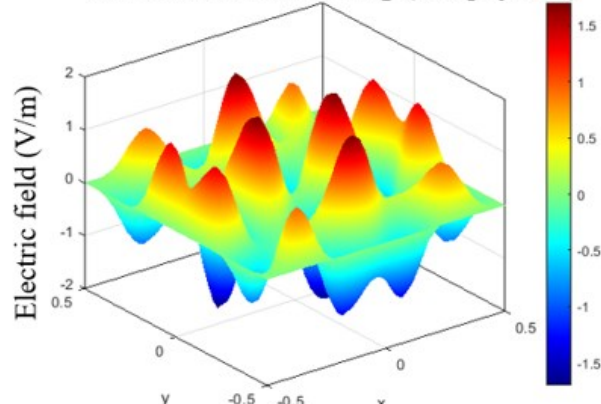


Nonphysical

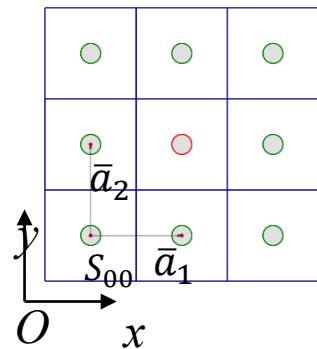
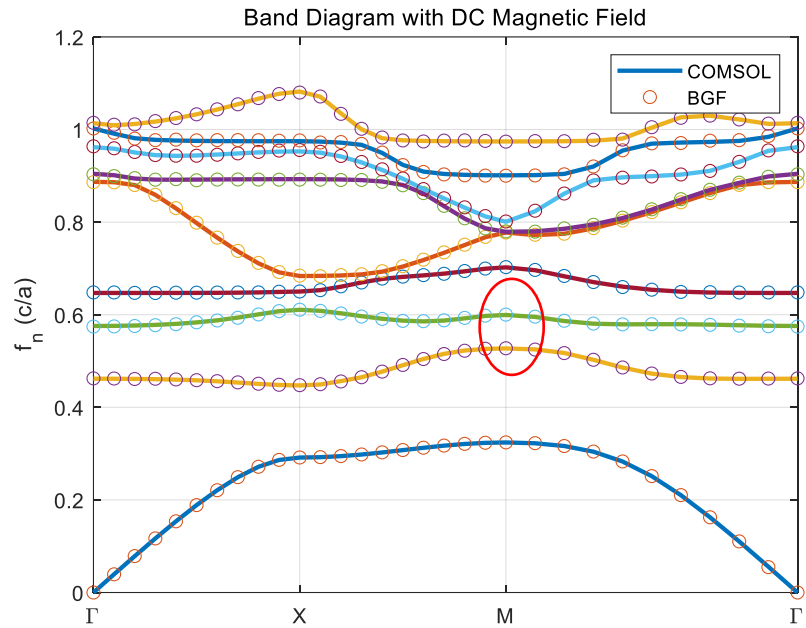
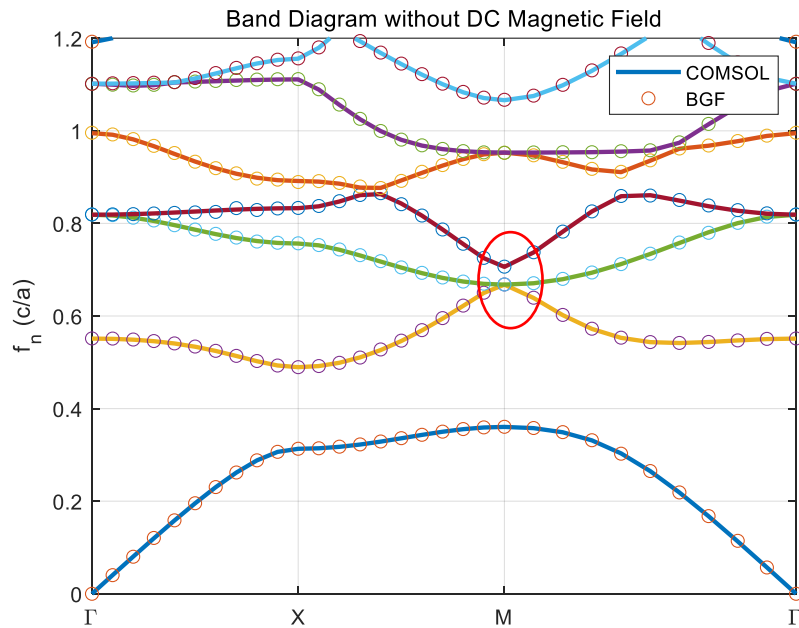
Extinction theorem of E_0 (Nonphysical)



Extinction theorem of E_1 (Nonphysical)



Physical Band Solutions to Gyromagnetic Photonic Crystals without/with DC Magnetic Fields



$$r = 0.11a$$

$$\varepsilon_1 = 15\varepsilon_0$$

$$\bar{\mu} = \begin{bmatrix} 14\mu_0 & 12.4i\mu_0 & 0 \\ -12.4i\mu_0\kappa & 14\mu_0 & 0 \\ 0 & 0 & \mu_0 \end{bmatrix}$$

Feng, Z., Tan, S., Tsang, L., & Li, E. (2020). Spurious mode free broadband Green's function technique for periodic scatterers using the combined field integral equation formulation. NEMO 2020 Hangzhou. (*Paper*)

Feng, Z., Gao, R., Bai, X. & Tan, S. (2020). Eigen-analysis of cavity perturbations by combining vector potential electromagnetics with broadband periodic Green's function. NEMO 2020 Hangzhou.

Overcome The Spurious Mode Issue

PEC Crystal Revisit: EFIE, MFIE, CFIE, and the Nyström method

The complementary problem: a linear eigenvalue problem formulation for cavity modes

Nyström/CFIE applied to dielectric crystal

The PEC Scatterer Array, TMz Case: Revisit

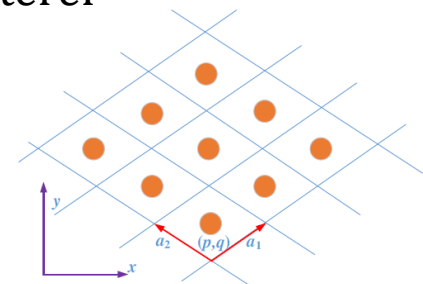
EFIE

$$\int_{S_{00}} dl' \left[g_P(k, \bar{k}_i; \bar{r}, \bar{r}') \frac{\partial \psi(\bar{r}')}{\partial n'} \right] = \begin{cases} \psi(\bar{r}) & \bar{r} \text{ outside scatterer} \\ 0 & \bar{r} \text{ inside scatterer} \end{cases}$$

$$\hat{n} \times \bar{H} = \bar{J} = \frac{1}{-i\omega\mu} \frac{\partial \psi}{\partial n}$$

MFIE

$$\frac{1}{-i\omega\mu} \int_{S_{00}} dl' \left[\frac{\partial g_P(k, \bar{k}_i; \bar{r}, \bar{r}')}{\partial n} \frac{\partial \psi(\bar{r}')}{\partial n'} \right] = \begin{cases} \frac{1}{-i\omega\mu} \frac{\partial \psi(\bar{r})}{\partial n} & \bar{r} \text{ outside scatterer} \\ 0 & \bar{r} \text{ inside scatterer} \end{cases}$$



CFIE

$$\int_{S_{00}} dl' \left[g_P(k, \bar{k}_i; \bar{r}, \bar{r}') + \frac{\eta}{-i\omega\mu} \frac{\partial g_P(k, \bar{k}_i; \bar{r}, \bar{r}')}{\partial n} \right] \frac{\partial \psi(\bar{r}')}{\partial n'} = 0, \quad \bar{r} \rightarrow S^-$$

Convert CFIE into A Linear Eigenvalue Problem

Fix ω in the CFIE combining coefficient

Matrix form of SIEs

$$\begin{array}{ll}
 \text{EFI} & \left[\bar{\bar{B}} + \bar{\bar{R}}(i\xi, \bar{r}) \bar{\bar{W}}(k, i\xi) \bar{\bar{R}}^\dagger(i\xi, \bar{r}') \right] \frac{\partial \bar{\psi}(\bar{r}')}{\partial n'} = \bar{0} \\
 \text{E} & \\
 \text{MFI} & \left[\bar{\bar{A}} + \bar{\bar{Q}}(i\xi, \bar{r}) \bar{\bar{W}}(k, i\xi) \bar{\bar{R}}^\dagger(i\xi, \bar{r}') \right] \frac{\partial \bar{\psi}(\bar{r}')}{\partial n'} = \bar{0} \\
 \text{E} & \\
 \text{CFI} & \left[\bar{\bar{B}} + \bar{\bar{R}}(i\xi, \bar{r}) \bar{\bar{W}}(k, i\xi) \bar{\bar{R}}^\dagger(i\xi, \bar{r}') + \frac{\eta}{-i\omega\mu} \bar{\bar{A}} \right. \\
 \text{E} & \left. + \frac{\eta}{-i\omega\mu} \bar{\bar{Q}}(i\xi, \bar{r}) \bar{\bar{W}}(k, i\xi) \bar{\bar{R}}^\dagger(i\xi, \bar{r}') \right] \frac{\partial \bar{\psi}(\bar{r}')}{\partial n'} = \bar{0}
 \end{array}$$

Define

$$\begin{aligned}
 \bar{b} &= \bar{\bar{W}}(k, i\xi) \bar{\bar{R}}^\dagger(i\xi, \bar{r}') \frac{\partial \bar{\psi}(\bar{r}')}{\partial n'} \\
 &= [\lambda(i\xi, k) - \bar{\bar{D}}(i\xi)] \bar{b} \\
 &= \bar{\bar{R}}^\dagger(i\xi, \bar{r}') \frac{\partial \bar{\psi}(\bar{r}')}{\partial n'}
 \end{aligned}$$

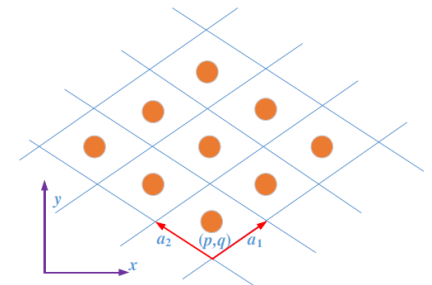
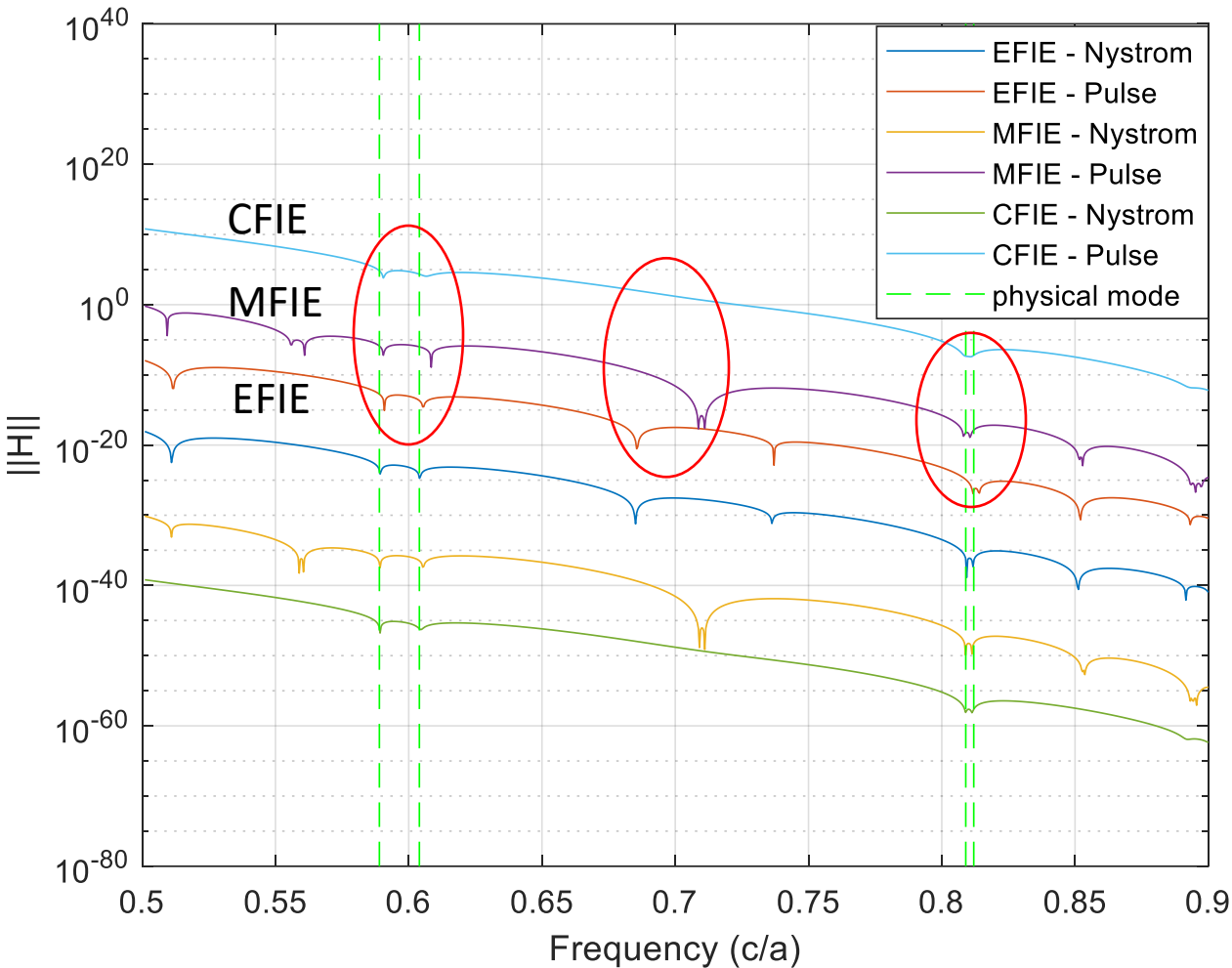

 Eliminating $\frac{\partial \bar{\psi}(\bar{r}')}{\partial n'}$
 $\bar{\bar{P}}\bar{b} = \lambda\bar{b}$

Eigenvalue problem
(EVP)

$$\bar{\bar{P}} = \bar{\bar{D}} - \bar{\bar{R}}^\dagger(i\xi, \bar{r}') \left[\bar{\bar{B}} + \frac{\eta}{i\omega\mu_0} \bar{\bar{A}} \right]^{-1} \left[\bar{\bar{R}}(i\xi, \bar{r}) + \frac{\eta}{-i\omega\mu_0} \bar{\bar{Q}}(i\xi, \bar{r}) \right]$$

EFIE, MFIE, and CFIE Results with Pulse Basis

$$r = 0.4a \quad \bar{k}_b = 0.1\bar{b}_1 + 0.05\bar{b}_2$$



- Dips in $\|H\|$ is consistent with real eigenvalues
- Both EFIE and MFIE yield spurious modes
- EFIE and MFIE with pulse basis are not accurate enough to capture the physical modes.
- CFIE with pulse basis yields promising yet degraded results.

Apply Nyström Method to Improve Accuracy

$$\int_{S_{00}} dl' \left[g_P(k, \bar{k}_i; \bar{r}, \bar{r}') \frac{\partial \psi(\bar{r}')}{\partial n'} \right] = \sum_{p \in near S_p} \int dl' \left[g_P(k, \bar{k}_i; \bar{r}, \bar{r}') \frac{\partial \psi(\bar{r}')}{\partial n'} \right] + \sum_{p \in far S_p} \int dl' \left[g_P(k, \bar{k}_i; \bar{r}, \bar{r}') \frac{\partial \psi(\bar{r}')}{\partial n'} \right]$$

Gaussian-Legendre quadrature to compute integral of **far region**

$$\int_{S_p} dl' \left[g_P(k, \bar{k}_i; \bar{r}, \bar{r}') \frac{\partial \psi(\bar{r}')}{\partial n'} \right] = \frac{\Delta t}{2} \sum_{q=1}^{N_q} \omega_q g_P(k, \bar{k}_i; \bar{r}, \bar{r}'_q) \frac{\partial \psi(\bar{r}'_q)}{\partial n'}$$

Local correction for near region

$$\int_{S_p} dl' \left[g_P(k, \bar{k}_i; \bar{r}, \bar{r}') f_k(\bar{r}') \right] = \sum_{q=1}^{N_q} \tilde{\omega}_q f_k(\bar{r}'_q)$$

$$\tilde{\omega} = [\bar{L}]^{-1} \bar{\kappa}$$

$$[\bar{L}]_{k,q} = f_k(\bar{r}_q) \quad [\bar{\kappa}]_k = \int_{S_p} dl' \left[g_P(k, \bar{k}_i; \bar{r}, \bar{r}') f_k(\bar{r}') \right]$$

$$\frac{\partial \psi(\bar{r}')}{\partial n'} = \sum_{k=1}^{N_k} b_k f_k(\bar{r}')$$

$f_k(t)$ commonly taken as Gaussian-Legendre polynomials

$$\int_{S_p} dl' \left[g_P(k, \bar{k}_i; \bar{r}, \bar{r}') \frac{\partial \psi(\bar{r}')}{\partial n'} \right] = \int_{S_p} dl' \left[g_P(k, \bar{k}_i; \bar{r}, \bar{r}') \sum_{k=1}^{N_k} b_k f_k(\bar{r}') \right]$$

$$= \sum_{k=1}^{N_k} b_k \int_{S_p} dl' \left[g_P(k, \bar{k}_i; \bar{r}, \bar{r}') f_k(\bar{r}') \right] = \sum_{k=1}^{N_k} b_k \sum_{q=1}^{N_q} \tilde{\omega}_q f_k(\bar{r}'_q)$$

$$= \sum_{q=1}^{N_q} \tilde{\omega}_q \sum_{k=1}^{N_k} b_k f_k(\bar{r}'_q) = \sum_{q=1}^{N_q} \tilde{\omega}_q \frac{\partial \psi(\bar{r}'_q)}{\partial n'}$$

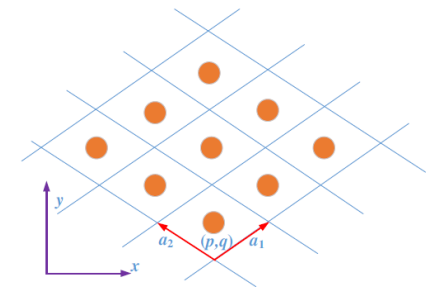
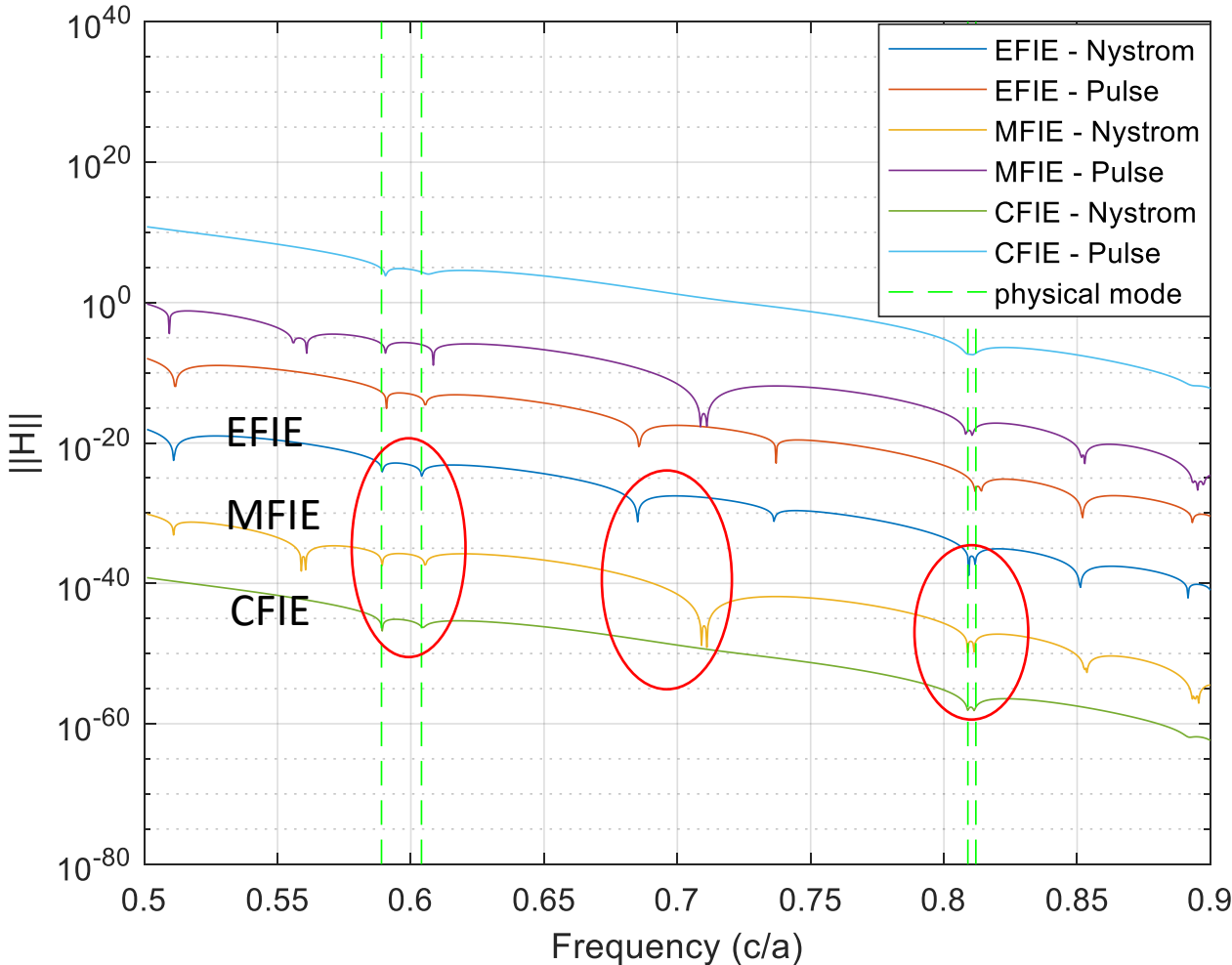
N_q : Number of quadrature points

N_k : Number of Legendre polynomial

$$N_q = N_k$$

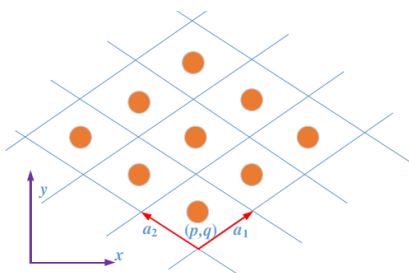
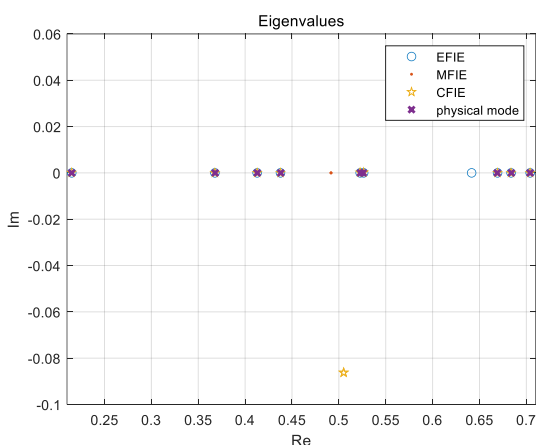
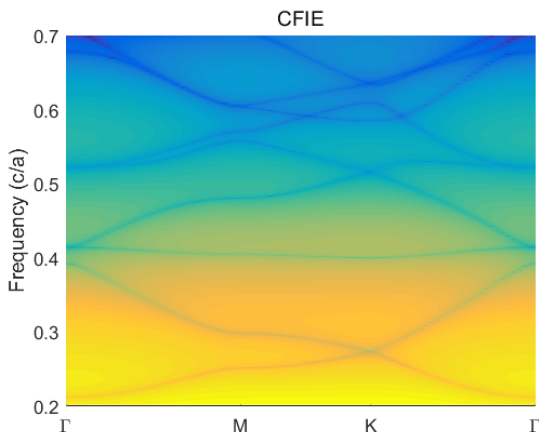
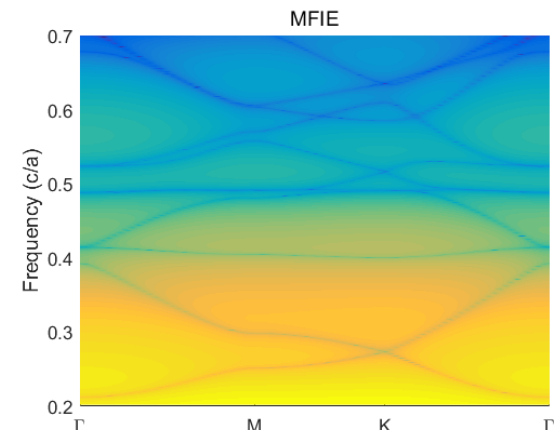
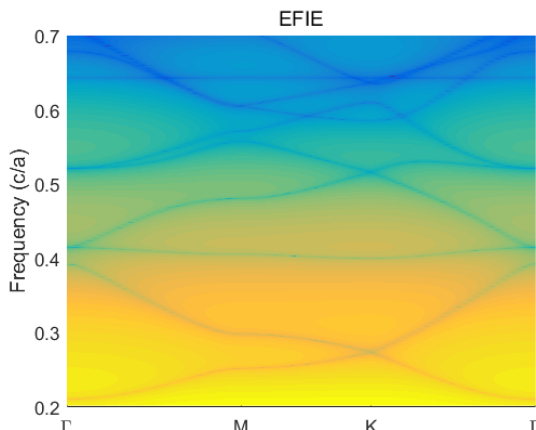
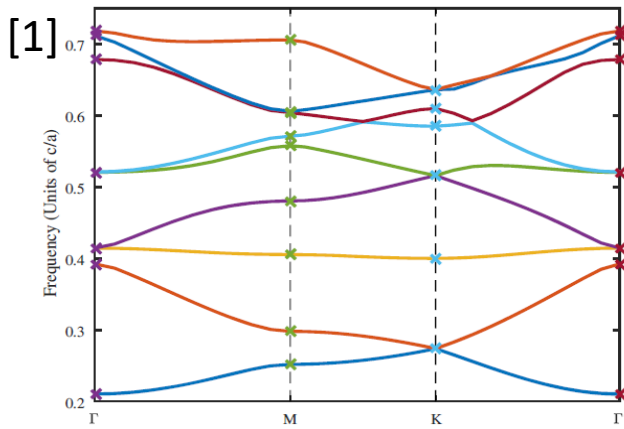
EFIE, MFIE, and CFIE Results: Nystrom Method

$$r = 0.4a \quad \bar{k}_b = 0.1\bar{b}_1 + 0.05\bar{b}_2$$



- Nystrom method significantly improves the accuracy of EFIE, MFIE, and CFIE.
- CFIE with Nystrom method effectively rejects spurious modes on real axis

Band Diagrams with EFIE, MFIE, and CFIE

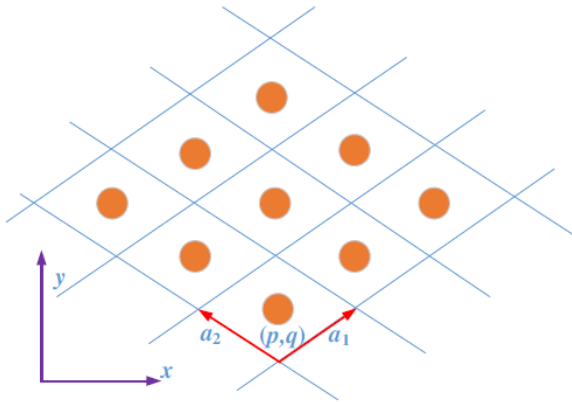


$$r = 0.2a \quad \bar{k}_b = 0.1\bar{b}_1 + 0.05\bar{b}_2$$

- CFIE with Nystrom method effectively rejects spurious modes on real axis
- With CFIE/Nystrom, all eigenvalues lying on real axis are physical

The Complementary Internal Resonance Problem

The photonic band problem



EFIE:

$$\int_{S_{00}} dl' \left[g_P(k, \bar{k}_i; \bar{r}, \bar{r}') \frac{\partial \psi(\bar{r}')}{\partial n'} \right] = 0, \quad \bar{r} \rightarrow S^-$$

MFIE:

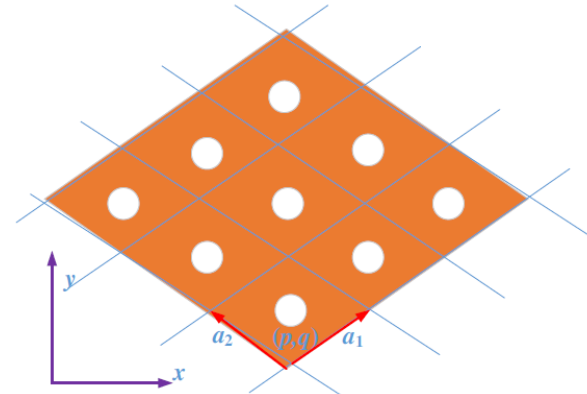
$$\frac{1}{-i\omega\mu} \int_{S_{00}} dl' \left[\frac{\partial g_P(k, \bar{k}_i; \bar{r}, \bar{r}')}{\partial n} \frac{\partial \psi(\bar{r}')}{\partial n'} \right] = 0, \quad \bar{r} \rightarrow S^-$$

CFIE:

$$\int_{S_{00}} dl' \left[g_P(k, \bar{k}_i; \bar{r}, \bar{r}') + \frac{\eta}{-i\omega\mu} \frac{\partial g_P(k, \bar{k}_i; \bar{r}, \bar{r}')}{\partial n} \right] \frac{\partial \psi(\bar{r}')}{\partial n'} = 0$$

\bar{r} approaches surface from inside

The cavity resonance problem



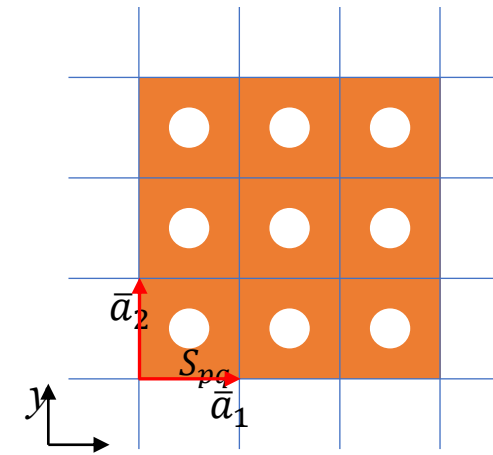
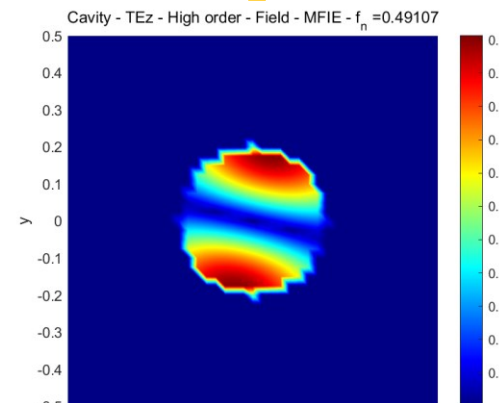
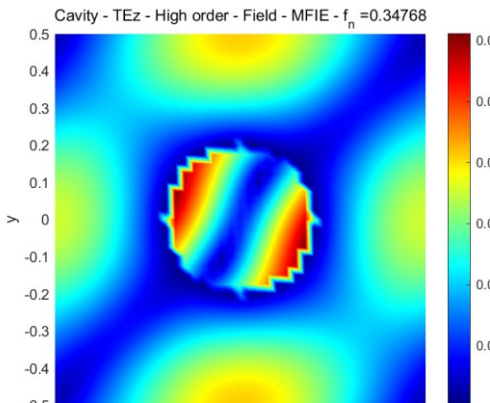
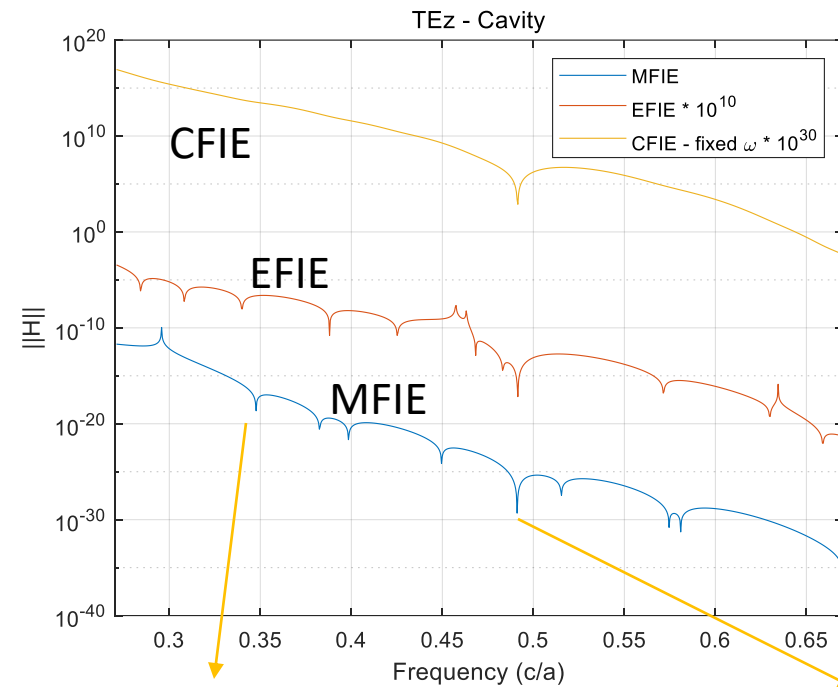
$$\int_{S_{00}} dl' \left[g_P(k, \bar{k}_i; \bar{r}, \bar{r}') \frac{\partial \psi(\bar{r}')}{\partial n'} \right] = 0, \quad \bar{r} \rightarrow S^+$$

$$\frac{1}{-i\omega\mu} \int_{S_{00}} dl' \left[\frac{\partial g_P(k, \bar{k}_i; \bar{r}, \bar{r}')}{\partial n} \frac{\partial \psi(\bar{r}')}{\partial n'} \right] = 0, \quad \bar{r} \rightarrow S^+$$

$$\int_{S_{00}} dl' \left[g_P(k, \bar{k}_i; \bar{r}, \bar{r}') + \frac{\eta}{-i\omega\mu} \frac{\partial g_P(k, \bar{k}_i; \bar{r}, \bar{r}')}{\partial n} \right] \frac{\partial \psi(\bar{r}')}{\partial n'} = 0$$

\bar{r} approaches surface from outside

One Stone, Two Birds: CFIE/Nystrom Also Predicts Accurately The Cavity Modes



$$r = 0.2a \quad \bar{k}_b = 0.1\bar{b}_1 + 0.05\bar{b}_2$$

- CFIE/Nystrom yields the physical cavity modes on real axis
- Physical modes satisfy the extinction theorem.

CFIE/Nystrom Applied to Dielectric Crystals: BGF with High-order Extraction Yields A Non-linear Eigenvalue Problem

EFIE:

$$\int_{S_{00}} d\bar{\rho}' \left[\psi_0(\bar{\rho}') \frac{\partial g_P^0}{\partial n'} - g_P^0 \frac{\partial \psi_0(\bar{\rho}')}{\partial n'} \right] = 0, \quad \bar{\rho} \rightarrow 0^-$$

$$\int_{S_{00}} d\bar{\rho}' \left[\psi_0(\bar{\rho}') \frac{\partial g_P^1}{\partial n'} - \frac{\mu_1}{\mu_0} g_P^1 \frac{\partial \psi_0(\bar{\rho}')}{\partial n'} \right] = 0, \quad \bar{\rho} \rightarrow 0^+$$

MFIE:

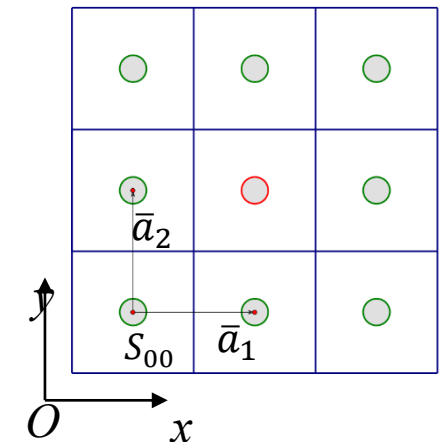
$$\int_{S_{00}} d\bar{\rho}' \left[\psi_0(\bar{\rho}') \frac{\partial^2}{\partial n \partial n'} g_P^0 - \frac{\partial}{\partial n} g_P^0 u_0(\bar{\rho}') \right] = 0, \quad \bar{\rho} \rightarrow 0^-$$

$$\int_{S_{00}} d\bar{\rho}' \left[\psi_0(\bar{\rho}') \frac{\partial^2}{\partial n \partial n'} g_P^1 - \frac{\mu_1}{\mu_0} \frac{\partial}{\partial n} g_P^1 u_0(\bar{\rho}') \right] = 0, \quad \bar{\rho} \rightarrow 0^+$$

CFIE:

$$\int_{S_{00}} d\bar{\rho}' \left[\psi_0(\bar{\rho}') \frac{\partial g_P^0}{\partial n'} - g_P^0 \frac{\partial \psi_0(\bar{\rho}')}{\partial n'} \right] + \frac{\eta_0}{-i\omega\mu_0} \int_{S_{00}} d\bar{\rho}' \left[\psi_0(\bar{\rho}') \frac{\partial^2}{\partial n \partial n'} g_P^0 - \frac{\partial}{\partial n} g_P^0 u_0(\bar{\rho}') \right] = 0$$

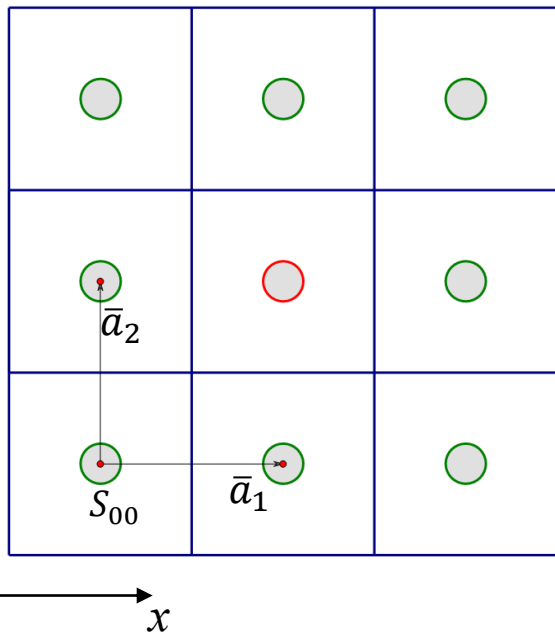
$$\int_{S_{00}} d\bar{\rho}' \left[\psi_0(\bar{\rho}') \frac{\partial g_P^1}{\partial n'} - \frac{\mu_1}{\mu_0} g_P^1 \frac{\partial \psi_0(\bar{\rho}')}{\partial n'} \right] + \frac{\eta_1}{-i\omega\mu_1} \int_{S_{00}} d\bar{\rho}' \left[\psi_0(\bar{\rho}') \frac{\partial^2}{\partial n \partial n'} g_P^1 - \frac{\mu_1}{\mu_0} \frac{\partial}{\partial n} g_P^1 u_0(\bar{\rho}') \right] = 0$$



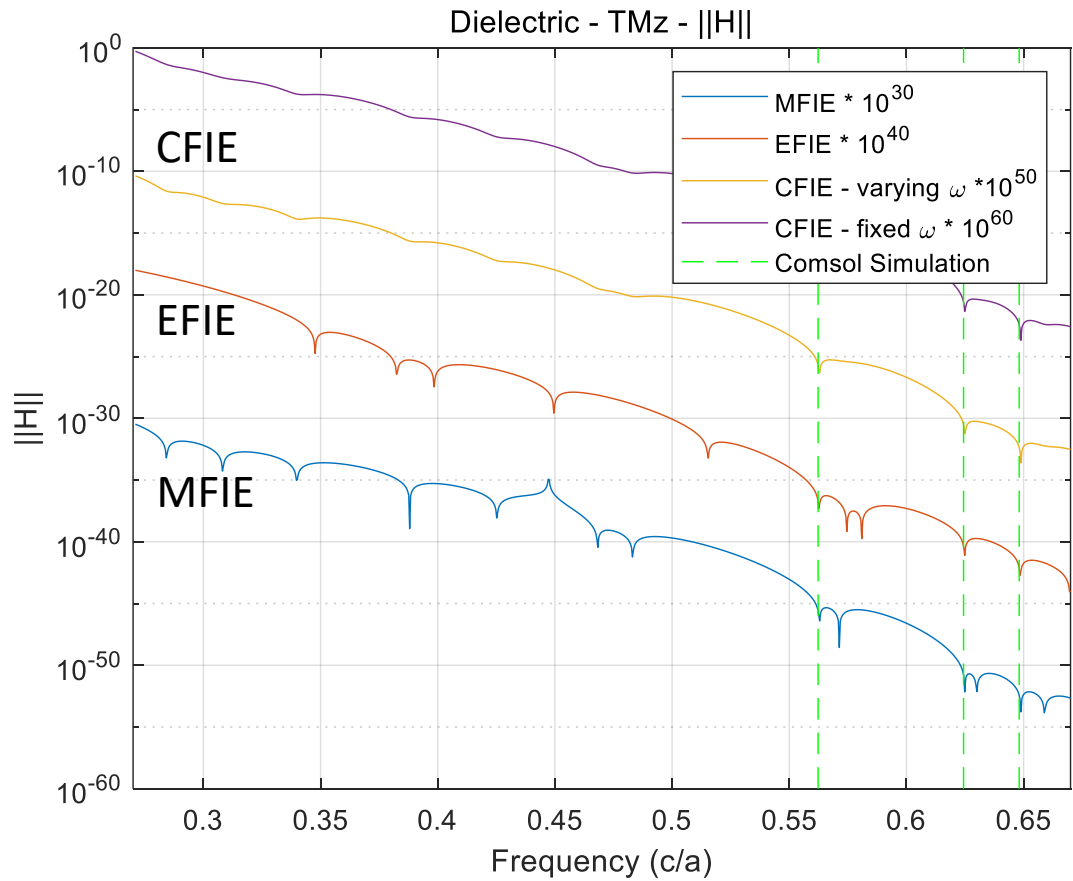
Necessity to apply BGF with high-order extraction:

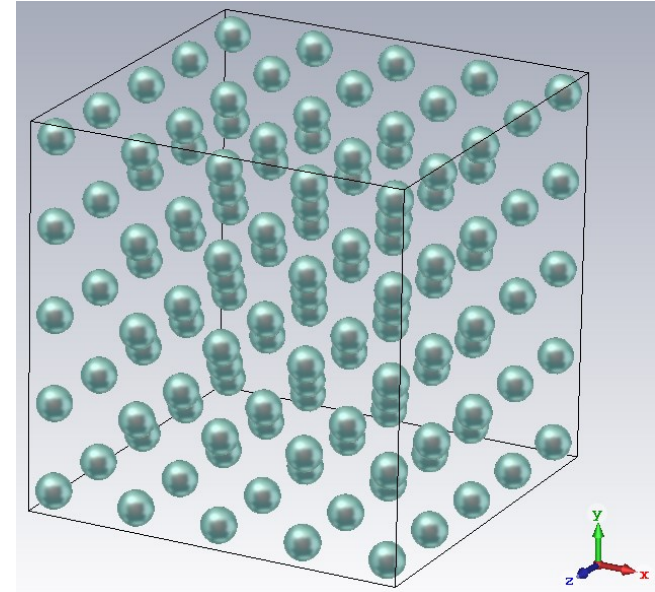
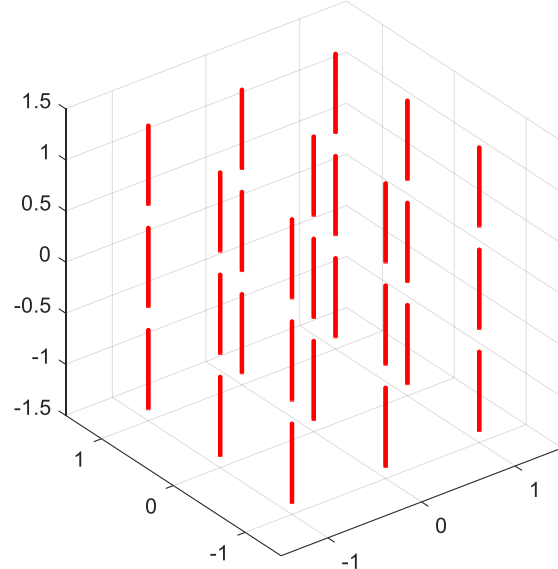
Dielectric Crystal: CFIE/Nystrom Effectively Rejects Spurious Modes on Real Frequencies

$$r = 0.2a \quad \bar{k}_b = 0.1\bar{b}_1 + 0.05\bar{b}_2$$



Background: air
 Scatterer: $\mu_r = 1 \quad \varepsilon_r = 8.9$





Broadband Green's Function in 3D Problems with 3D Periodicity

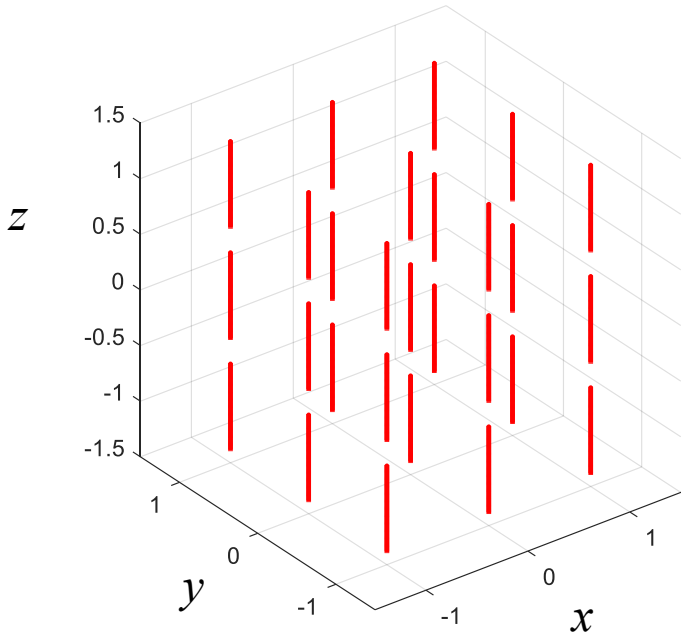
A simple case: wire medium

A generalized case: 3D scatterers

Nonlinear vs. Linear Eigenvalue Problem Formulation

Tan, S., & Tsang, L. (2017). Broadband Green's Function with Low Wavenumber Extraction (BBGFL) in 3D Vector Wave Equations Applied to Arbitrary Wire Medium Characterization. PIERS 2017 Singapore.

Band Structure of The Wire Medium Using A Line Integral (3D Demonstration)



❖ Thin wire approximation

$$\bar{J}(\bar{r}) = \hat{z} J_z(\rho = r_0, \phi, z) = \frac{I_z(z)}{2\pi r_0}$$

❖ Enforce $E_z^S(\bar{r}) = 0$ at the axis of the wires

$$0 = -\frac{1}{i\omega\epsilon} \int_{(0)} dz' I_z(z') \left(k^2 + \frac{\partial^2}{\partial z^2} \right) \tilde{g}_P(\bar{k}_i, k; z, z')$$

$$\tilde{g}_P(\bar{k}_i, k; z, z') = \frac{1}{2\pi} \int_0^{2\pi} d\phi' g_P(\bar{k}_i, k; \bar{r}, \vec{r}') \Big|_{\rho=0, \rho'=r_0}$$

❖ Demonstration of 3D vector wave interactions using 1 scalar equation

$$\left(1 + \frac{1}{k^2} \frac{\partial^2}{\partial z^2} \right) \tilde{g}_P = \hat{z} \cdot \left(\bar{\bar{I}} + \frac{\nabla \nabla}{k^2} \right) \tilde{g}_P \cdot \hat{z}$$

High-Order BGF Applied to Wire Media Characterization

□ Line Integral Equation

$$0 = -\frac{1}{i\omega\epsilon} \int_{(0)} dz' I_z(z') \left(k^2 + \frac{\partial^2}{\partial z^2} \right) \tilde{g}_P(\bar{k}_i, k; z, z')$$

$\partial^2/\partial z^2$ slows down the convergence rate

□ The high order BGF representation with $k_L = 0$

$$\tilde{g}_P(k) = \tilde{g}_P(0) + (k^2) \left[\frac{1}{2} \frac{d^2 \tilde{g}_P(k)}{dk^2} \Big|_{k=0} \right] + \frac{1}{\Omega} \sum_{\alpha} \frac{k^4}{(|\bar{k}_{i,\alpha}|^2 - k^2) |\bar{k}_{i,\alpha}|^4} \exp(ik_z^{i\alpha}(z-z')) J_0(|\bar{k}_{\rho}^{i\alpha}| r_0)$$

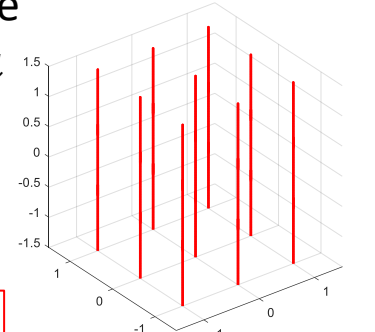
✓ converge up to $1/|\bar{k}_{i,\alpha}|^6$

✓ Possible for further improvement

Connected Wire Medium

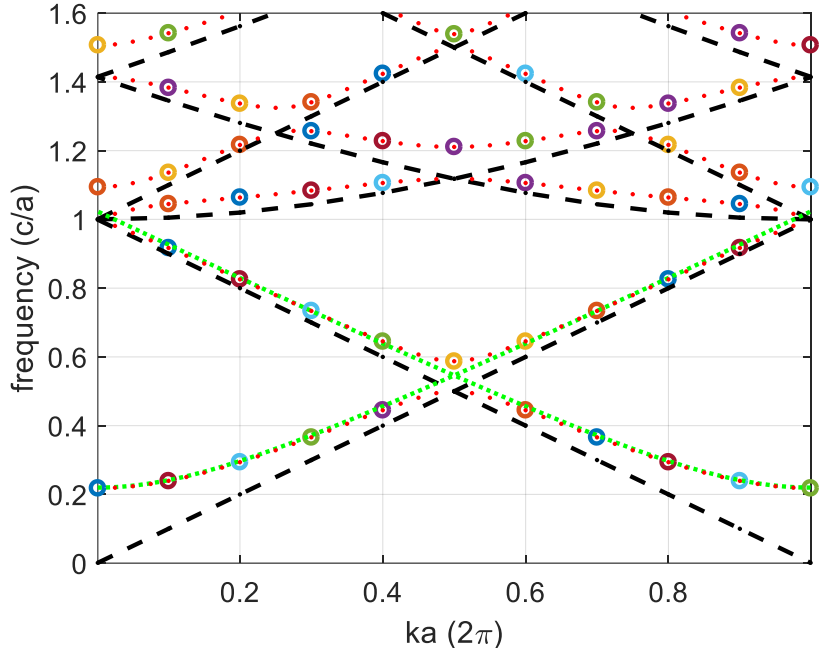
Cubic lattice

$$L \geq a$$



$$r_0 = 0.01a$$

$$0 = Ak^2 + B + Ck^4 + Dk^2 + \frac{a}{\Omega} k^4 \sum_{\alpha} \frac{k^2 - (k_z^{i\alpha})^2}{(\bar{k}_{i\alpha}^2 - k^2) |\bar{k}_{i\alpha}|^4} J_0(|\bar{k}_{i\alpha}| r_0) \sin c((k_{iz} - k_z^{i\alpha}) a / 2)$$



- Good agreements with plasma homogenization for the lowest band
- Agree with Belov's results for higher bands
- Extendable to arbitrary wire media

Circles: BBGFL;
Red dots: Belov et al. 2002
Green dots: Homogenization
Black dash: $k = |\bar{k}_{i\alpha}|$

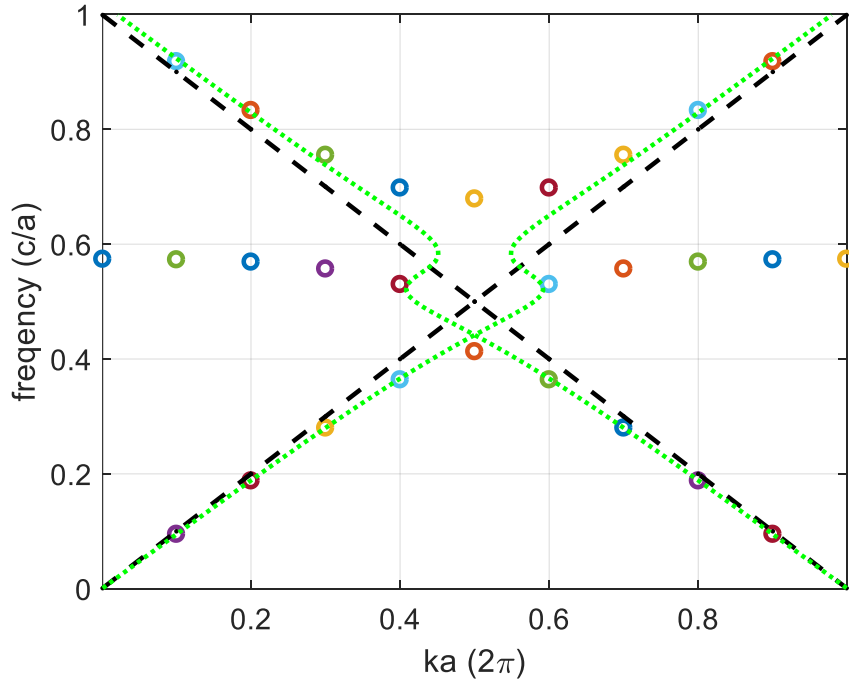
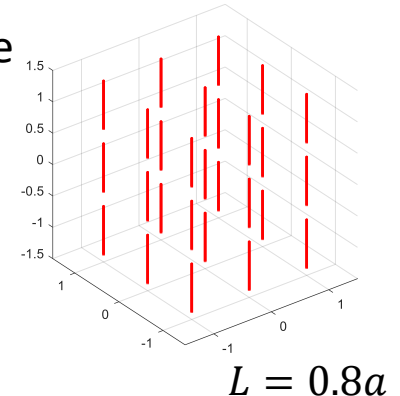
Disconnected Wire Medium

$$I_z(z') = \sum_{n=1}^N I_n p_n(z')$$

$$\lambda \bar{b} = \bar{\bar{D}} \left(\bar{\bar{I}} - \frac{1}{\lambda} \bar{\bar{R}}^\dagger \left[\bar{\bar{S}} + \frac{1}{\lambda} \left(\bar{\bar{L}} + \bar{\bar{S}}_d \right) + \frac{1}{\lambda^2} \bar{\bar{L}}_d \right]^{-1} \bar{\bar{R}} \left(\frac{1}{\lambda} \bar{\bar{I}} - \bar{\bar{T}} \right) \right) \bar{b}$$

Cubic lattice
 $L < a$

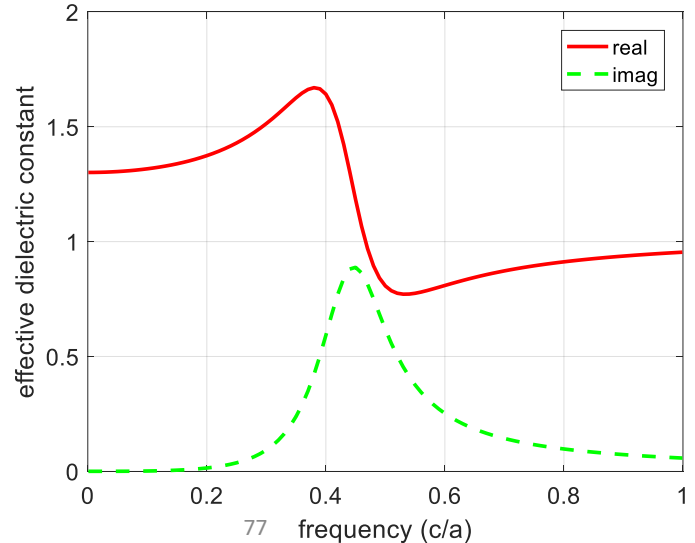
$$\lambda = \frac{1}{k^2}$$



- Distinct behavior from continuous wire medium
- Good agreements with Foldy's Approximation in the lowest band except at resonance
- BGF predicts an extra band

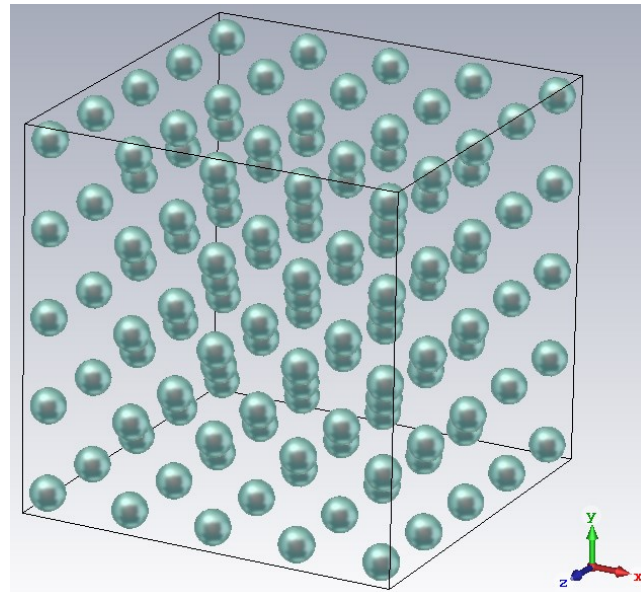
Effective Permittivity from Foldy's Approximation

$$k_{eff} = k + n_0 \frac{2\pi}{k} \langle f(\hat{k}_i; \hat{k}_i) \rangle$$



Feng, Z. & Tan, S. (2020). Band calculation of 3D periodic scatterers using broadband dyadic Green's function of vector potential A. NEMO 2020 Hangzhou.

Feng, Z. & Tan, S. (2020). Efficient band characterization of 3D periodic scatterers using broadband dyadic Green's function of vector potential A. APS/URSI 2020 Montréal. (*Paper*)



Broadband Green's Function in 3D Problems with 3D Periodicity

The $A\text{-}\Phi$ formulation

Nonlinear vs. Linear Eigenvalue Problem Formulation

E-H formulation vs. A- ϕ formulation

E-H formulation

Maxwell
equation

$$\nabla \times \bar{E} = i\omega\mu\bar{H}$$

$$\nabla \times \bar{H} = -i\omega\epsilon\bar{E} + \bar{J}$$

$$\nabla \cdot \bar{D} = \rho$$

$$\nabla \cdot \bar{B} = 0$$

Boundary
condition

$$\hat{n} \times (\bar{E}_1 - \bar{E}_0) = 0$$

$$\hat{n} \times (\bar{H}_1 - \bar{H}_0) = 0$$

$$\hat{n} \cdot (\bar{B}_1 - \bar{B}_0) = 0$$

$$\hat{n} \cdot (\bar{D}_1 - \bar{D}_0) = 0$$

Wave
equation

$$\nabla \times \nabla \times \bar{E} - \omega^2\mu\epsilon\bar{E} = i\omega\mu\bar{J}$$

$$\nabla \times \nabla \times \bar{H} - \omega^2\mu\epsilon\bar{H} = \nabla \times \bar{J}$$

A- ϕ formulation

$$\begin{aligned}\bar{E} &= i\omega\bar{A} - \nabla\phi \\ \bar{B} &= \nabla \times \bar{A}\end{aligned}$$

$$\nabla \times (i\omega\bar{A} - \nabla\phi) = i\omega(\nabla \times \bar{A})$$

$$\nabla \times (\nabla \times \bar{A}) = -i\omega\epsilon\mu(i\omega\bar{A} - \nabla\phi) + \mu\bar{J}$$

$$\nabla \cdot (i\omega\bar{A} - \nabla\phi) = \frac{\rho}{\epsilon}$$

$$\nabla \cdot (\nabla \times \bar{A}) = 0$$

$$\hat{n} \times [(i\omega\bar{A}_1 - \nabla\phi_1) - (i\omega\bar{A}_0 - \nabla\phi_0)] = 0$$

$$\hat{n} \times \left[\frac{(\nabla \times \bar{A}_1)}{\mu_1} - \frac{(\nabla \times \bar{A}_0)}{\mu_0} \right] = 0$$

$$\hat{n} \cdot [(\nabla \times \bar{A}_1) - (\nabla \times \bar{A}_0)] = 0$$

$$\hat{n} \cdot [\epsilon_1(i\omega\bar{A}_1 - \nabla\phi_1) - \epsilon_0(i\omega\bar{A}_0 - \nabla\phi_0)] = 0$$

$$\nabla \cdot \bar{A} = i\omega\mu\epsilon\phi \quad \text{Lorentz gauge}$$

$$\nabla^2\phi + k^2\phi = -\frac{\rho}{\epsilon}$$

$$\nabla \times \nabla \times \bar{A} - \nabla \nabla \cdot \bar{A} - k^2\bar{A} = \mu\bar{J}$$

3D periodic structure: Dyadic Green's Function in EFIE

For source free region

$$\begin{aligned} \nabla \times \nabla \times \bar{E} - \omega^2 \mu \epsilon \bar{E} &= \bar{0} \\ \nabla \times \nabla \times \bar{\bar{G}}(\bar{r}, \bar{r}') - \omega^2 \mu \epsilon \bar{\bar{G}}(\bar{r}, \bar{r}') &= \bar{I}\delta(\bar{r} - \bar{r}') \\ &\downarrow \\ \bar{E} &= i\omega\mu \int d\bar{r}' \bar{\bar{G}}(\bar{r}, \bar{r}') \cdot \bar{J}(\bar{r}') \\ \bar{\bar{G}}(\bar{r}, \bar{r}') &= \left(\bar{I} + \frac{1}{k^2} \cancel{\nabla \nabla} \right) g_P(\bar{r}, \bar{r}') \end{aligned}$$

$$g_P^0(k, \bar{k}_i; \bar{\rho}, \bar{\rho}') = \sum_{\bar{R}} g^0(i\xi; \bar{\rho}, \bar{\rho}' + \bar{R}) \exp(i\bar{k}_i \cdot \bar{R}) + \sum_{\bar{K}} \frac{1}{\frac{1}{k^2 + \xi^2} - \frac{1}{|\bar{K}|^2 + \xi^2}} \frac{\exp(i\bar{K} \cdot (\bar{\rho} - \bar{\rho}'))}{(|\bar{K}|^2 + \xi^2)^2} \Omega$$

Due to the $\frac{\nabla \nabla}{k^2}$ operator, the E-H formulation leads to

1. Nonlinear eigenvalue problem;
2. Poor convergence.

The disadvantage will disappear in A- ϕ formulation.

The A-Φ Formulation: Green's Function and Extinction Theorem

Wave function of magnetic vector potential \bar{A}

$$\nabla \times \nabla \times \bar{A}(\bar{r}) - \nabla \nabla \cdot \bar{A}(\bar{r}) - k^2 \bar{A}(\bar{r}) = \mu \bar{J}(\bar{r})$$

Define Dyadic Green's function

$$\nabla \times \nabla \times \bar{\bar{G}}_A(\bar{r}, \bar{r}') - \nabla \nabla \cdot \bar{\bar{G}}_A(\bar{r}, \bar{r}') - k^2 \bar{\bar{G}}_A(\bar{r}, \bar{r}') = \bar{\bar{I}}\delta(\bar{r} - \bar{r}')$$

$$\boxed{\bar{\bar{G}}_A(\bar{r}, \bar{r}') = \bar{\bar{I}}g(\bar{r}, \bar{r}')}}$$

$$\nabla^2 g(\bar{r}, \bar{r}') + k^2 g(\bar{r}, \bar{r}') = -\delta(\bar{r} - \bar{r}')$$

$$\bar{A}_{inc}(\bar{r}) + \iint_S dS' \left[\mu g(\bar{r}, \bar{r}') \hat{n}' \times \bar{H}(\bar{r}') - \nabla' g(\bar{r}, \bar{r}') \times \hat{n}' \times \bar{A}(\bar{r}') \right]$$

$$\xrightarrow{\hspace{1cm}} + \iint_S dS' \left[-\hat{n}' g(\bar{r}, \bar{r}') \nabla' \cdot \bar{A}(\bar{r}') + \nabla' g(\bar{r}, \bar{r}') \hat{n}' \cdot \bar{A}(\bar{r}') \right] = \begin{cases} \bar{A}(\bar{r}) & \bar{r} \text{ is outside scatterer} \\ 0 & \bar{r} \text{ is inside scatterer} \end{cases}$$

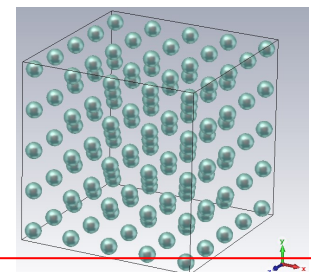
For PEC scatterers (electric potential $\varphi = 0$ on PEC surface)

Boundary condition

$$\hat{n} \times \bar{A}(\bar{r}) = 0$$

Lorentz gauge

$$\nabla \cdot \bar{A}(\bar{r}) = i\omega \epsilon \mu \phi = 0$$



$$\xrightarrow{\hspace{1cm}} \bar{A}_{inc}(\bar{r}) + \iint_S dS' \mu g(\bar{r}, \bar{r}') \hat{n}' \times \bar{H}(\bar{r}') + \iint_S dS' \nabla' g(\bar{r}, \bar{r}') \hat{n}' \cdot \bar{A}(\bar{r}') = \begin{cases} \bar{A}(\bar{r}) & \bar{r} \text{ is outside scatterer} \\ 0 & \bar{r} \text{ is inside scatterer} \end{cases}$$

The A-Φ Formulation: Surface Integral Equation

Extinction theorem of A

$$\iint_{S_{000}} dS' \mu g_P(k, \bar{k}_i; \bar{r}, \bar{r}') \hat{n}' \times \bar{H}(\bar{r}') + \iint_{S_{000}} dS' \nabla' g_P(k, \bar{k}_i; \bar{r}, \bar{r}') \hat{n}' \cdot \bar{A}(\bar{r}') \\ = \begin{cases} \bar{A}(\bar{r}) & \bar{r} \text{ is outside scatterer} \\ 0 & \bar{r} \text{ is inside scatterer} \end{cases}$$

Since

$$\bar{J}_s = \hat{n} \times \bar{H}$$

$$\sigma(\bar{r}') = \hat{n}' \cdot \bar{A}(\bar{r}')$$

Surface integral equation

$$\iint_{\substack{S_{000} \\ \bar{r} \rightarrow S^-}} dS' \mu g_P(k, \bar{k}_i; \bar{r}, \bar{r}') \bar{J}_s(\bar{r}') + \iint_{S_{000}} dS' \nabla' g_P(k, \bar{k}_i; \bar{r}, \bar{r}') \sigma(\bar{r}') = 0,$$

Unknowns: surface current $\bar{J}_s(\bar{r}')$ and charge $\sigma(\bar{r}')$

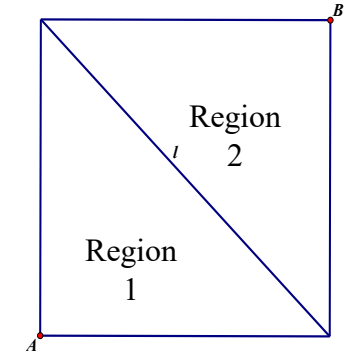
Basis function: RWG Roof-top

Solve SIE with RWG/Roof-Top Basis Functions and The Galerkin method

Represent surface current with RWG basis function

$$\bar{J}(\bar{r}) = \sum_{m=1}^M j_m \bar{J}_m(\bar{r})$$

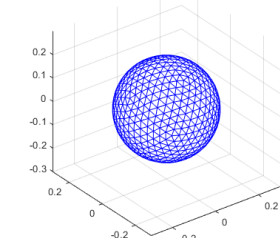
$$\bar{J}_m(\bar{r}) = \begin{cases} \frac{l}{2S_1} (\bar{r} - \bar{r}_A) & \bar{r} \text{ in region 1} \\ \frac{l}{2S_2} (\bar{r}_B - \bar{r}) & \bar{r} \text{ in region 2} \end{cases}$$



Apply Galerkin's method

$$\sum_{m=1}^M \iint_{S_{000}^m} d\bar{r} \bar{J}_m(\bar{r}') \cdot \sum_{n=1}^N \iint_{S_{000}^n} d\bar{r}' \mu g_P(k, \bar{k}_i; \bar{r}, \bar{r}') \bar{J}_n(\bar{r}') j_n + \sum_{m=1}^M \iint_{S_{000}^m} d\bar{r} \bar{J}_m(\bar{r}') \cdot \sum_{n=1}^N \iint_{S_{000}^n} d\bar{r}' s_n \sigma_n(\bar{r}') \nabla' g_P(k, \bar{k}_i; \bar{r}, \bar{r}') = 0$$

$$\sum_{n=1}^N \iint_{S_{000}^n} d\bar{r} \sigma_n \hat{n} \cdot \sum_{m=1}^M \iint_{S_{000}^m} d\bar{r}' \mu g_P(k, \bar{k}_i; \bar{r}, \bar{r}') \bar{J}_n(\bar{r}') j_n + \sum_{m=1}^N \iint_{S_{000}^m} d\bar{r} \sigma_n \hat{n} \cdot \sum_{n=1}^M \iint_{S_{000}^n} d\bar{r}' s_n \sigma_n(\bar{r}') \nabla' g_P(k, \bar{k}_i; \bar{r}, \bar{r}') = 0$$



Apply BGF in 3D SIE

Matrix Form of SIE $\left[\bar{\bar{A}} + \bar{\bar{R}}(i\xi, \bar{r}) \bar{\bar{W}}(k, i\xi) \bar{\bar{R}}^\dagger(i\xi, \bar{r}') \right]_{\bar{J}} + \left[\bar{\bar{B}} + \bar{\bar{R}}(i\xi, \bar{r}) \bar{\bar{W}}(k, i\xi) \bar{\bar{Q}}^\dagger(i\xi, \bar{r}') \right]_{\bar{s}} = \bar{0}$

$$\left[\bar{\bar{C}} + \bar{\bar{V}}(i\xi, \bar{r}) \bar{\bar{W}}(k, i\xi) \bar{\bar{R}}^\dagger(i\xi, \bar{r}') \right]_{\bar{J}} + \left[\bar{\bar{D}} + \bar{\bar{V}}(i\xi, \bar{r}) \bar{\bar{W}}(k, i\xi) \bar{\bar{Q}}^\dagger(i\xi, \bar{r}') \right]_{\bar{s}} = \bar{0}$$

$\bar{\bar{W}}$ is a diagonal matrix

$$[\bar{\bar{W}}(k, i\xi)]_{\alpha\alpha} = \frac{1}{\lambda(i\xi, k) - [\bar{\bar{\Lambda}}(i\xi)]_{\alpha\alpha}}$$

$$[\bar{\bar{R}}(i\xi, \bar{r})]_{m\alpha} = \frac{1}{\sqrt{\Omega}} \iint_{S_{000}^m} d\bar{r} \bar{J}_m(\bar{r}) \frac{\exp(i\bar{k}_\alpha \cdot \bar{r})}{(|\bar{k}_\alpha|^2 + \xi^2)}$$

$$[\bar{\bar{Q}}(i\xi, \bar{r})]_{n\alpha} = \frac{1}{\sqrt{\Omega}} \iint_{S_{000}^n} d\bar{r} \sigma_n(\bar{r})(i\bar{k}_\alpha) \frac{\exp(i\bar{k}_\alpha \cdot \bar{r})}{(|\bar{k}_\alpha|^2 + \xi^2)}$$

$$[\bar{\bar{V}}(i\xi, \bar{r})]_{n\alpha} = \frac{1}{\sqrt{\Omega}} \iint_{S_{000}^n} d\bar{r} \sigma_n(\bar{r}) \hat{n} \frac{\exp(i\bar{k}_\alpha \cdot \bar{r})}{(|\bar{k}_\alpha|^2 + \xi^2)}$$

$\bar{\bar{R}}, \bar{\bar{Q}}$ and $\bar{\bar{V}}$ are related to spectral series of BGF

Convert SIE into A Linear Eigenvalue Problem

Define $\bar{b} = \overline{\overline{W}}(k, i\xi) \bar{R}^\dagger(i\xi, \bar{r}') \mu \bar{j} + \overline{\overline{W}}(k, i\xi) \bar{Q}^\dagger(i\xi, \bar{r}') \bar{s}$



$$[\bar{W}(k, i\xi)]^{-1} \bar{b} = [\lambda(i\xi, k) - \bar{\Lambda}(i\xi)] \bar{b} = \bar{R}^\dagger(i\xi, \bar{r}') \mu \bar{j} + \bar{Q}^\dagger(i\xi, \bar{r}') \bar{s}$$

$$\begin{aligned} & \lambda(i\xi, k) \bar{b} \\ &= \bar{\Lambda}(i\xi) \bar{b} + [\bar{R}^\dagger(i\xi, \bar{r}') \quad \bar{Q}^\dagger(i\xi, \bar{r}')] \begin{bmatrix} \mu \bar{j} \\ \bar{s} \end{bmatrix} \end{aligned}$$

$$\begin{aligned} \overline{\overline{A}} \mu \bar{j} + \overline{\overline{B}} \bar{s} + \overline{\overline{R}}(i\xi, \bar{r}) \bar{b} &= \overline{0} \\ \overline{\overline{C}} \mu \bar{j} + \overline{\overline{D}} \bar{s} + \overline{\overline{V}}(i\xi, \bar{r}) \bar{b} &= \overline{0} \end{aligned}$$


$$\begin{bmatrix} \mu \bar{j} \\ \bar{s} \end{bmatrix} = - \begin{bmatrix} \overline{\overline{A}} & \overline{\overline{B}} \\ \overline{\overline{C}} & \overline{\overline{D}} \end{bmatrix}^{-1} \begin{bmatrix} \overline{\overline{R}}(i\xi, \bar{r}) \\ \overline{\overline{V}}(i\xi, \bar{r}) \end{bmatrix} \bar{b}$$

Linear eigenvalue problem

$$\lambda(i\xi, k) \bar{b} = \bar{P} \bar{b}$$

$$\bar{P} = \bar{\Lambda}(i\xi) - [\bar{R}^\dagger(i\xi, \bar{r}') \quad \bar{Q}^\dagger(i\xi, \bar{r}')] \begin{bmatrix} \overline{\overline{A}} & \overline{\overline{B}} \\ \overline{\overline{C}} & \overline{\overline{D}} \end{bmatrix}^{-1} \begin{bmatrix} \overline{\overline{R}}(i\xi, \bar{r}) \\ \overline{\overline{V}}(i\xi, \bar{r}) \end{bmatrix}$$

Surface Unknowns and Modal Fields

Eigen-frequency from eigenvalue

$$\lambda = \frac{1}{\xi^2 + k^2}$$

Surface unknowns from eigenvector

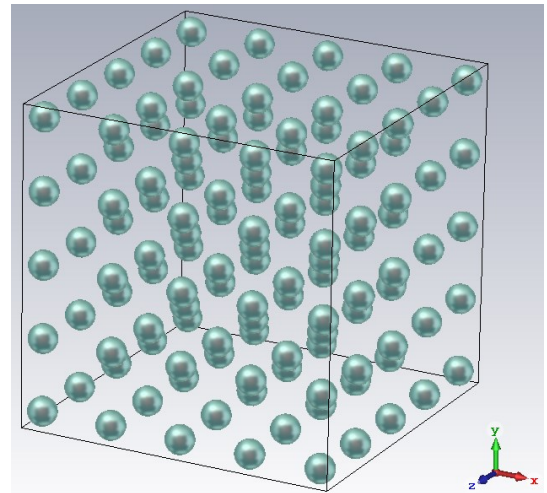
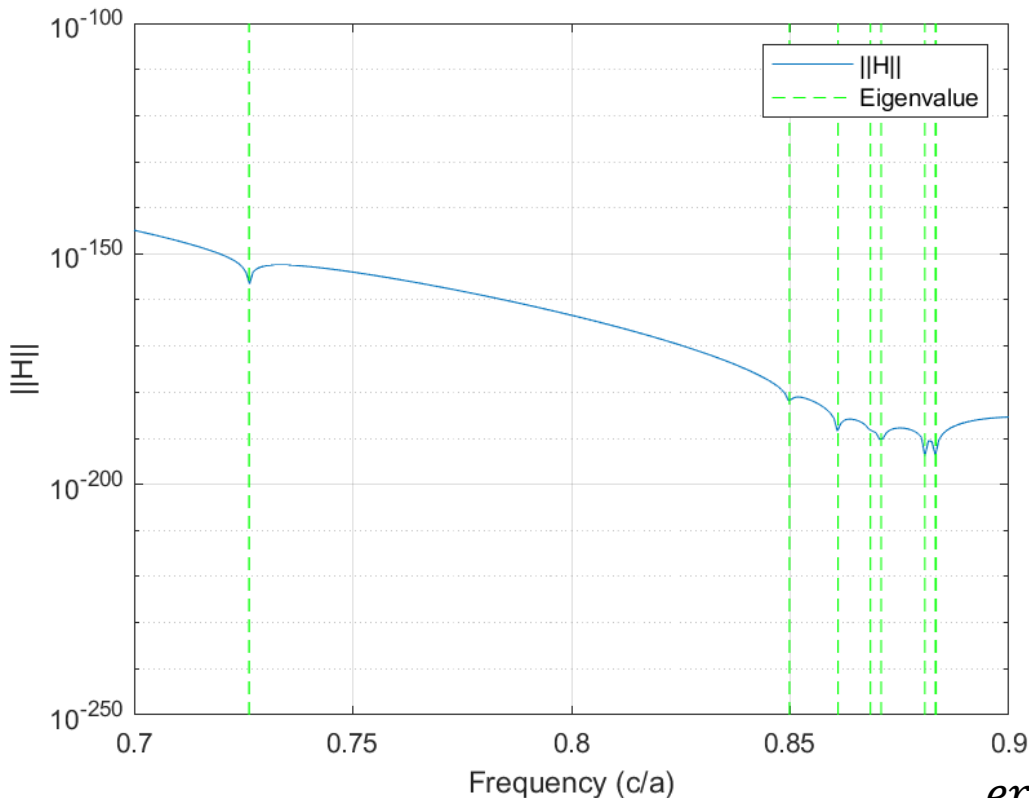
$$\begin{bmatrix} \mu \bar{J} \\ \bar{s} \end{bmatrix} = - \begin{bmatrix} \bar{\bar{A}} & \bar{\bar{B}} \\ \bar{\bar{C}} & \bar{\bar{D}} \end{bmatrix}^{-1} \begin{bmatrix} \bar{\bar{R}}(i\xi, \bar{r}) \\ \bar{\bar{V}}(i\xi, \bar{r}) \end{bmatrix} \bar{b}$$

Computing modal fields

$$\begin{aligned} & \iint_{S_{000}} dS' \mu g_P(k, \bar{k}_i; \bar{r}, \bar{r}') \bar{J}_s(\bar{r}') + \iint_{S_{000}} dS' \nabla' g_P(k, \bar{k}_i; \bar{r}, \bar{r}') \sigma(\bar{r}') \\ &= \begin{cases} \bar{A}(\bar{r}) & \bar{r} \text{ is outside scatterer} \\ 0 & \bar{r} \text{ is inside scatterer} \end{cases} \end{aligned}$$

This equation can also be used to distinguish physical modes from nonphysical modes.

The BGF A-Φ Formulation: Band Results



$$error = \frac{|f_{n,COMSOL} - f_{n,BGF}|}{f_{n,COMSOL}} \times 100\%$$

COMSOL	0.731867	0.846267	0.859433	0.868633	0.952367
BBGF	0.72631	0.84985	0.86093	0.87079	0.96087
Error(%)	0.76%	0.42%	0.17%	0.25%	0.89%

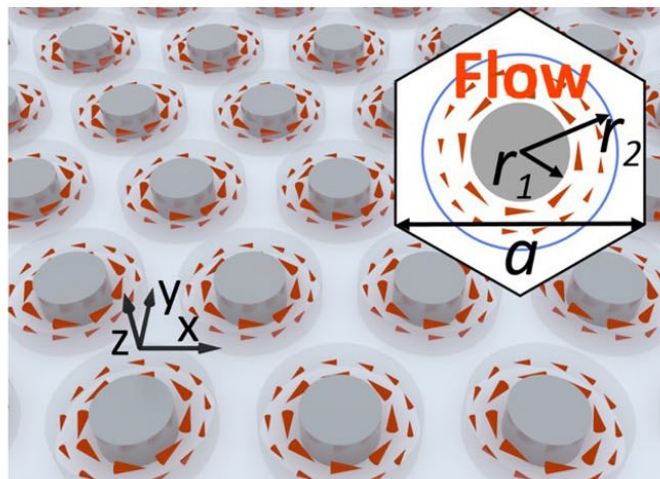
Tan, S., and Tsang, L. (2019). Band structures and modal fields in topological acoustics: an integral formulation. APS/URSI 2019 Atlanta. (*Paper*)

Tan, S., and Tsang, L. (2019). Efficient characterizations of topological acoustics using the broadband Green's function. PIERS 2019 Rome.

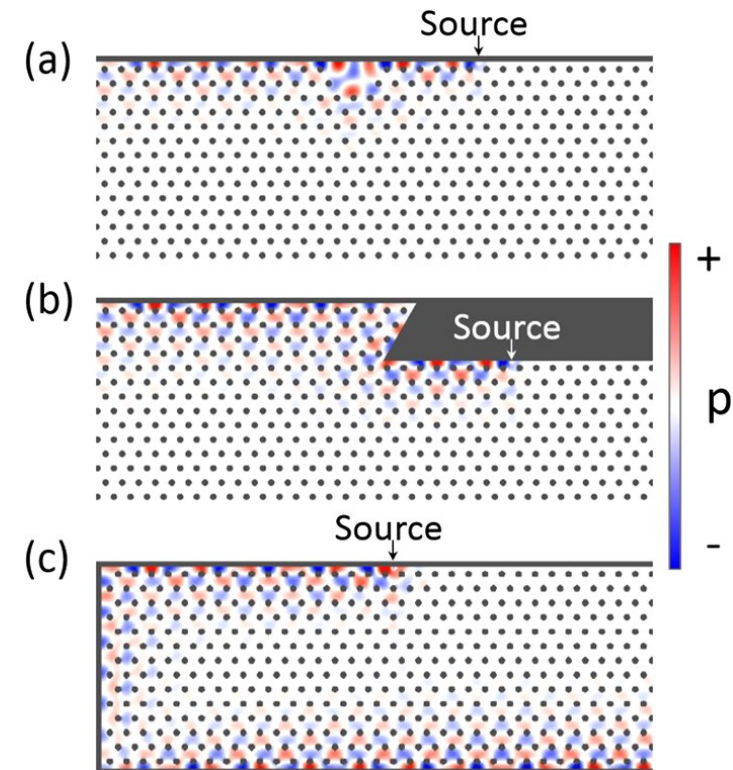
Topological Acoustics

BGF in Combined SIE and VIE

Topological Acoustics



Illustrations courtesy Yang et al. PRL 114: 114301, 2015.



- Rotation induced one-way edge states
- Can apply the broadband method to characterize the band diagram and modal solution

The Governing Wave Equations

- The sound master equation

$$V = \nabla \Phi$$

$$\frac{1}{\rho} \nabla \cdot \rho \nabla \Phi - \left(\frac{\partial}{\partial t} + \bar{v}_0 \cdot \nabla \right) \frac{1}{c^2} \left(\frac{\partial}{\partial t} + \bar{v}_0 \cdot \nabla \right) \Phi = 0$$

- Boundary conditions:

$$\hat{n} \cdot \nabla \Phi = 0, \quad r = r_1$$

$$\Phi, \hat{n} \cdot \nabla \Phi \text{ continuous at } r = r_2$$

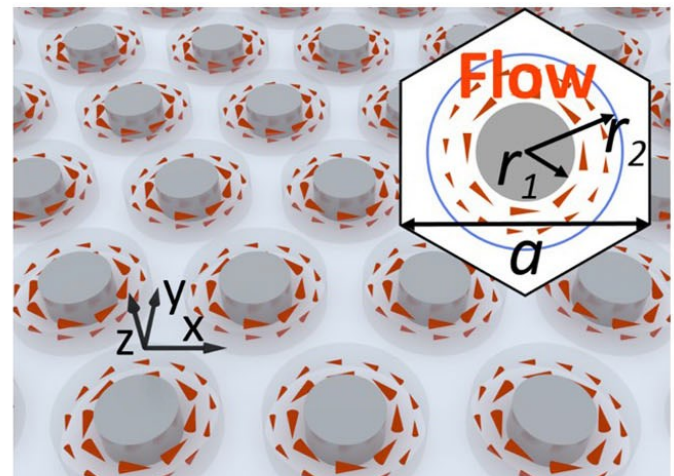
- Harmonic wave equation

Assuming ρ and c are constant, and $|\bar{v}_0/c| \ll 1$,

$$\left[(\nabla - i\bar{A})^2 + k^2 \right] \Phi = 0 \quad \bar{A}(k; \bar{r}) = -k \frac{\bar{v}_0(\bar{r})}{c}$$

$$\bar{v}_0(\bar{r}) = \Omega \left[-\frac{r_1^2}{r_2^2 - r_1^2} r + \frac{r_1^2 r_2^2}{r_2^2 - r_1^2} \frac{1}{r} \right] \hat{\theta}$$

Illustrations courtesy Yang et al. PRL 114: 114301, 2015.



Φ : acoustic velocity potential

An Integral Formulation

$$\left[(\nabla - i\bar{A})^2 + k^2 \right] \Phi = 0 \quad \hat{n} \cdot \nabla \Phi = 0, \quad r = r_1 \\ \Phi, \hat{n} \cdot \nabla \Phi \text{ continuous at } r = r_2$$

Ignoring $\bar{A} \cdot \bar{A}$ term

$$[\nabla^2 + k^2] \Phi = i2\bar{A} \cdot \nabla \Phi$$

$$[\nabla^2 + k^2] g(\bar{r}, \bar{r}') = -\delta(\bar{r} - \bar{r}')$$

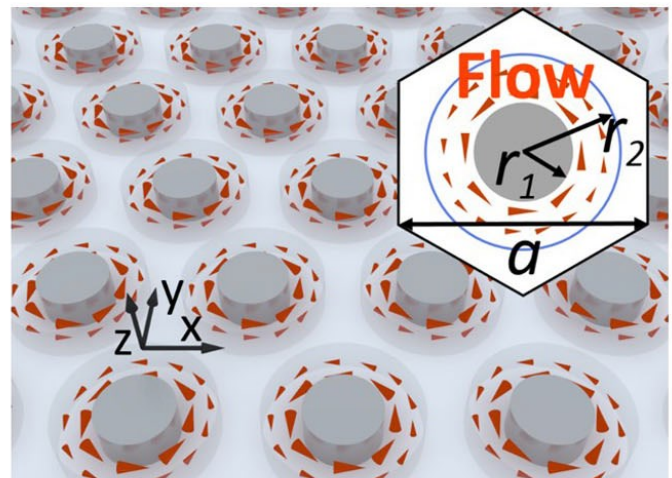
Formulate integral equation outside the scatterers

$$\int_{C_{00}} d\bar{r}' \Phi \frac{\partial g_P}{\partial n'} = \iint_{r_1 < r < r_2} d\bar{r}' g_P i2\bar{A} \cdot \nabla' \Phi + \Phi(\bar{r}), \quad r_1 < r < r_2$$

where
$$g_P(k, \bar{k}_b; \bar{r}, \bar{r}') = \sum_{m,n} g(k; \bar{r}, \bar{r}' + \bar{R}_{mn}) \exp(i\bar{k}_b \cdot \bar{R}_{mn})$$

The broadband Green's function technique can be used to compute g_P .

Illustrations courtesy Yang et al. PRL 114: 114301, 2015.



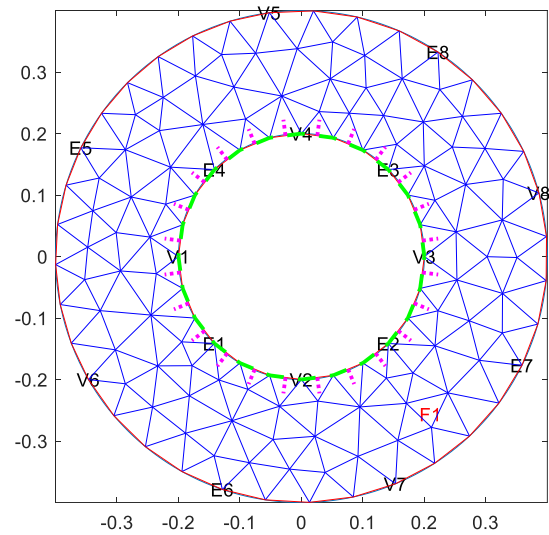
Deriving the Band Solution

$$\int_{C_{00}} d\bar{r}' \Phi \frac{\partial g_p}{\partial n'} = \iint_{r_1 < r < r_2} d\bar{r}' g_p i 2 \bar{A} \cdot \nabla' \Phi + \Phi(\bar{r}), \quad r_1 < r < r_2$$

- Discretize the integral domain with triangular patches
- Apply Method of Moments to solved the coupled volume surface integral equations with piece-wise linear (roof-top) basis functions
- Convert the integral equation into a non-linear eigenvalue problem

$$\sum_{n=1}^{N_p} Z_{mn} \Phi_n = 0$$

$$\bar{Z}(\lambda) \bar{\Phi} = 0$$



Solving the Non-linear Eigenvalue Problem

- The governing non-linear eigenvalue problem

$$\bar{\bar{Z}}(\lambda)\bar{\Phi} = 0 \quad \bar{\Phi} \neq 0$$

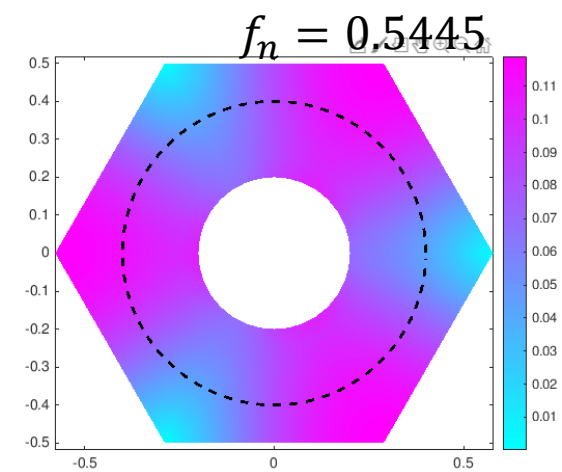
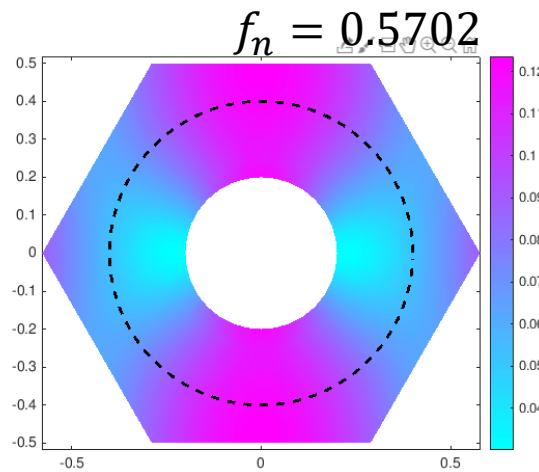
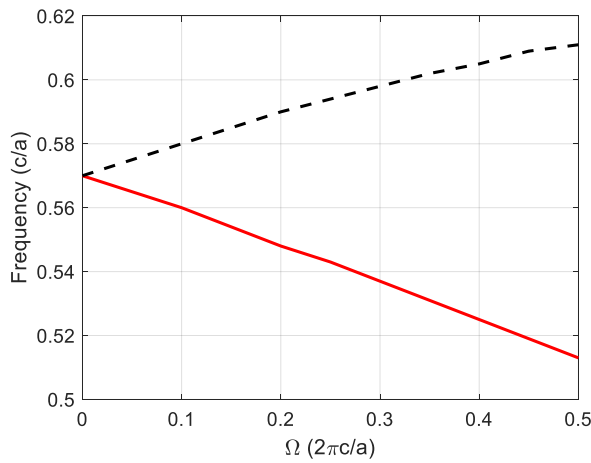
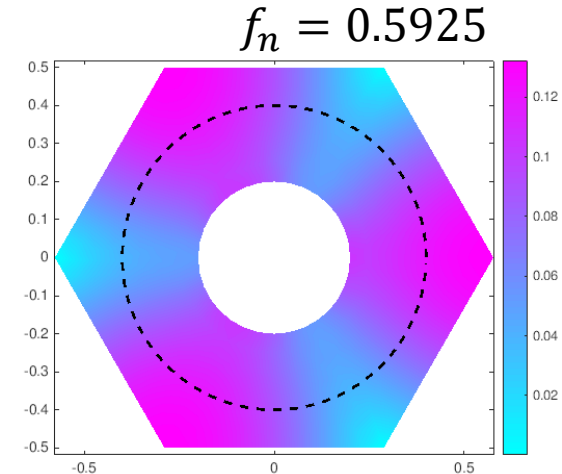
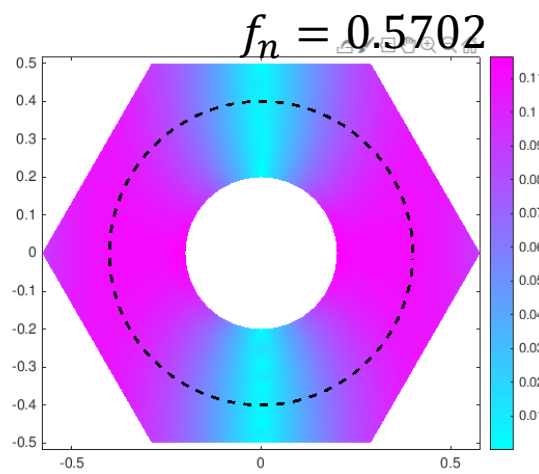
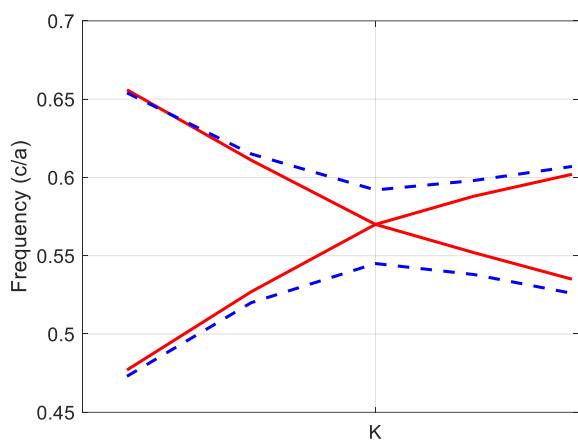
- To solve for the eigenvalue $\det(\bar{\bar{Z}}(\lambda)) = 0$
- To solve for the eigenvector $\bar{\bar{Z}}\bar{\Phi} = 0\bar{\Phi} \quad \bar{\Phi} \neq 0$

Thus we are solving the linear eigenvalue problem

$$\bar{\bar{Z}}\bar{\Phi} = \lambda\bar{\Phi}$$

And looking for the eigenvectors corresponding to eigenvalue 0.

Band Diagrams and Modal Solutions



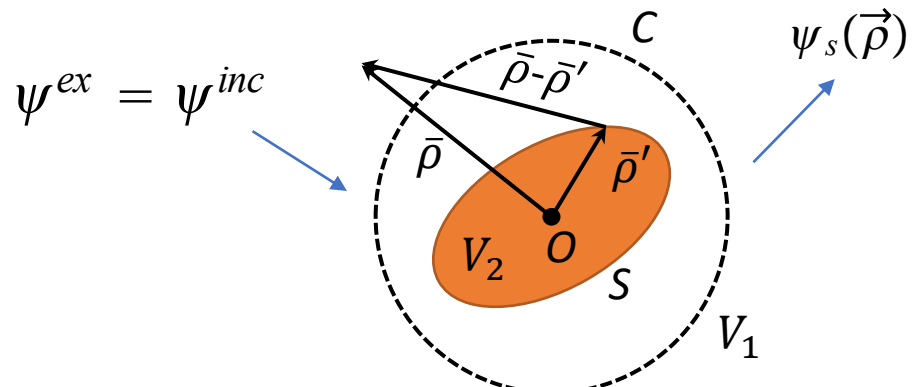
Top: band diagram around K point;
 Bottom: splitting of bands vs
 rotation speeds at K point;

Field distributions for the two degenerated modes
 (left, $\Omega_n = 0$) and their lifted counterparts (right,
 $\Omega_n = 0.2332$)

The Foldy-Lax Multiple Scattering Theory

Scattering from A Single Scatterer and The T-Matrix

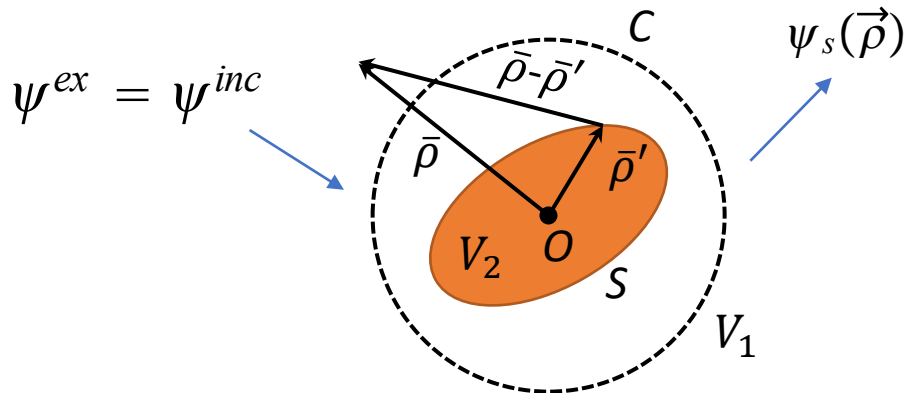
The Extinction Theorem



$$\left. \begin{array}{ll} \vec{\rho} \in V_1 & \psi_1(\vec{\rho}) \\ \vec{\rho} \in V_2 & 0 \end{array} \right\} = \psi_{inc}(\vec{\rho}) - \int_S d\vec{\rho}' \left[g_1(\vec{\rho}, \vec{\rho}') \frac{\partial \psi_1(\vec{\rho}')}{\partial n'} - \psi_1(\vec{\rho}') \frac{\partial g_1(\vec{\rho}, \vec{\rho}')}{\partial n'} \right]$$

$$\left. \begin{array}{ll} \vec{\rho} \in V_1 & 0 \\ \vec{\rho} \in V_2 & \psi_2(\vec{\rho}) \end{array} \right\} = \int_S d\vec{\rho}' \left[g_2(\vec{\rho}, \vec{\rho}') \frac{\partial \psi_2(\vec{\rho}')}{\partial n'} - \psi_2(\vec{\rho}') \frac{\partial g_2(\vec{\rho}, \vec{\rho}')}{\partial n'} \right]$$

Represent Scattering Fields with Cylindrical Wave



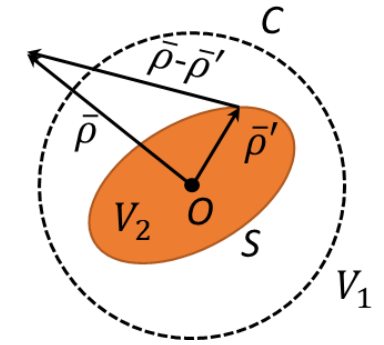
$$\begin{aligned}
 \psi_s(\vec{\rho}) &= \int_s d\vec{\rho}' \psi_1(\vec{\rho}') \frac{\partial g_1(\vec{\rho}'; \vec{\rho})}{\partial n'} - \frac{\partial \psi_1(\vec{\rho}')}{\partial n'} g_1(\vec{\rho}'; \vec{\rho}) \\
 &= \int_s d\vec{\rho}' \left[\psi_1(\vec{\rho}') \frac{\partial}{\partial n'} \frac{i}{4} H_0^{(1)}(k_1 |\vec{\rho} - \vec{\rho}'|) - \frac{\partial \psi_1(\vec{\rho}')}{\partial n'} \frac{i}{4} H_0^{(1)}(k_1 |\vec{\rho} - \vec{\rho}'|) \right]
 \end{aligned}$$

Addition theorem:

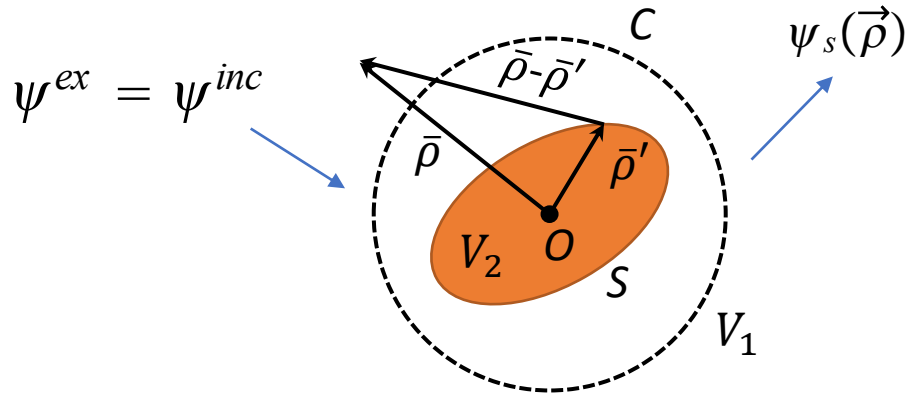
$$H_0^{(1)}(k_1 |\vec{\rho}' - \vec{\rho}|) = \sum_{n=-\infty}^{\infty} J_n(k_1 |\vec{\rho}'|) e^{-in\phi_{\vec{\rho}'}} H_n^{(1)}(k_1 |\vec{\rho}|) e^{in\phi_{\vec{\rho}}} \quad |\vec{\rho}| > |\vec{\rho}'|$$

Represent Scattering Field with Cylindrical Wave (Cont)

$$\begin{aligned}
\psi_s(\vec{\rho}) &= \int_s d\vec{\rho}' \left[\psi_1(\vec{\rho}') \frac{\partial}{\partial n'} \frac{i}{4} H_0^{(1)}(k_1 |\vec{\rho} - \vec{\rho}'|) - \frac{\partial \psi_1(\vec{\rho}')}{\partial n'} \frac{i}{4} H_0^{(1)}(k_1 |\vec{\rho} - \vec{\rho}'|) \right] \\
&= \frac{i}{4} \int_s d\vec{\rho}' \left[\psi_1(\vec{\rho}') \frac{\partial}{\partial n'} \sum_{n=-\infty}^{\infty} J_n(k_1 \rho') e^{-in\phi_{\vec{\rho}'}} H_n^{(1)}(k_1 \rho) e^{in\phi_{\vec{\rho}}} \right. \\
&\quad \left. - \frac{\partial \psi_1(\vec{\rho}')}{\partial n'} \sum_{n=-\infty}^{\infty} J_n(k_1 \rho') e^{-in\phi_{\vec{\rho}'}} H_n^{(1)}(k_1 \rho) e^{in\phi_{\vec{\rho}}} \right] \\
&= \sum_{n=-\infty}^{\infty} H_n^{(1)}(k_1 \rho) e^{in\phi_{\vec{\rho}}} \frac{i}{4} \int_s d\vec{\rho}' \left[\psi_1(\vec{\rho}') \frac{\partial}{\partial n'} J_n(k_1 \rho) e^{-in\phi_{\vec{\rho}'}} - \frac{\partial \psi_1(\vec{\rho}')}{\partial n'} J_n(k_1 \rho) e^{-in\phi_{\vec{\rho}'}} \right] \\
\psi_s(\vec{\rho}) &= \sum_{n=-\infty}^{\infty} a_n^s H_n^{(1)}(k_1 \rho) e^{in\phi_{\vec{\rho}}} \\
a_n^s &= \frac{i}{4} \int_s d\vec{\rho}' \left[\psi_1(\vec{\rho}') \frac{\partial}{\partial n'} J_n(k_1 \rho') e^{-in\phi_{\vec{\rho}'}} - \frac{\partial \psi_1(\vec{\rho}')}{\partial n'} J_n(k_1 \rho') e^{-in\phi_{\vec{\rho}'}} \right]
\end{aligned}$$



Scattering from a Single Scatterer- Definition of The T-matrix



$$\psi^{ex}(\vec{\rho}) = \sum_{m=-\infty}^{\infty} a_m^{ex} J_m(k_1 \rho) e^{in\phi_\rho} \quad \psi_s(\vec{\rho}) = \sum_{n=-\infty}^{\infty} a_n^s H_n^{(1)}(k_1 \rho) e^{in\phi_\rho}$$

$$\overline{a^s} = \bar{T} \overline{a^{ex}}$$

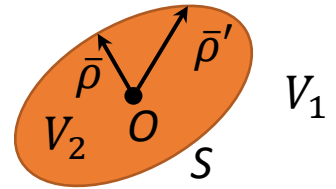
$$a_n^s = \frac{i}{4} \int_S d\vec{\rho}'' \left[\psi_1(\vec{\rho}'') \frac{\partial}{\partial n'} J_n(k_1 \rho'') e^{-in\phi_{\vec{\rho}''}} - \frac{\partial \psi_1(\vec{\rho}'')}{\partial n'} J_n(k_1 \rho'') e^{-in\phi_{\vec{\rho}''}} \right]$$

How to calculate $\psi(\vec{\rho}')$ and $\frac{\partial \psi(\vec{\rho}')}{\partial n'}$?

Approach I: Surface Field Calculation by SIE Method

$$\psi_{inc} - \int_s d\vec{\rho}' \left[g_1(\vec{\rho}; \vec{\rho}') \frac{\partial \psi_1(\vec{\rho}')}{\partial n'} - \psi_1(\vec{\rho}') \frac{\partial g_1(\vec{\rho}; \vec{\rho}')}{\partial n'} \right] = 0, \vec{\rho}' \text{ on } S^-$$

$$\int_s d\vec{\rho}' \left[g_2(\vec{\rho}; \vec{\rho}') \frac{\partial \psi_2(\vec{\rho}')}{\partial n'} - \psi_2(\vec{\rho}') \frac{\partial g_2(\vec{\rho}; \vec{\rho}')}{\partial n'} \right] = 0, \vec{\rho}' \text{ on } S^+$$



Boundary condition:

	$\psi_1 = \psi_2$	$p_1 = \frac{1}{\epsilon_1}$	$p_2 = \frac{1}{\epsilon_2}, TE (H_z)$
	$p_1 \frac{\partial \psi_1}{\partial n} = p_2 \frac{\partial \psi_2}{\partial n}$	$p_1 = \frac{1}{\mu_1}$	$p_2 = \frac{1}{\mu_2}, TM (E_z)$

SIE:

$$\psi_{inc} - \int_s d\vec{\rho}' \left[g_1(\vec{\rho}; \vec{\rho}') \frac{\partial \psi_1(\vec{\rho}')}{\partial n'} - \psi_1(\vec{\rho}') \frac{\partial g_1(\vec{\rho}; \vec{\rho}')}{\partial n'} \right] = 0, \vec{\rho}' \text{ on } S^-$$

$$\int_s d\vec{\rho}' \left[g_2(\vec{\rho}; \vec{\rho}') \frac{p_1}{p_2} \frac{\partial \psi_1(\vec{\rho}')}{\partial n'} - \psi_1(\vec{\rho}') \frac{\partial g_2(\vec{\rho}; \vec{\rho}')}{\partial n'} \right] = 0, \vec{\rho}' \text{ on } S^+$$

Matrix equation:

$$\xrightarrow{\quad} \bar{\bar{Z}} \begin{bmatrix} \overline{\frac{\partial \psi_1(\vec{\rho}')}{\partial n'}} \\ \overline{\psi_1(\vec{\rho}')} \end{bmatrix} = \begin{bmatrix} \overline{\psi}_{inc} \\ \bar{0} \end{bmatrix}$$

MOM(pulse), Nystrom ...

Approach II: Surface Field Representation with The Extended Boundary Condition (EBC) Method

Extinction theorem

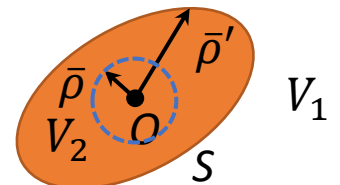
$$\psi_{inc}(\vec{\rho}) = \int_S d\vec{\rho}' \left[g_1(\vec{\rho}, \vec{\rho}') \frac{\partial \psi_1(\vec{\rho}')}{\partial n'} - \psi_1(\vec{\rho}') \frac{\partial g_1(\vec{\rho}, \vec{\rho}')}{\partial n'} \right], \quad \vec{\rho} \in V_2$$

Addition theorem

$$g_1(\vec{\rho}, \vec{\rho}') = \frac{i}{4} \sum_{n=-\infty}^{\infty} J_n(k_1 |\vec{\rho}|) e^{in\phi_{\vec{\rho}}} H_n^{(1)}(k_1 |\vec{\rho}'|) e^{-in\phi_{\vec{\rho}'}} \quad |\vec{\rho}| < |\vec{\rho}'|$$

Expansion and Eliminate Jn

$$\begin{aligned} \sum_{n=-\infty}^{\infty} a_n^{inc} J_n(k\rho) e^{in\phi} &= \int_S d\vec{\rho}' \left[\frac{i}{4} \sum_{n=-\infty}^{\infty} J_n(k|\vec{\rho}|) e^{in\phi_{\vec{\rho}}} H_n^{(1)}(k|\vec{\rho}'|) e^{-in\phi_{\vec{\rho}'}} \frac{\partial \psi_1(\vec{\rho}')}{\partial n'} \right. \\ &\quad \left. - \psi_1(\vec{\rho}') \frac{\partial \frac{i}{4} \sum_{n=-\infty}^{\infty} J_n(k|\vec{\rho}|) e^{in\phi_{\vec{\rho}}} H_n^{(1)}(k|\vec{\rho}'|) e^{-in\phi_{\vec{\rho}'}}}{\partial n'} \right] \\ a_n^{inc} &= \int_S d\vec{\rho}' \left[\frac{i}{4} H_n^{(1)}(k_1 |\vec{\rho}'|) e^{-in\phi_{\vec{\rho}'}} \frac{\partial \psi_1(\vec{\rho}')}{\partial n'} - \psi_1(\vec{\rho}') \frac{\partial \frac{i}{4} H_n^{(1)}(k_1 |\vec{\rho}'|) e^{-in\phi_{\vec{\rho}'}}}{\partial n'} \right], \quad \forall n \end{aligned}$$



Relation between The Incident and Total Field Coefficients

$$a_n^{inc} = \int_S d\vec{\rho}'' \left[\frac{i}{4} H_n^{(1)}(k_1 |\vec{\rho}''|) e^{-in\phi_{\vec{\rho}''}} \frac{\partial \psi_1(\vec{\rho}'')}{\partial n'} - \psi_1(\vec{\rho}'') \frac{\partial \frac{i}{4} H_n^{(1)}(k_1 |\vec{\rho}''|) e^{-in\phi_{\vec{\rho}''}}}{\partial n'} \right], \quad \forall n$$

Represent internal fields

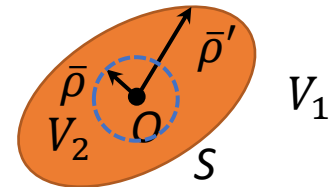
Apply BC

$$\psi_2 = \sum_{m=-\infty}^{\infty} a_m J_m(k_2 \rho) e^{im\phi}$$

$$\frac{\partial \psi_2}{\partial n} = \sum_{m=-\infty}^{\infty} a_m \frac{\partial J_m(k_2 \rho) e^{im\phi}}{\partial n}$$

$$\psi_1 = \psi_2$$

$$p_1 \frac{\partial \psi_1}{\partial n} = p_2 \frac{\partial \psi_2}{\partial n}$$



Relationship of a_n^{inc} and a_n

$$a_n^{inc} = \sum_{m=-\infty}^{\infty} a_m \int_S d\vec{\rho}'' \left[\frac{i}{4} H_n^{(1)}(k_1 \rho'') e^{-in\phi''} \frac{p_2}{p_1} \frac{\partial J_m(k_2 \rho'') e^{im\phi''}}{\partial n'} - J_m(k_2 \rho'') e^{im\phi''} \frac{\partial \frac{i}{4} H_n^{(1)}(k_1 \rho'') e^{-in\phi''}}{\partial n'} \right], \quad \forall n$$

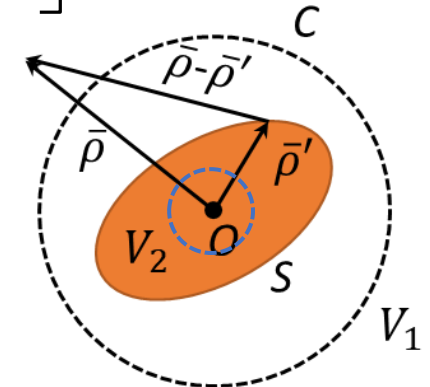
In matrix form

$$\overline{a}^{inc} = \bar{P} \bar{a}$$

Relation between The Scattering and Total Field Coefficients

From before:

$$\begin{aligned}
 a_n^s &= \frac{i}{4} \int_s d\vec{\rho}' \left[\psi_1(\vec{\rho}') \frac{\partial}{\partial n'} J_n(k_1 \rho') e^{-in\phi_{\vec{\rho}'}} - \frac{\partial \psi_1(\vec{\rho}')}{\partial n'} J_n(k_1 \rho') e^{-in\phi_{\vec{\rho}'}} \right] \\
 &= \frac{i}{4} \int_s d\vec{\rho}' \left[\sum_{m=-\infty}^{\infty} a_m J_m(k_2 \rho') e^{im\phi'} \frac{\partial}{\partial n'} J_n(k_1 \rho') e^{-in\phi_{\vec{\rho}'}} \right. \\
 &\quad \left. - \frac{p_2}{p_1} \sum_{m=-\infty}^{\infty} a_m \frac{\partial J_m(k_2 \rho') e^{im\phi'}}{\partial n'} J_n(k_1 \rho') e^{-in\phi_{\vec{\rho}'}} \right]
 \end{aligned}$$



Relationship of a_n^s and a_n

$$a_n^s = \sum_{m=-\infty}^{\infty} a_m \frac{i}{4} \int_s d\vec{\rho}' \left[J_m(k_2 \rho') e^{im\phi'} \frac{\partial}{\partial n'} J_n(k_1 \rho') e^{-in\phi_{\vec{\rho}'}} - \frac{p_2}{p_1} \frac{\partial J_m(k_2 \rho') e^{im\phi'}}{\partial n'} J_n(k_1 \rho') e^{-in\phi_{\vec{\rho}'}} \right]$$

In matrix form

$$\bar{a}^s = \bar{Q} \bar{a}$$

T-matrix Calculation with Surface Field Derived from The EBC Method

a_n^{inc} and a_n

$$\overline{a}^{inc} = \bar{\bar{P}}\bar{a}$$

$$P_{nm} = \frac{i}{4} \int_S d\vec{\rho}' \left[H_n^{(1)}(k_1\rho') e^{-in\phi'} \frac{p_2}{p_1} \frac{\partial J_m(k_2\rho') e^{im\phi'}}{\partial n'} - J_m(k_2\rho') e^{im\phi'} \frac{\partial H_n^{(1)}(k_1\rho') e^{-in\phi'}}{\partial n'} \right]$$

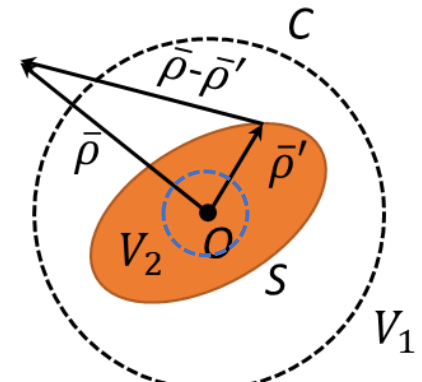
a_n^s and a_n

$$\overline{a}^s = \bar{\bar{Q}}\bar{a}$$

$$Q_{nm} = \frac{i}{4} \int_S d\vec{\rho}' \left[J_m(k_2\rho') e^{im\phi'} \frac{\partial}{\partial n'} J_n(k_1\rho') e^{-in\phi_{\vec{\rho}'}} - \frac{p_2}{p_1} \frac{\partial J_m(k_2\rho') e^{im\phi'}}{\partial n'} J_n(k_1\rho') e^{-in\phi_{\vec{\rho}'}} \right]$$

$$\overline{a}^s = \bar{\bar{Q}}\bar{\bar{P}}^{-1}\overline{a}^{inc}$$

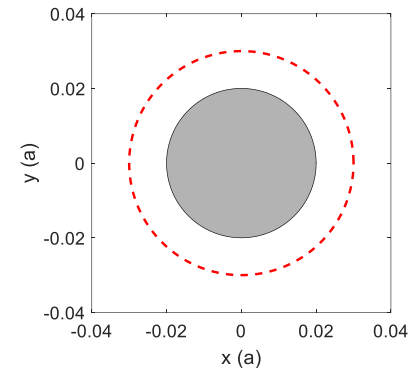
$$\bar{\bar{T}} = \bar{\bar{Q}}\bar{\bar{P}}^{-1}$$



Chee, W. C., *Waves and Fields in Inhomogeneous Media*, Van Nostrand Reinhold, New York, 1990.

Comparing SIE and EBC Approaches

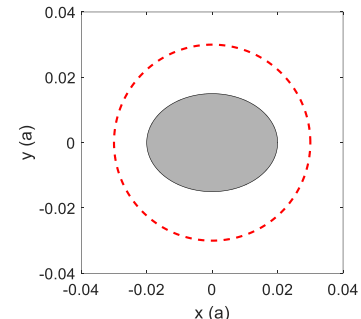
For a cylindrical PEC structure



	Tmatrix-EBC approach	Tmatrix-SIE approach
Minimum order required	3	3
calculating time (s)	0.292	0.011
Required fraction	300	20
Scattering field results comparing with MOM		

Comparing SIE and EBC Approaches (Cont.)

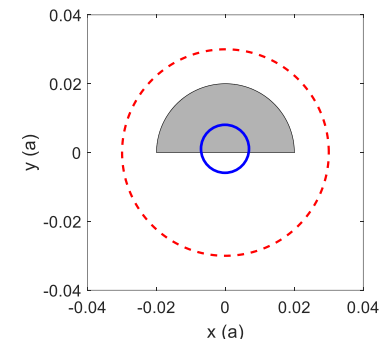
For an semicircle PEC structure



	Tmatrix-EBC approach	Tmatrix-SIE approach
Minimum order required	17	5
calculating time (s)	109.18	0.031
Required fraction	4000	60
Scattering field results comparing with MOM		

Comparing SIE and EBC Approaches (Cont.)

For an ellipse PEC structure



	Tmatrix-EBC approach	Tmatrix-SIE approach
Minimum order required	Limited applicability: not converge in the selected coordinate	5
calculating time (s)	Limited applicability: not converge in the selected coordinate	0.026
Required fraction	Limited applicability: not converge in the selected coordinate	50
Scattering field results comparing with MOM		

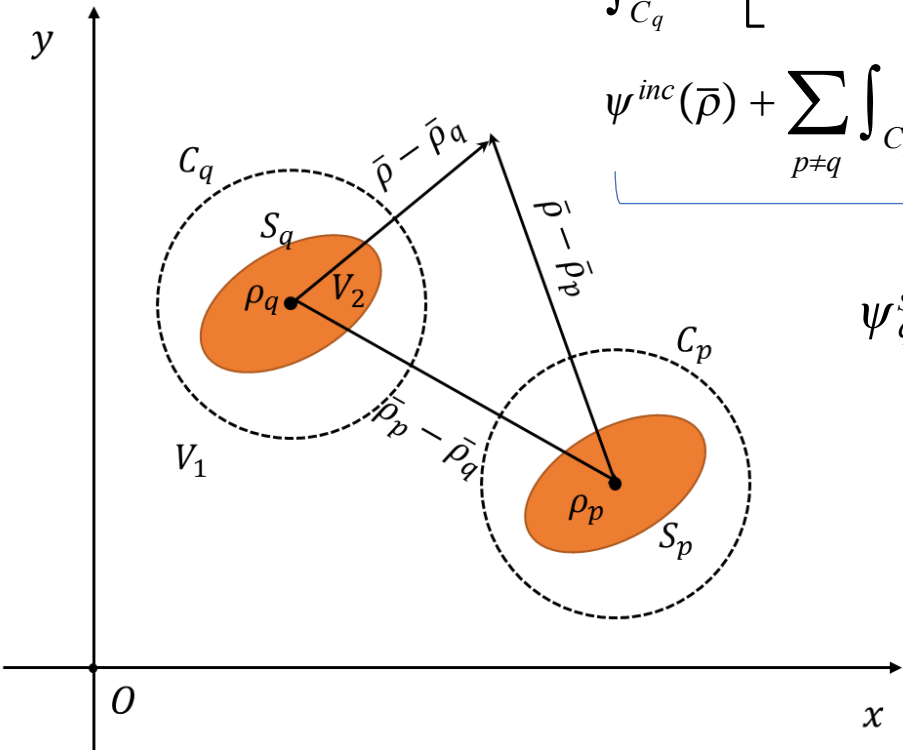
Scattering from Multiple Scatterers and The Foldy-Lax Multiple Scattering Theory (MST)

From Extinction Theorem to Multiple Scattering Equation (MSE)

$$\left. \begin{array}{ll} \bar{\rho} \in V_1 & \psi_1(\bar{\rho}) \\ \bar{\rho} \notin V_1 & 0 \end{array} \right\} = \psi^{inc}(\bar{\rho}) + \sum_p \int_{C_p} d\bar{\rho}' \left[\psi_1(\bar{\rho}') \frac{\partial g_1(\bar{\rho}, \bar{\rho}')}{\partial n'} - g_1(\bar{\rho}, \bar{\rho}') \frac{\partial \psi_1(\bar{\rho}')}{\partial n'} \right]$$

$$= \int_{C_q} d\bar{\rho}' \left[\psi_1(\bar{\rho}') \frac{\partial g_1(\bar{\rho}, \bar{\rho}')}{\partial n'} - g_1(\bar{\rho}, \bar{\rho}') \frac{\partial \psi_1(\bar{\rho}')}{\partial n'} \right] +$$

$$\psi^{inc}(\bar{\rho}) + \sum_{p \neq q} \int_{C_p} d\bar{\rho}' \left[\psi_1(\bar{\rho}') \frac{\partial g_1(\bar{\rho}, \bar{\rho}')}{\partial n'} - g_1(\bar{\rho}, \bar{\rho}') \frac{\partial \psi_1(\bar{\rho}')}{\partial n'} \right]$$



$$\psi_q^s(\vec{\rho}) \quad \psi_q^{ex}(\vec{\rho})$$

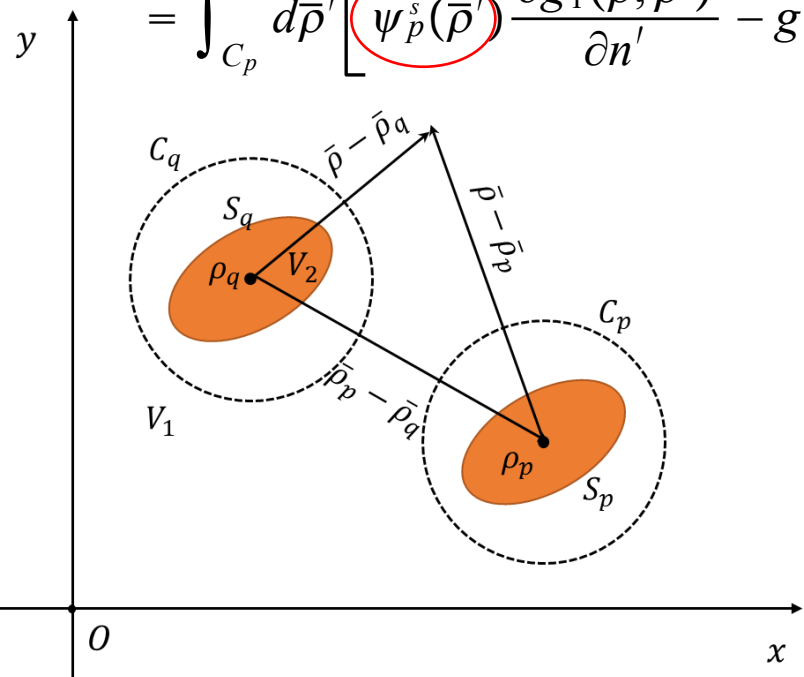
Foldy-Lax MSE:

$$\boxed{\psi_q^{ex}(\bar{\rho}) = \psi^{inc}(\bar{\rho}) + \sum_{p \neq q} \psi_p^s(\bar{\rho})}$$

Foldy-Lax MST: Key Relations

$$\psi_q^{ex}(\bar{\rho}) = \psi^{inc}(\bar{\rho}) + \sum_{p \neq q} \psi_p^s(\bar{\rho})$$

$$\begin{aligned}\psi_p^s(\bar{\rho}) &= \int_{C_p} d\bar{\rho}' \left[\psi_1(\bar{\rho}') \frac{\partial g_1(\bar{\rho}, \bar{\rho}')}{\partial n'} - g_1(\bar{\rho}, \bar{\rho}') \frac{\partial \psi_1(\bar{\rho}')}{\partial n'} \right] \\ &= \int_{S_p} d\bar{\rho}' \left[\psi_1(\bar{\rho}') \frac{\partial g_1(\bar{\rho}, \bar{\rho}')}{\partial n'} - g_1(\bar{\rho}, \bar{\rho}') \frac{\partial \psi_1(\bar{\rho}')}{\partial n'} \right] \\ &= \int_{C_p} d\bar{\rho}' \left[\psi_p^s(\bar{\rho}') \frac{\partial g_1(\bar{\rho}, \bar{\rho}')}{\partial n'} - g_1(\bar{\rho}, \bar{\rho}') \frac{\partial \psi_p^s(\bar{\rho}')}{\partial n'} \right]\end{aligned}$$



↗

$$\begin{aligned}\psi_p^s(\bar{\rho}) &= \sum_{n=-\infty}^{\infty} a_{p,n} H_n^{(1)}(k|\bar{\rho} - \bar{\rho}_p|) e^{in\phi_{\bar{\rho}\bar{\rho}_p}} \\ \bar{a}_p^s &= \bar{T}_p \bar{a}_p^{ex}\end{aligned}$$

↘

Wronskian:

$$H_m^{(1)\prime}(kb)J_m(kb) - H_m^{(1)}(kb)J'_m(kb) = \frac{2i}{\pi kb}$$

Multiple Scattering Eqn Governing \bar{a}^{ex}

$$\psi_q^{ex}(\bar{\rho}) = \psi^{inc}(\bar{\rho}) + \sum_{p \neq q} \psi_p^s(\bar{\rho})$$



$$\psi_q^{ex}(\bar{\rho}) = \sum_{n=-\infty}^{\infty} a_{q,n}^{ex} J_n(k|\bar{\rho} - \bar{\rho}_q|) e^{in\phi_{\bar{\rho}\bar{\rho}_q}}$$

$$\psi^{inc}(\bar{\rho}) = \sum_{n=-\infty}^{\infty} a_{q,n}^{inc} J_n(k|\bar{\rho} - \bar{\rho}_q|) e^{in\phi_{\bar{\rho}\bar{\rho}_q}}$$

$$\psi_p^s(\bar{\rho}) = \sum_{n=-\infty}^{\infty} a_{p,n}^s H_n^{(1)}(k|\bar{\rho} - \bar{\rho}_p|) e^{in\phi_{\bar{\rho}\bar{\rho}_p}}$$

$$H_n^{(1)}(k|\bar{\rho} - \bar{\rho}_p|) e^{in\phi_{\bar{\rho}\bar{\rho}_p}}$$

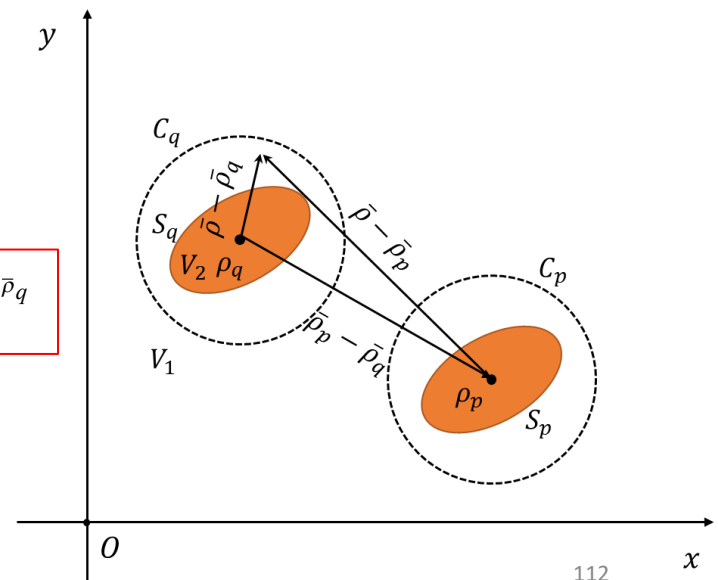
$$= \sum_{l=-\infty}^{\infty} J_l(k|\bar{\rho} - \bar{\rho}_q|) e^{il\phi_{\bar{\rho}\bar{\rho}_q}} H_{l-n}^{(1)}(k|\bar{\rho}_p - \bar{\rho}_q|) e^{-i(l-n)\phi_{\bar{\rho}_p\bar{\rho}_q}}$$



$$a_{q,n}^{ex} = a_{q,n}^{inc} + \sum_{p \neq q} \sum_{l=-\infty}^{\infty} a_{p,n}^s H_{l-n}^{(1)}(k|\bar{\rho}_p - \bar{\rho}_q|) e^{-i(l-n)\phi_{\bar{\rho}_p\bar{\rho}_q}}$$



$$\bar{a}_p^s = \bar{T}_p \bar{a}_p^{ex}$$



MSE Governing \bar{a}^{ex} : A Green Function Formulation

$$\psi_q^{ex}(\bar{\rho}) = \psi^{inc}(\bar{\rho}) + \sum_{p \neq q} \int_{C_p} d\bar{\rho}' \left[\psi_p^s(\bar{\rho}') \frac{\partial g_1(\bar{\rho}, \bar{\rho}')}{\partial n'} - g_1(\bar{\rho}, \bar{\rho}') \frac{\partial \psi_p^s(\bar{\rho}')}{\partial n'} \right]$$

+

$$\psi_q^{ex}(\bar{\rho}) = \sum_{n=-\infty}^{\infty} a_{q,n}^{ex} J_n(k |\bar{\rho} - \bar{\rho}_q|) e^{in\phi_{\bar{\rho}\bar{\rho}_q}}$$

$$\psi^{inc}(\bar{\rho}) = \sum_{n=-\infty}^{\infty} a_{q,n}^{inc} J_n(k \left| \bar{\rho} - \bar{\rho}_q \right|) e^{in\phi_{\bar{\rho}\bar{\rho}_q}}$$

$$\psi_p^s(\bar{\rho}) = \sum_{n=-\infty}^{\infty} a_{p,n}^s H_n^{(1)}(k|\bar{\rho} - \bar{\rho}_p|) e^{in\phi_{\bar{\rho}\bar{\rho}_p}}$$

$$g(\bar{\rho}, \bar{\rho}') = \frac{i}{4} H_0^{(1)}(k_0 |\bar{\rho} - \bar{\rho}'|)$$

$$= \frac{i}{4} \sum_{l=-\infty}^{\infty} J_l(k|\bar{\rho}' - \bar{\rho}_p|) e^{-il\phi_{\bar{\rho}'_p - \bar{\rho}_p}} H_l^{(1)}(k|\bar{\rho} - \bar{\rho}_p|) e^{il\phi_{\bar{\rho} - \bar{\rho}_p}}$$

$$= \frac{i}{4} \sum_{l=-\infty}^{\infty} J_l(k|\vec{p}' - \vec{p}_p|) e^{-il\phi_{\vec{p}' - \vec{p}_p}}$$

$$\sum_{n=-\infty}^{\infty} J_n(k|\bar{p} - \bar{\rho}_q|) e^{in\phi_{\bar{p}-\bar{\rho}_q}} H_{n-l}^{(1)}(k|\bar{p}_p - \bar{\rho}_q|) e^{-i(n-l)\phi_{\bar{p}_p-\bar{\rho}_q}}$$

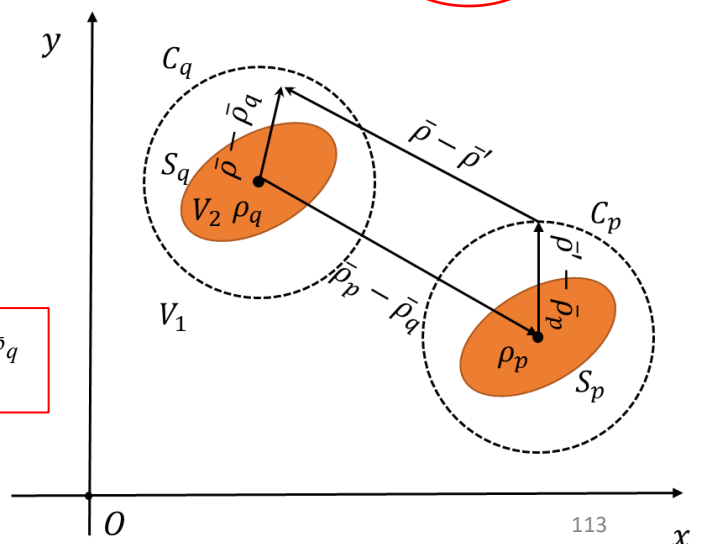
γ

$$H_m^{(1)'}(kb)J_m(kb) - H_m^{(1)}(kb)J_m'(kb) = \frac{2i}{\pi kb}$$

$$a_{q,n}^{ex} = a_{q,n}^{inc} + \sum_{p \neq q} \sum_{l=-\infty}^{\infty} a_{p,n}^s H_{l-n}^{(1)}(k|\bar{\rho}_p - \bar{\rho}_q|) e^{-i(l-n)\phi_{\bar{\rho}_p - \bar{\rho}_q}}$$

+

$$\bar{a}_p^s = \bar{\bar{T}}_p \bar{a}_p^{ex}$$



Liao, T.-H., Tsang, L., & Tan, S. (2021). Broadband Green's Function-KKR-Multiple Scattering Method for the Calculations of Band Structures in Topological Acoustics. APS/URSI 2021 Singapore. (Paper)

Tsang, L., Liao, T.-H., & Tan, S. (2021). Calculations of Bands and Band Field Solutions in Topological Acoustics Using The Broadband Green's Function-KKR-Multiple Scattering Method. *Prog. Electromagn. Res.*, 171, 137-158.

Gao, R., Tsang, L., Tan, S., & Liao, T.-H. (2021). Broadband Green's Function-KKR-Multiple Scattering Method for Calculations of Normalized Band Field Solutions in Magnetic-Optics Crystals. *J. Opt. Soc. Am. B*, 38(10), 3159-3171.

Gao, R., Tsang, L., Tan, S. & Liao, T. (2020). Band calculations using broadband Green's functions and the KKR method with applications to magneto-optics and photonic crystals, *J. Opt. Soc. Am. B*, 37 (12): 3896-3907.

Scattering from Infinite Periodic Scatterers and Band Characterization

The BGF-KKR-MST Approach

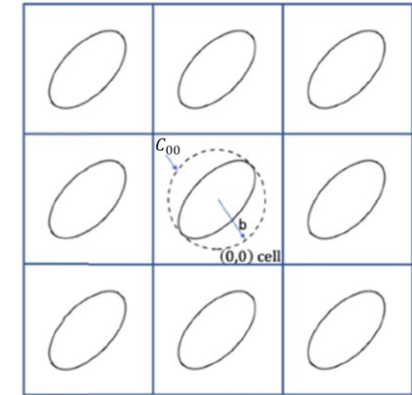
Foldy-Lax MST Applied to Periodic Scatterers

$$\psi_q^{ex}(\bar{\rho}) = \psi^{inc}(\bar{\rho}) + \sum_{p \neq q} \int_{C_p} d\bar{\rho}' \left[\psi_p^s(\bar{\rho}') \frac{\partial g_1(\bar{\rho}, \bar{\rho}')}{\partial n'} - g_1(\bar{\rho}, \bar{\rho}') \frac{\partial \psi_p^s(\bar{\rho}')}{\partial n'} \right]$$

Apply Bloch Theorem: $\psi(\bar{\rho} + \bar{R}) = \psi(\bar{\rho}) \exp(i\bar{k}_b \cdot \bar{R})$

Define the residual Green's function

$$\begin{aligned} g_R(\vec{\rho}, \vec{\rho}') &= \sum_{pq \neq 00} g_1(\vec{\rho}, \vec{\rho}') e^{i\bar{k}_b \cdot \bar{R}_{pq}} \\ &= g_P(\bar{k}_b; \vec{\rho}, \vec{\rho}') - g_1(\vec{\rho}, \vec{\rho}') \end{aligned}$$



The governing multiple scattering equation

$$\psi_{00}^{ex}(\bar{\rho}) = \psi^{inc}(\bar{\rho}) + \int_{C_{00}} d\bar{\rho}' \left[\psi_{00}^s(\bar{\rho}') \frac{\partial g_R(\bar{\rho}, \bar{\rho}')}{\partial n'} - g_R(\bar{\rho}, \bar{\rho}') \frac{\partial \psi_{00}^s(\bar{\rho}')}{\partial n'} \right]$$

The Korringa-Kohn-Rostoker (KKR) Formulation

$$\psi_{00}^{ex}(\bar{\rho}) = \psi^{inc}(\bar{\rho}) + \int_{C_{00}} d\bar{\rho}' \left[\psi_{00}^s(\bar{\rho}') \frac{\partial g_R(\bar{\rho}, \bar{\rho}')}{\partial n'} - g_R(\bar{\rho}, \bar{\rho}') \frac{\partial \psi_{00}^s(\bar{\rho}')}{\partial n'} \right]$$

$$g_R(\vec{\rho}, \vec{\rho}') = \sum_{pq \neq 00} g_1(\vec{\rho}, \vec{\rho}') e^{i\vec{k}_b \cdot \vec{R}_{pq}} = g_P(\vec{k}_b; \vec{\rho}, \vec{\rho}') - g_1(\vec{\rho}, \vec{\rho}')$$

$$\psi^{ex}(\bar{\rho}) = \sum_{n=-\infty}^{\infty} a_n^{ex} J_n(k\rho) e^{in\phi_{\bar{\rho}}}$$

$$\psi^{inc}(\bar{\rho}) = \sum_{n=-\infty}^{\infty} a_n^{inc} J_n(k\rho) e^{in\phi_{\bar{\rho}}}$$

$$\psi^s(\bar{\rho}) = \sum_{n=-\infty}^{\infty} a_n^s H_n^{(1)}(k\rho) e^{in\phi_{\bar{\rho}}}$$

+

$$g_R(\vec{\rho}, \vec{\rho}') = \sum_{l=-\infty}^{\infty} D_l J_l(k|\vec{\rho} - \vec{\rho}'|) e^{il\phi_{\bar{\rho}\bar{\rho}'}}$$

$$= \sum_{l=-\infty}^{\infty} D_l \sum_{n=-\infty}^{\infty} J_n(k\rho) e^{in\phi_{\bar{\rho}}} J_{n-l}(k\rho') e^{-i(n-l)\phi'}$$

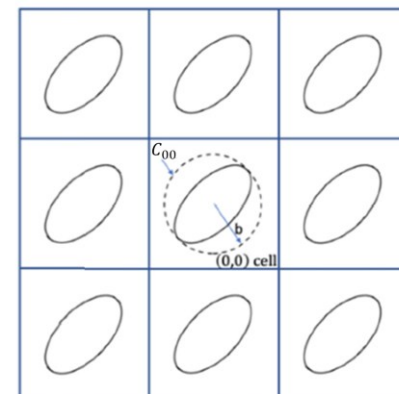


$$H_m^{(1)'}(kb) J_m(kb) - H_m^{(1)}(kb) J_m'(kb) = \frac{2i}{\pi kb}$$

$$\overline{a^s} = \overline{\bar{T}a^{ex}}$$



$$(\bar{I} + 4i\bar{\bar{D}}\bar{\bar{T}})\overline{a^{ex}} = \overline{a^{inc}}$$



KKR-BGF-MST: Evaluation D_l in the Residual Green's Function with BGF

Assuming ρ' to be 0

$$g_R = \sum_{l=-\infty}^{\infty} D_l J_l(k|\vec{\rho}|) e^{il\phi_{\vec{\rho}}}$$

$$\int_0^{2\pi} g_R(\vec{\rho}, \vec{\rho}') e^{-im\phi} d\phi = \int_0^{2\pi} \sum_{l=-\infty}^{\infty} D_l J_l(k|\vec{\rho}|) e^{il\phi_{\vec{\rho}}} e^{-im\phi} d\phi = 2\pi D_m J_m(k|\vec{\rho}|)$$

$$D_m = \frac{\int_0^{2\pi} g_R(\vec{\rho}, \vec{\rho}'=0) e^{-im\phi} d\phi}{2\pi J_m(k|\vec{\rho}|)}$$

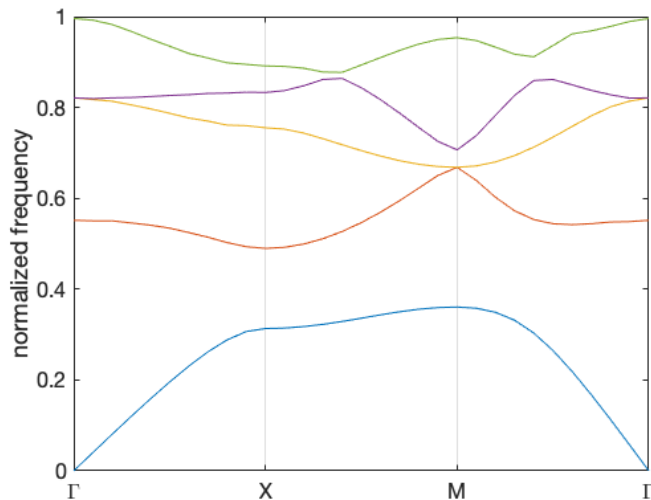
BBGF with sixth-order convergence and imaginary extractions

$$\begin{aligned} g_p^{(6)}(k, \bar{k}_i, \bar{\rho}) &= g_p^{spa}(i\xi, \bar{k}_i, \bar{\rho}) - \\ &\quad \frac{\xi^2 + k^2}{2\xi} \frac{d}{d\xi} g_p^{spa}(i\xi, \bar{k}_i, \bar{\rho}) + \sum_{p=-\infty}^{\infty} \sum_{q=-\infty}^{\infty} \frac{(\xi^2 + k^2)^2}{(|k_{ipq}|^2 + \xi^2)^2} \frac{e^{i\bar{k}_{ipq} \cdot \bar{\rho}}}{|k_{ipq}|^2 - k^2} \end{aligned}$$

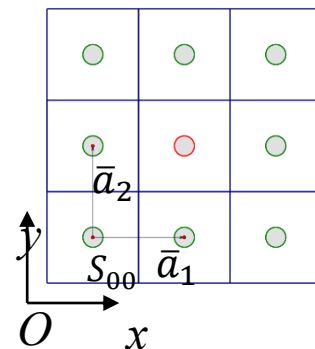
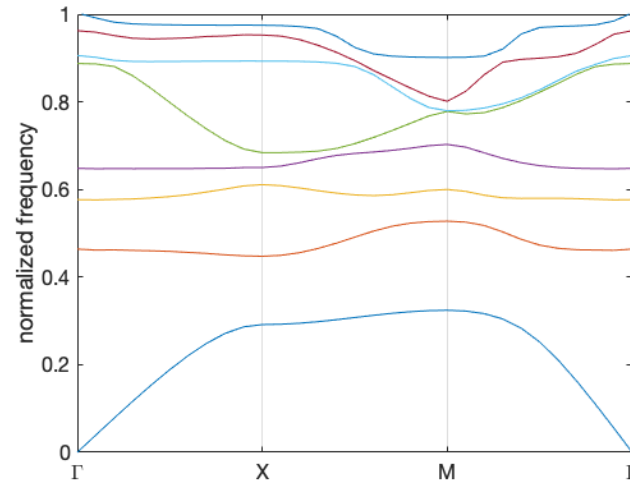
This allows efficient evaluation of $D_m(\bar{k}_i, k)$ as a function of k over a broadband.

KKR-BGF-MST Applied to Characterize Band of Gyromagnetic Photonic Crystals

Without external DC field



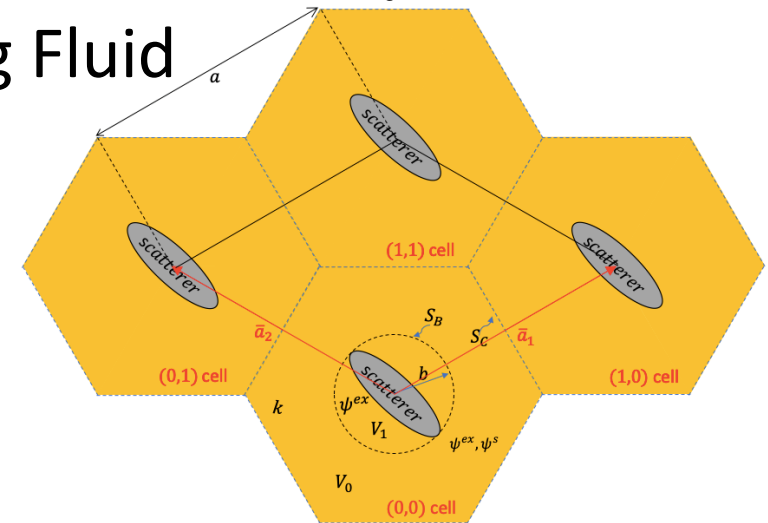
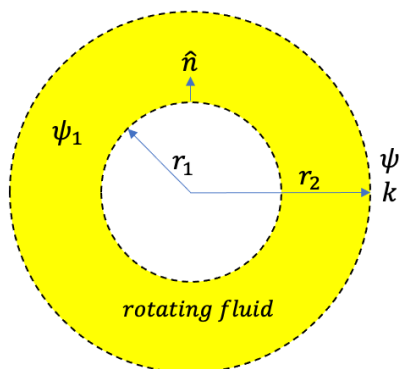
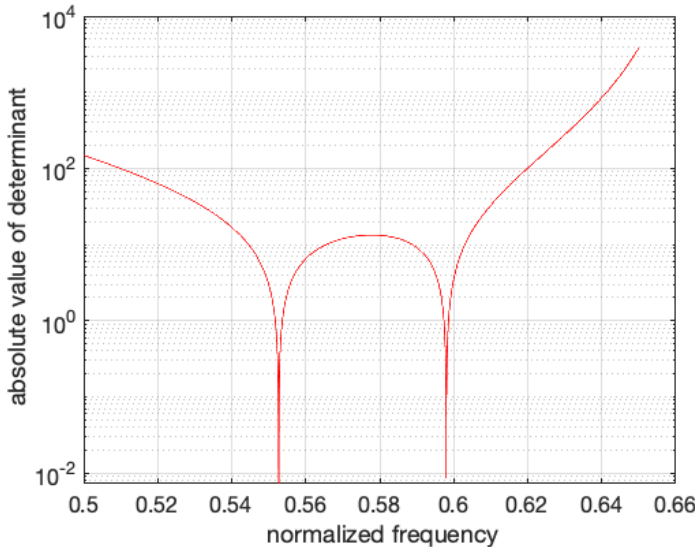
With external DC field



$$\bar{\mu} = \begin{bmatrix} r = 0.11a & 14\mu_0 & 12.4i\mu_0 & 0 \\ \varepsilon_1 = 15\varepsilon_0 & -12.4i\mu_0\kappa & 14\mu_0 & 0 \\ 0 & 0 & 0 & \mu_0 \end{bmatrix}$$

Gao, R., Tsang, L., Tan, S. & Liao, T. (2020). Band calculations using broadband Green's functions and the KKR method with applications to magneto-optics and photonic crystals, J. Opt. Soc. Am. B, 37 (12): 3896-3907.

KKR-BGF-MST Applied to Characterize Band of Acoustic Crystals with Rotating Fluid



CPU Time Comparisons for computing Band eigenvalue frequencies. $N_{spa} = 4$, $N_{spe} = 4$

Method	Set-up (milliseconds)	Number of bands N_L	Number frequencies of	D_l and $\det(P)$ (milliseconds)	Total CPU time (milliseconds)
Frequency scanning	1.7	1	2	1000	124.9
Frequency scanning	2.6	1	3	1000	183.4
Bisection	2.1	1	2	14	2.9
Bisection	3.4	1	3	14	5.1
					8.5

Tsang, L., Liao, T.-H., & Tan, S. (2021). Calculations of Bands and Band Field Solutions in Topological Acoustics Using The Broadband Green's Function-KKR-Multiple Scattering Method. *Prog. Electromagn. Res.*, 171, 137-158.

Represent D_m in Lattice Summation

$$D_m = \frac{\int_0^{2\pi} g_R(\vec{\rho}, \vec{\rho}'=0) e^{-im\phi} d\phi}{2\pi J_m(k|\vec{\rho}|)} \quad g_R(k, k_b; \rho, \phi) = \sum_{pq \neq 00} \frac{i}{4} H_0^{(1)}(k|\vec{\rho} - \bar{R}_{pq}|) e^{i\bar{k}_b \cdot \bar{R}_{pq}}$$



$$H_0^{(1)}(k|\vec{\rho} - \bar{R}_{pq}|) = \sum_{n=-\infty}^{\infty} J_n(k|\vec{\rho}|) e^{in\phi} H_n^{(1)}(k|\bar{R}_{pq}|) e^{-in\phi_{\bar{R}_{pq}}} \quad for \quad |\vec{\rho}| < |\bar{R}_{pq}|$$

$$\begin{aligned} D_m(k) &= \frac{\int_0^{2\pi} \sum_{pq \neq 00} \frac{i}{4} H_0^{(1)}(k_0|\vec{\rho} - \bar{R}_{pq}|) e^{i\bar{k}_b \cdot \bar{R}_{pq}} e^{-im\phi} d\phi}{2\pi J_m(k\rho)} \\ &= \frac{\frac{i}{4} \sum_{pq \neq 00} J_m(k\rho) H_m^{(1)}(|\bar{R}_{pq}|) e^{-im\phi_{\bar{R}_{pq}}} e^{i\bar{k}_b \cdot \bar{R}_{pq}} \cdot 2\pi}{2\pi J_m(k\rho)} \\ &= \frac{i}{4} \sum_{pq \neq 00} H_m^{(1)}(|\bar{R}_{pq}|) e^{-im\phi_{\bar{R}_{pq}}} e^{i\bar{k}_b \cdot \bar{R}_{pq}} \end{aligned}$$

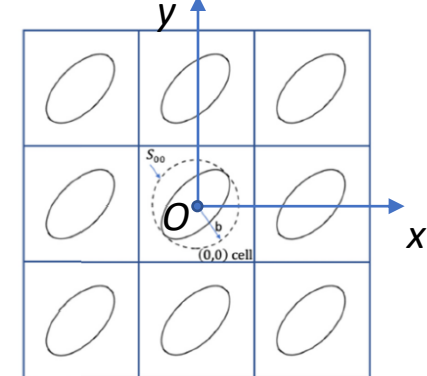
Rediscover D_m in Foldy-Lax MSE Applied to Periodic Scatterers: Another Formulation of The KKR MSE

$$\psi_{00}^{ex}(\bar{\rho}) = \psi_{00}^{inc}(\bar{\rho}) + \sum_{pq \neq 00} \psi_{pq}^s(\bar{\rho})$$

$$\psi_{00}^{ex}(\bar{\rho}) = \sum_{n=-\infty}^{\infty} a_n^{ex} J_n(k\rho) e^{in\phi}$$

$$\psi_{00}^{inc}(\bar{\rho}) = \psi_0 e^{i\bar{k}_b \cdot \bar{\rho}} = \sum_{n=-\infty}^{\infty} a_n^{inc} J_n(k\rho) e^{in\phi}$$

$$\psi_{pq}^s(\bar{\rho}) = \sum_{l=-\infty}^{\infty} a_{pq,l}^s H_l^{(1)}(k|\bar{\rho} - \bar{R}_{pq}|) e^{in\phi_{\bar{\rho} - \bar{R}_{pq}}} \quad +$$



$$H_l^{(1)}(k|\bar{\rho} - \bar{R}_{pq}|) e^{il\phi_{\bar{\rho} - \bar{R}_{pq}}} \\ = \sum_{n=-\infty}^{\infty} J_n(k|\bar{\rho}|) e^{in\phi} H_{n-l}^{(1)}(k|\bar{R}_{pq}|) e^{-i(n-l)\phi_{\bar{R}_{pq}}}$$



Bloch Theorem

$$a_{pq,l}^s = a_l^s e^{i\bar{k}_b \cdot \bar{R}_{pq}}$$

$$a_n^{ex} = a_n^{inc} + \sum_{l=-\infty}^{\infty} a_l^s \sum_{pq \neq 00} H_{n-l}^{(1)}(k|\bar{R}_{pq}|) e^{-i(n-l)\phi_{\bar{R}_{pq}}} e^{i\bar{k}_b \cdot \bar{R}_{pq}}$$

Realizing

$$D_m(k) = \frac{i}{4} \sum_{pq \neq 00} H_m^{(1)}(|\bar{R}_{pq}|) e^{-im\phi_{\bar{R}_{pq}}} e^{i\bar{k}_b \cdot \bar{R}_{pq}}$$

$$\rightarrow \bar{a}^{ex} = \bar{a}^{inc} - 4i\bar{D}\bar{a}^s \quad + \quad \bar{a}^s = \bar{\bar{T}}\bar{a}^{ex}$$

$$(\bar{I} + 4i\bar{\bar{D}}\bar{\bar{T}})\bar{a}^{ex} = \bar{a}^{inc}$$

Feng, Z., & Tan, S. (2022). Characterization of One-Way Edge Modes at the Interface of Topological Photonic Crystals and A PEC Wall Using the Coupled Integral Equation - Foldy-Lax Multiple Scattering Method. PIERS 2021 Hangzhou.

Feng, Z., & Tan, S. (2021). Topological Edge-Mode Characterization Using Foldy-Lax Multiple Scattering Theory and Interpretation with Classical EM Theory. APS/URSI 2021 Singapore. (Paper)

Feng, Z., & Tan, S. (2021). Modeling Reflection-Free One-Way Edge Modes Using Foldy-Lax Multiple Scattering Theory. ACES 2021. (Paper)

Scattering from Finite Periodic Scatterers: Topological Edge State Characterization and Interpretation

MST generalized to handle boundary

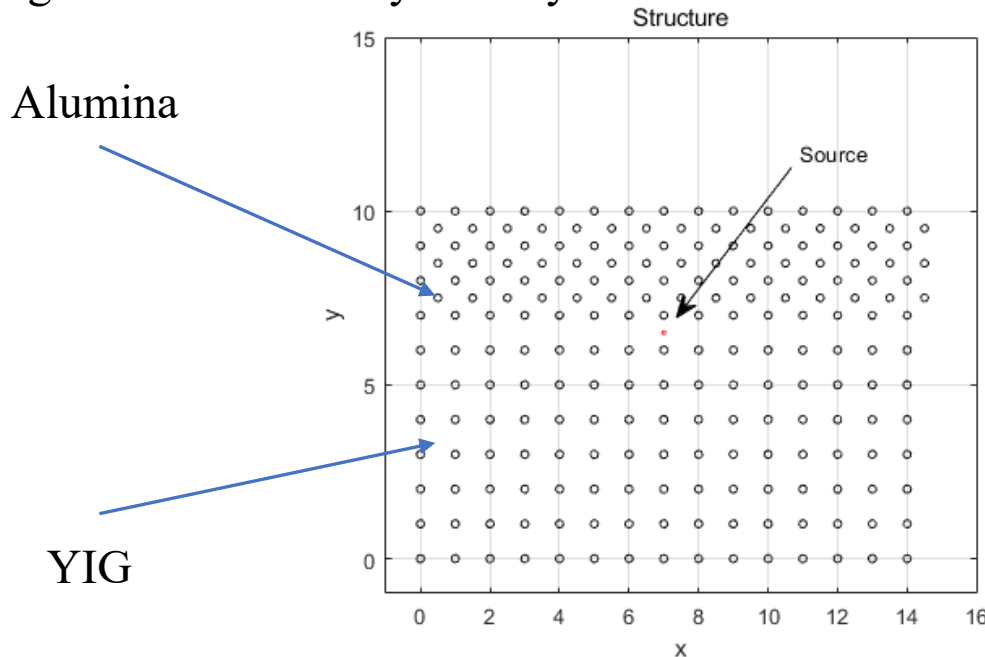
Edge modes and the robustness

Interpretation in terms of Green's function and waveguide theory

Dispersion of edge modes

Apply Foldy-Lax MST to Characterize Uni-directional Edge States

Edge state confined by two crystals



Foldy-Lax MST

$$\bar{\psi}_p^{\text{ex}} = \bar{\psi}_p^{\text{inc}} + \sum_{\substack{q=1, \\ q \neq p}}^N \bar{\psi}_q^s$$

$$\bar{\psi}_p^{\text{inc}} = \frac{i}{4} H_0^{(1)}(k|\bar{\rho} - \bar{\rho}_{\text{inc}}|)$$

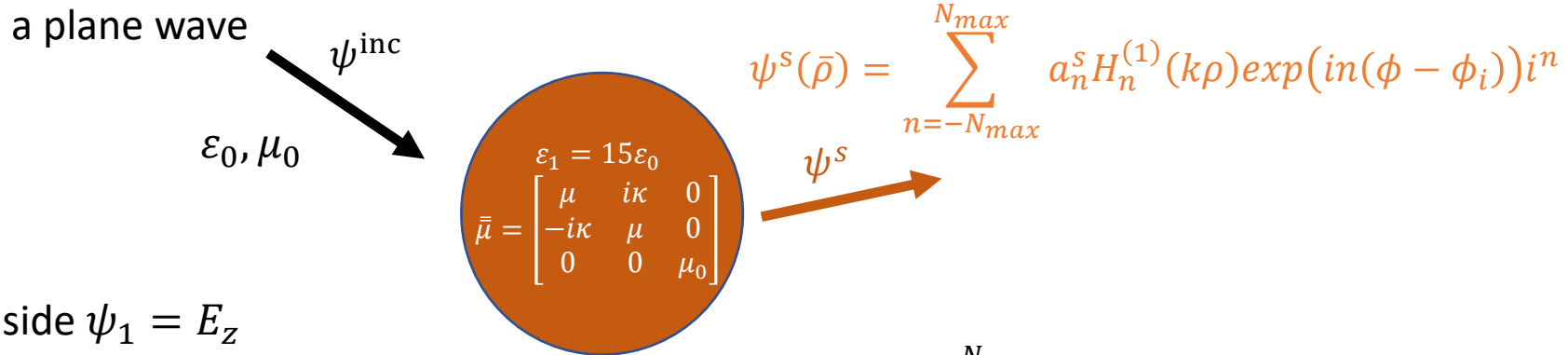
$$\sum_{n=-N_{\max}}^{N_{\max}} \omega_n^{(p)} J_n(k |\bar{\rho} - \bar{\rho}_p|) \exp(in\phi_{\bar{\rho}\bar{\rho}_p}) = \psi_{\text{inc}} + \sum_{q=1, q \neq p}^N \sum_{m=-M_{\max}}^{M_{\max}} T_m \omega_m^{(q)} H_m^{(1)}(k |\bar{\rho} - \bar{\rho}_q|) \exp(im\phi_{\bar{\rho}\bar{\rho}_q})$$

$$a_{q,n}^{\text{ex}} = a_n^{\text{inc}} + \sum_{p \neq q} \sum_{l=-\infty}^{\infty} a_{p,n}^s H_{l-n}^{(1)}(k |\bar{\rho}_p - \bar{\rho}_q|) e^{-i(l-n)\phi_{\bar{\rho}_p - \bar{\rho}_q}}$$

$$\overline{a^s} = \overline{\bar{T}a^{\text{ex}}}$$

T matrix of a cylindrical scatterer of gyromagnetic material

$$\psi^{\text{inc}}(\bar{\rho}) = \sum_{n=-N_{\max}}^{N_{\max}} a_n J_n(k\rho) \exp(in(\phi - \phi_i)) i^n$$



Inside $\psi_1 = E_z$

$$\nabla^2 E_z + \omega^2 \epsilon \mu \left(1 - \frac{\kappa^2}{\mu^2} \right) E_z = 0$$

$$\psi_1(\bar{\rho}) = \sum_{n=-N_{\max}}^{N_{\max}} c_n J_n(k_1 \rho) \exp(in(\phi - \phi_i)) i^n$$

Boundary condition
(TMz polarized)

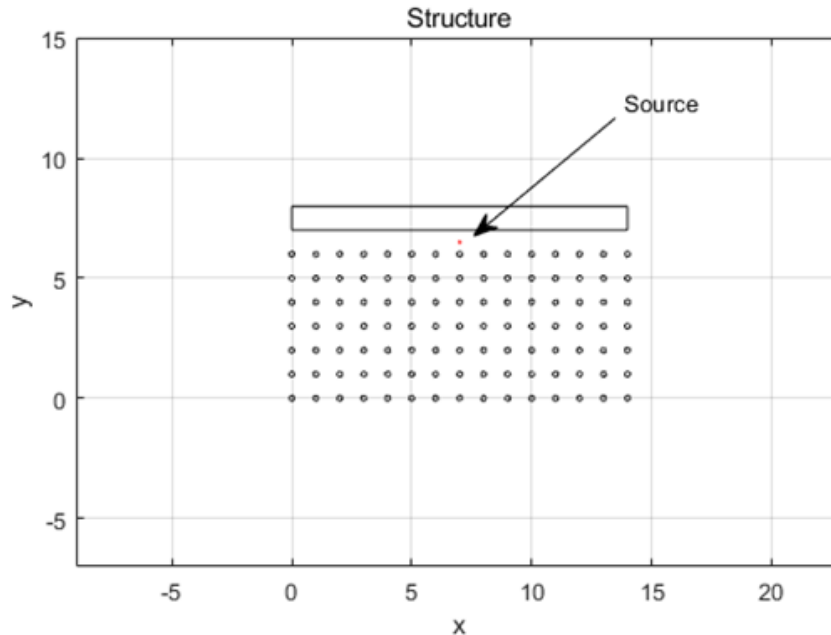
$$\begin{aligned} \psi_0 &= \psi_1 \\ \frac{1}{\mu_0} \hat{n} \cdot \nabla \psi_0 &= \frac{1}{\tilde{\mu}} \hat{n} \cdot \nabla \psi_1 + j\eta \hat{t} \cdot \nabla \psi_1 \end{aligned}$$

T matrix

$$T_n = \frac{a_n^s}{a_n} = \frac{\mu_0 \left[\frac{1}{\tilde{\mu}} J'_n(k_1 r) + \frac{1}{r} n \eta J_n(k_1 r) \right] J_n(k_0 r) - J'_n(k_0 r) J_n(k_1 r)}{H_n'^{(1)}(k_0 r) J_n(k_1 r) - \mu_0 \left[\frac{1}{\tilde{\mu}} J'_n(k_1 r) + \frac{1}{r} n \eta J_n(k_1 r) \right] H_n^{(1)}(k_0 r)}$$

Generalize Foldy-Lax MST to Handle Boundaries

Edge state confined by one crystal and a PEC boundary



Existence of the boundary complicates the excitation field on a scatterer.

$$\psi_{exc}^{(p)}(\bar{\rho}) = \psi_{inc}(\bar{\rho}) + \sum_{q \neq p} \psi_{sca}^{(q)}(\bar{\rho}) + \psi_{sca}^B(\bar{\rho})$$
$$\psi_{exc}^{(p)}(\bar{\rho}) = \psi_{inc}(\bar{\rho}) + \psi_{sca}^{(PEC,p,inc)}(\bar{\rho}) + \sum_{q=1, q \neq p}^N \psi_{sca}^{(p,q)}(\bar{\rho}) + \sum_{q=1}^N \psi_{sca}^{(PEC,p,q)}(\bar{\rho})$$

The Hybrid MST-SIE Approach: Handling Additional Scattering Fields from Boundaries

- Solve surface field on boundary with MoM
- Expand scattering field from boundary as cylindrical waves centered at the reference scatterer

$$\begin{aligned}
 \psi_{sca}^{(PEC,qm)}(\bar{\rho}) &= - \int_S d\bar{\rho}' \left[g_0(\bar{\rho}; \bar{\rho}') \bar{u}_m^{(q)}(\bar{\rho}') \right] \\
 &= -\frac{i}{4} \int_S d\bar{\rho}' \left[H_0^{(1)}(k_0 |\bar{\rho} - \bar{\rho}'|) \bar{u}_m^{(q)}(\bar{\rho}') \right] \\
 &= -\frac{i}{4} \int_S d\bar{\rho}' \left[\sum_{n=-\infty}^{+\infty} J_n(k_0 |\bar{\rho} - \bar{\rho}_p|) e^{in\phi_{\bar{\rho}\bar{\rho}_p}} H_n^{(1)}(k_0 |\bar{\rho}' - \bar{\rho}_p|) e^{-in\phi_{\bar{\rho}'\bar{\rho}_p}} \bar{u}_m^{(q)}(\bar{\rho}') \right] \\
 &= -\frac{i}{4} \left[\sum_{v=1}^{N_t} \sum_{n=-\infty}^{+\infty} J_n(k_0 |\bar{\rho} - \bar{\rho}_p|) e^{in\phi_{\bar{\rho}\bar{\rho}_p}} \textcircled{H}_n^{(1)}(k_0 |\bar{\rho}_v - \bar{\rho}_p|) e^{-in\phi_{\bar{\rho}_v\bar{\rho}_p}} \Delta t_v \bar{u}_m^{(q)}(\bar{\rho}_v) \right]
 \end{aligned}$$

$\bar{\gamma}_n^{(p)}$

Modified Foldy-Lax Multiple Scattering Equations

$$\psi_{exc}^{(p)}(\bar{\rho}) = \psi_{inc}(\bar{\rho}) + \psi_{sca}^{(PEC,p,inc)}(\bar{\rho}) + \sum_{q=1,q \neq p}^N \psi_{sca}^{(p,q)}(\bar{\rho}) + \sum_{q=1}^N \psi_{sca}^{(PEC,p,q)}(\bar{\rho})$$

$$\sum_n J_n(k_0 |\bar{\rho} - \bar{\rho}_p|) e^{in\phi_{\bar{\rho}\bar{\rho}_p}} \bar{w}_n^{(p)}$$



$$\begin{aligned}
 &= \sum_{n=-\infty}^{+\infty} J_n(k_0 |\bar{\rho} - \bar{\rho}_p|) e^{in\phi_{\bar{\rho}\bar{\rho}_p}} H_n^{(1)}(k_0 |\bar{\rho}_{inc} - \bar{\rho}_p|) e^{-in\phi_{\bar{\rho}_{inc}\bar{\rho}_p}} \\
 &+ \sum_{n=-\infty}^{+\infty} J_n(k_0 |\bar{\rho} - \bar{\rho}_p|) e^{in\phi_{\bar{\rho}\bar{\rho}_p}} \bar{\gamma}_n^{(PEC,p)} [\bar{Z}_0]^{-1} \bar{\Psi}_{inc} \\
 &+ \sum_{n=-\infty}^{+\infty} J_n(k_0 |\bar{\rho} - \bar{\rho}_p|) e^{in\phi_{\bar{\rho}\bar{\rho}_p}} \sum_{q=1,q \neq p}^N \sum_{m=-\infty}^{+\infty} \bar{T}_m^{(q)} \bar{w}_m^{(q)} H_{n-m}^{(1)}(k_0 |\bar{\rho}_q - \bar{\rho}_p|) e^{-i(n-m)\phi_{\bar{\rho}_q\bar{\rho}_p}} \\
 &+ \sum_{n=-\infty}^{+\infty} J_n(k_0 |\bar{\rho} - \bar{\rho}_p|) e^{in\phi_{\bar{\rho}\bar{\rho}_p}} \sum_{q=1}^N \sum_{m=-\infty}^{+\infty} \bar{\gamma}_n^{(PEC,p)} [\bar{Z}_0]^{-1} \bar{Q}_m^{(q)} \bar{T}_m^{(q)} \bar{w}_m^{(q)}
 \end{aligned}$$



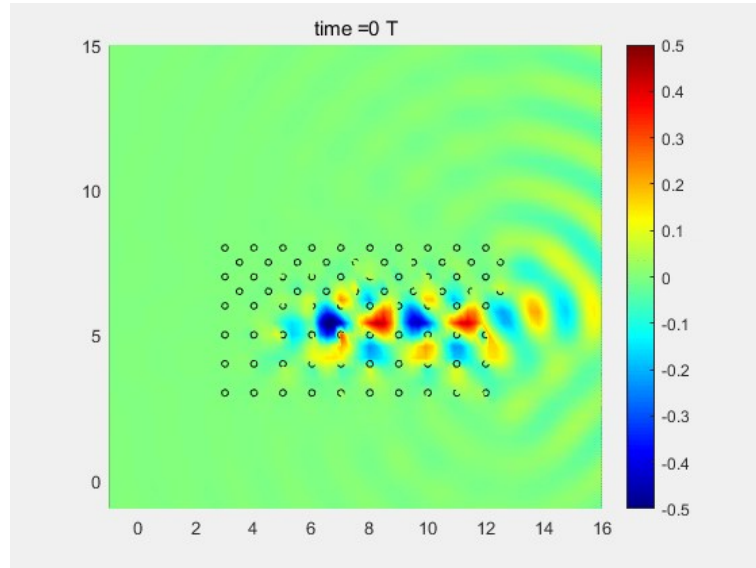
$$\begin{aligned}
 \bar{w}_n^{(p)} &= H_n^{(1)}(k_0 |\bar{\rho}_{inc} - \bar{\rho}_p|) e^{-in\phi_{\bar{\rho}_{inc}\bar{\rho}_p}} \\
 &+ \bar{\gamma}_n^{(PEC,p)} [\bar{Z}_0]^{-1} \bar{\Psi}_{inc}
 \end{aligned}$$

Extra terms due
to scattering
from boundary

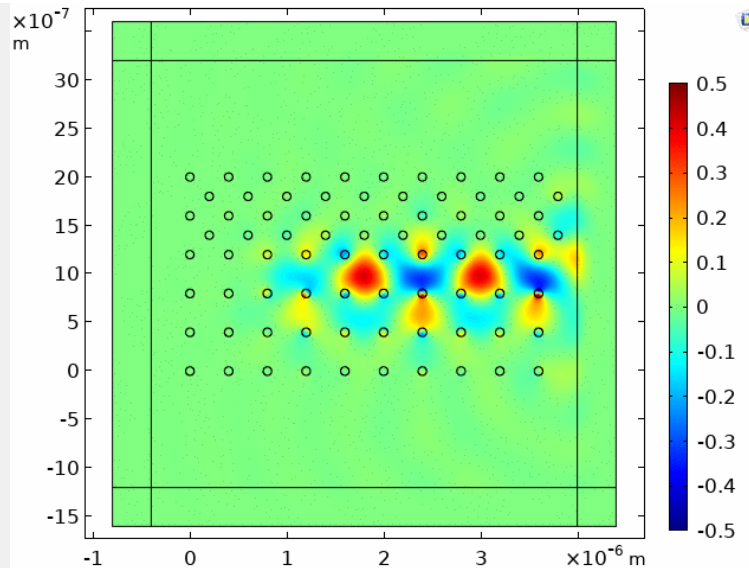
$$\begin{aligned}
 &+ \sum_{q=1,q \neq p}^N \sum_{m=-\infty}^{+\infty} \bar{T}_m^{(q)} \bar{w}_m^{(q)} H_{n-m}^{(1)}(k_0 |\bar{\rho}_q - \bar{\rho}_p|) e^{-i(n-m)\phi_{\bar{\rho}_q\bar{\rho}_p}} \\
 &+ \sum_{q=1}^N \sum_{m=-\infty}^{+\infty} \bar{\gamma}_n^{(PEC,p)} [\bar{Z}_0]^{-1} \bar{Q}_m^{(q)} \bar{T}_m^{(q)} \bar{w}_m^{(q)}
 \end{aligned}$$

Results of Edge States at The Interface of Two Photonic Crystals

Foldy-Lax MST



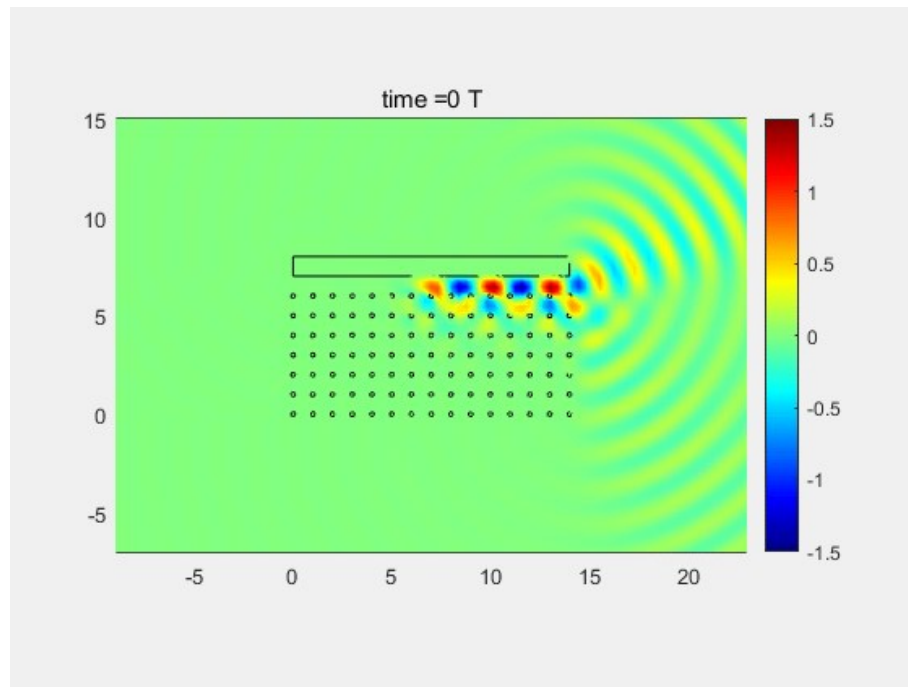
Comsol



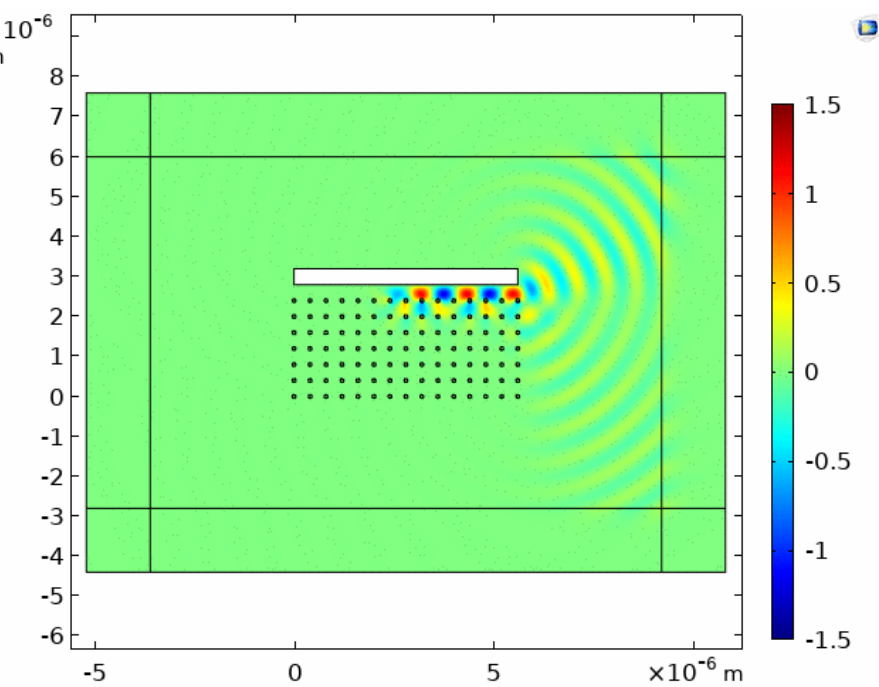
Method	Foldy-Lax	COMSOL	MoM
Unknowns	$80*5=400$	64854(mesh)	$80*30*2=4800$
CPU time	0.24s +2.69s=2.93s	9s	10021.5s+361.6s=10383.1s

Results of Edge States at The Interface of A Photonic Crystal and A PEC Boundary

Foldy-Lax MST

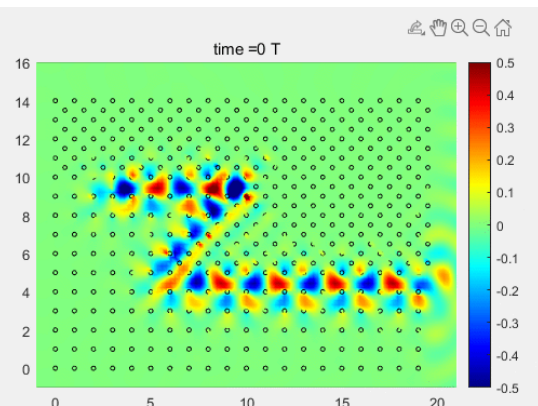
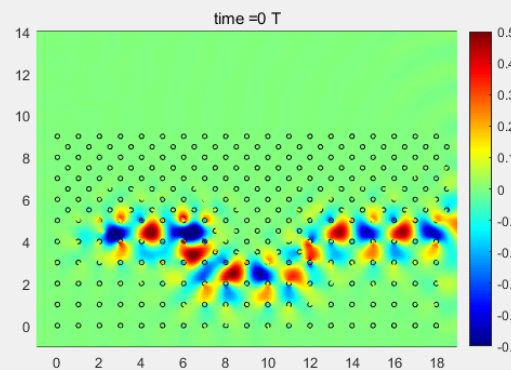
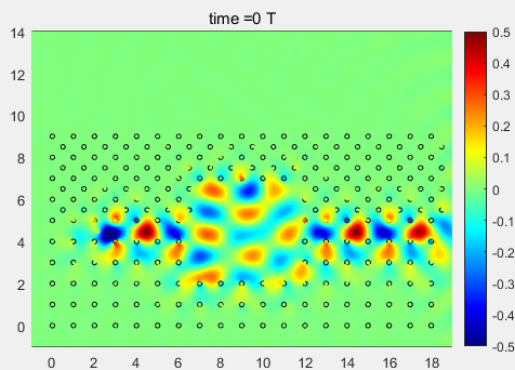
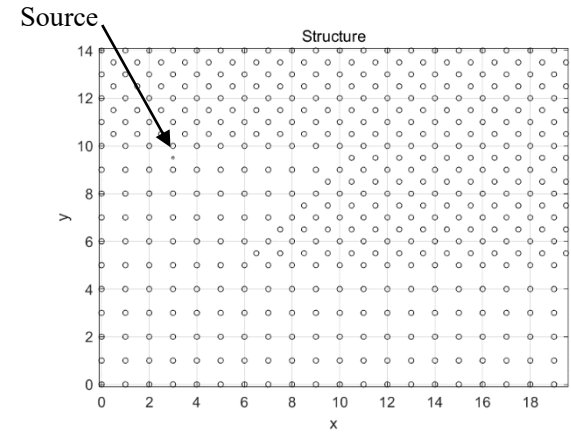
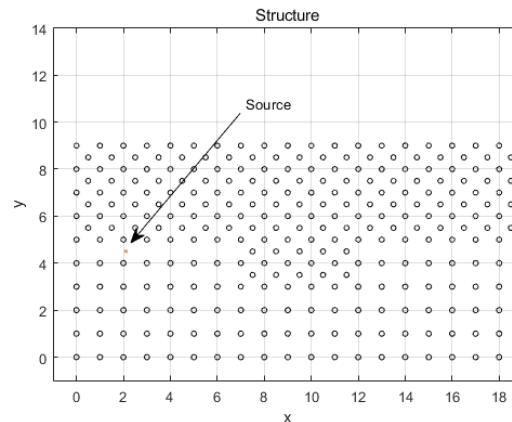
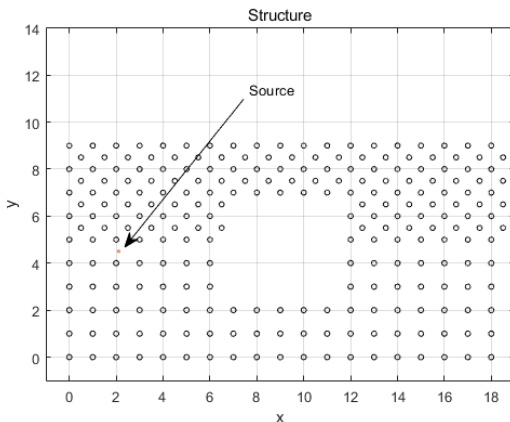


Comsol



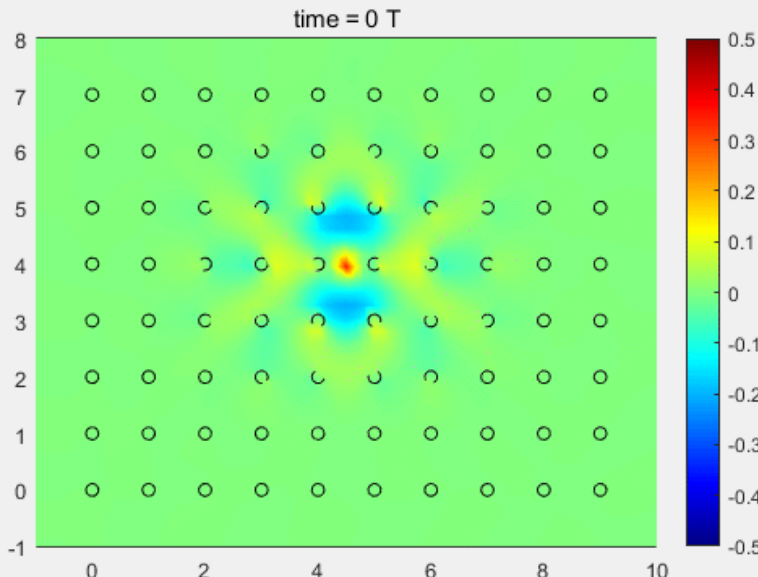
Method	Foldy-Lax MST	COMSOL
Unknowns	525	240810 (mesh)
CPU Time (s)	3.2+12.8=16	25

Robustness of The Topologically Protected One-Way Edge States

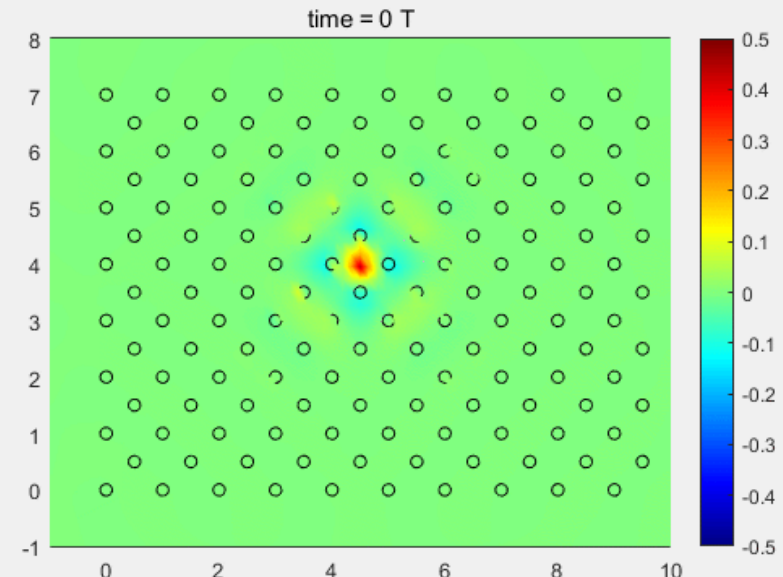


Green's Function: The Point Source Response in Photonic Crystals

YIG crystal

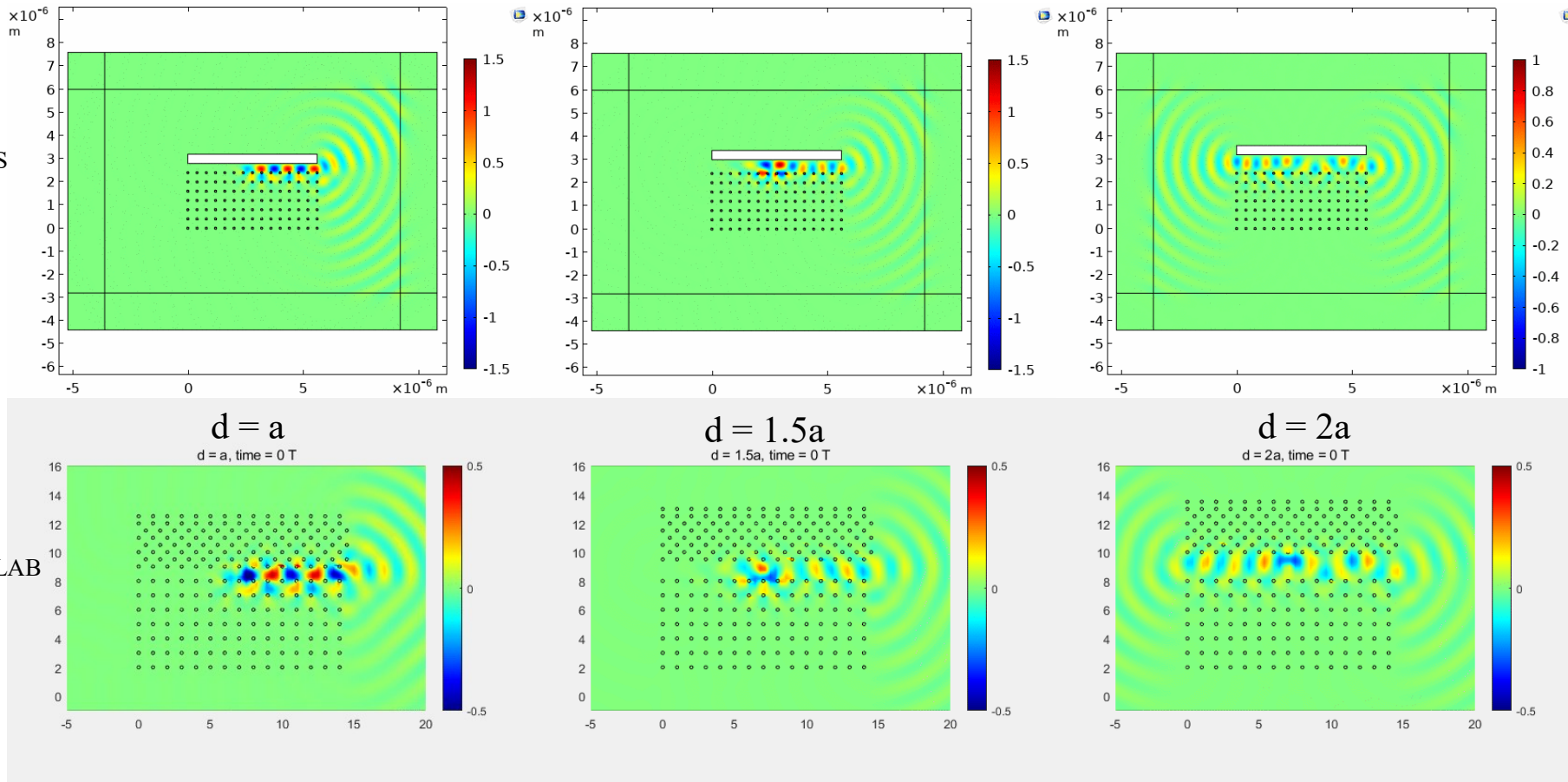


Alumina crystal



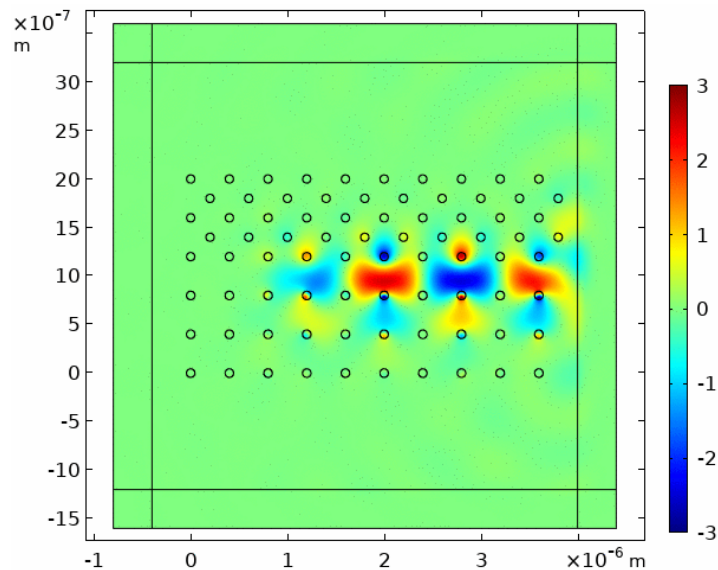
- The wave rotates counterclockwise in the YIG crystal;
- No rotation behavior in the regular alumina crystal
- Wave can not propagate in both crystal;
- Alumina crystal acts like total reflection interface like PEC.

One-way Edge Mode Interpretation in terms of The Green's Function and The Waveguide Theory

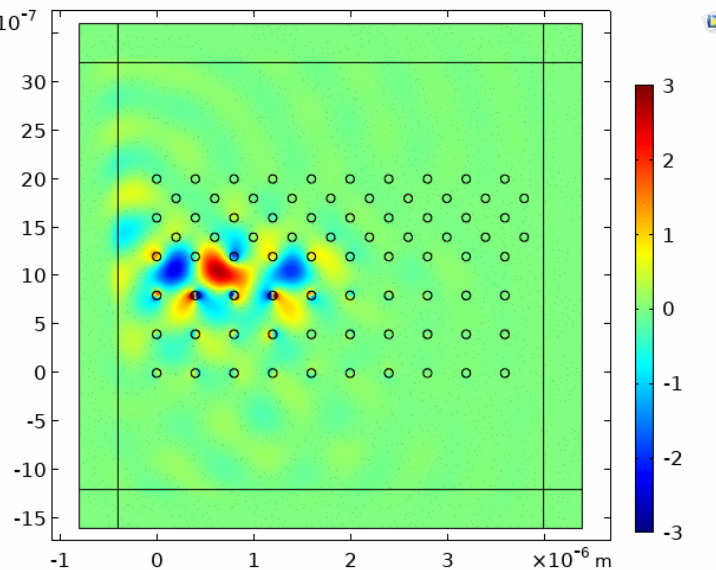


- Waveguide cut-off frequency f_c increases as the distance d decreases.
- When the operating frequency f is above the cut-off f_c , propagating modes are excited and can propagate along both directions.
- When $f < f_c$, wave is unidirectional due to the rotational wave behavior in the gyromagnetic crystal and the reflection at the interface from the other side.

Simultaneous Dual Unidirectional Edge Modes at Different Frequency Bands

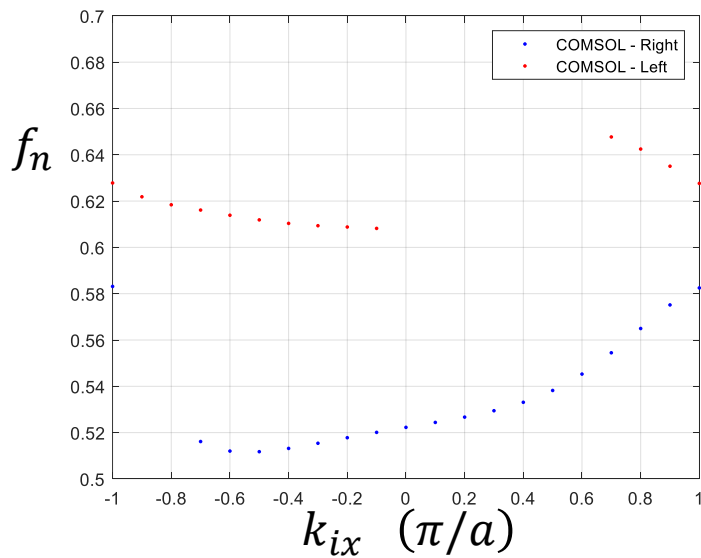
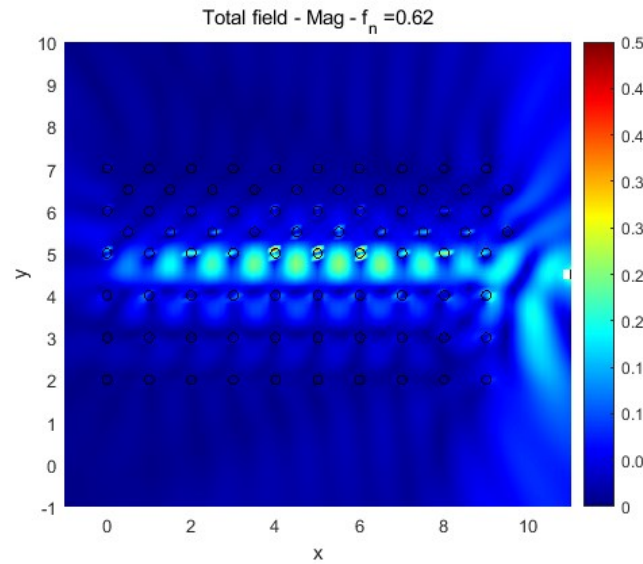
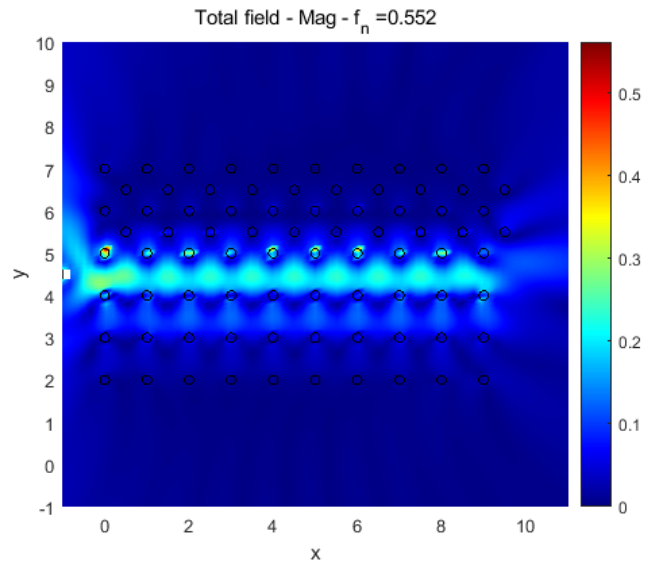


$$f_n = 0.5384$$



$$f_n = 0.6184$$

Dispersion Relations and Duplex Devices



- Working towards extracting dispersion relations numerically from edge mode calculation.
- Exploring ideas to design duplex connecting devices supporting unidirectional wave-guidance along both ways at different frequency bands

The Periodic Grating Scattering Problem

Bai, X., & Tan, S. (2022). An efficient and accurate Nystrom method for calculating scattering properties of 2D gratings with 1D periodicity. PIERS 2021 Hangzhou.

Bai, X., & Tan, S. (2021). An Accurate Solution to Periodic Grating Structure Scattering Using Nystrom Method with An Over-determined Testing Scheme. APS/URSI 2021 Singapore. (*Paper*) +

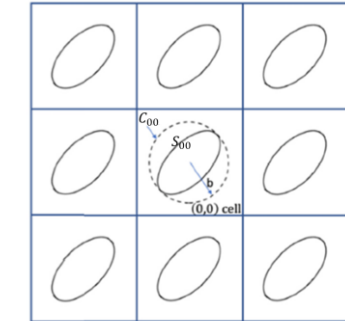
Bai, X., Tan, S., Wang, C., & Gao, F. (2021). An Accurate Integral Equation Formulation to Scattering of Periodic Grating Structures. ACES 2021. (*Paper*) ●

2D1D problem vs 2D2D problem

2D2D SIE

$$\psi_{inc} + \int_{S_{00}} d\bar{\rho}' \psi(\bar{\rho}') \frac{\partial g_P(\bar{\rho}; \bar{\rho}')}{\partial n'} = 0 \quad \bar{\rho}' \text{ on } S_{00}^- \text{ TE}$$

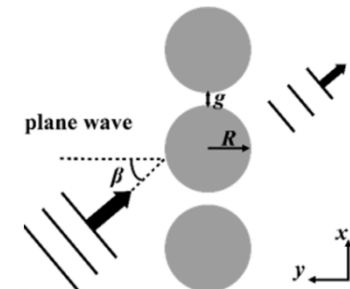
$$g_P(\bar{\rho}; \bar{\rho}') = \sum_{p,q} g(\bar{\rho}; \bar{\rho}' + \bar{R}_{pq}) \exp(i \bar{k}_b \cdot \bar{R}_{pq})$$



2D1D SIE

$$\psi_{inc} + \int_{S_0} d\bar{\rho}' \psi(\bar{\rho}') \frac{\partial g_{P_x}(\bar{\rho}; \bar{\rho}')}{\partial n'} = 0 \quad \bar{\rho}' \text{ on } S_0^- \text{ TE}$$

$$g_{P_x}(\bar{\rho}; \bar{\rho}') = \sum_q g(\bar{\rho}; \bar{\rho}' + \hat{x}qa) \exp(i \bar{k}_i \cdot \hat{x}qa)$$

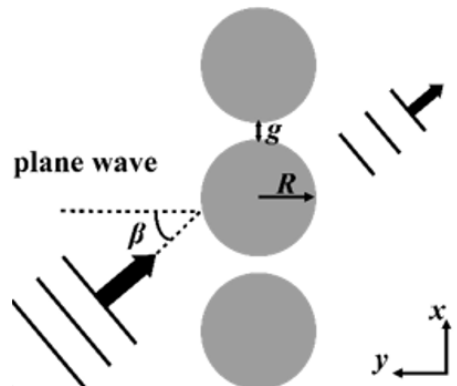


2D1D transmissivity coefficient

Scattering far fields $\psi_s(\vec{\rho}) = \frac{i}{2a} \int_{S_0} d\rho' \psi(\rho') \frac{\partial}{\partial n'} \sum_{m=\text{Prop}} \frac{\exp(i(k_{xm}x - k_{ym}y))}{k_{ym}} \exp(-i(k_{xm}x' - k_{ym}y'))$

$$t = \frac{k_0}{k_{y0}} \sum_{m=\text{Prop}} |\delta_{m0} + a_m|^2 \frac{k_{ym}}{k_0} \quad a_m = \frac{i}{2ak_{ym}} \int_{S_0} d\rho' \psi(\rho') \frac{\partial}{\partial n'} \exp(-i(k_{xm}x' - k_{ym}y'))$$

Efficient and accurate modeling of 2D1D arbitrary shape periodic gratings scattering



Integral equation based method

Arbitrary scatterer, accurate near field

Quadrature

Evaluation of
periodic Green's
function

Overcome
internal
resonance

Nystrom
approach

Imaginary
wave-
number
extraction

Laplace
transform

Over-
determined
testing

Multiple scattering theorem

Arbitrary scatterer, sparse configuration, efficient

T-matrix of arbitrary scatterer

Foldy-Lax MST

SIE

KKR, BGF-KKR

Evaluation of periodic Green's function

Imaginary wave number extraction technique

$$\frac{\partial}{\partial n'} g_{P_x}(\vec{\rho}, \vec{\rho}') = \frac{\partial}{\partial n'} [g_{P_x}(i\xi; \vec{\rho}, \vec{\rho}')]_{Spatial} + \frac{\partial}{\partial n'} [g_{P_x}(k; \vec{\rho}, \vec{\rho}') - g_{P_x}(i\xi; \vec{\rho}, \vec{\rho}')]_{Spectral}$$

$$\begin{aligned} & \frac{\partial}{\partial n'} [g_{P_x}(i\xi; \vec{\rho}, \vec{\rho}')]_{Spatial} \\ &= \sum_q \frac{\partial}{\partial n'} g(i\xi; \vec{\rho}, \vec{\rho}' + \hat{x}qa) e^{ik_{ix}qa} & k_{xm} &= k_{ix} + m \frac{2\pi}{a} \\ & & k_{ym} &= \sqrt{k_0^2 - k_{xm}^2} \\ & \frac{\partial}{\partial n'} [g_{P_x}(k; \vec{\rho}, \vec{\rho}') - g_{P_x}(i\xi; \vec{\rho}, \vec{\rho}')]_{Spectral} & \tilde{k}_{ym} &= \sqrt{\xi^2 + k_{xm}^2} \\ &= \frac{i}{2a} \frac{\partial}{\partial n'} \sum_m \left[\frac{\exp(ik_{ym}|y-y'|)}{k_{ym}} - \frac{\exp(-\tilde{k}_{ym}|y-y'|)}{i\tilde{k}_{ym}} \right] \exp(ik_{xm}(x-x')) \end{aligned}$$

Transformation method

$$g_P(\vec{\rho}, \vec{\rho}') = \sum_q \frac{i}{4} H_0^{(1)}(k | \vec{\rho} - (\vec{\rho}' + \hat{x}qa) |) e^{ik_{ix}qa}$$

Laplace transformation theorem $\sum_{m=1}^{\infty} e^{imt} Q(m) = e^{it} \int_0^{\infty} dv \frac{q(v)}{e^v - e^{it}} \quad Q(m) = \int_0^{\infty} dv e^{-mt} q(v)$

$$e^{-is} H_0^{(1)}(\sqrt{s^2 + a^2}) = -\frac{i2}{\pi} \int_0^{\infty} dy e^{-sy} \frac{\cos(a\sqrt{y^2 - 2iy})}{\sqrt{y^2 - 2iy}}$$

$$g_P = g_{P0} + g_{P0+} + g_{P0-}$$

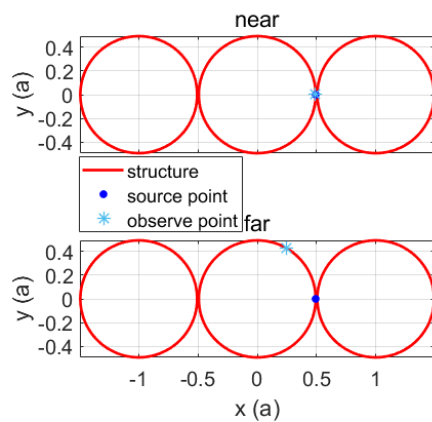
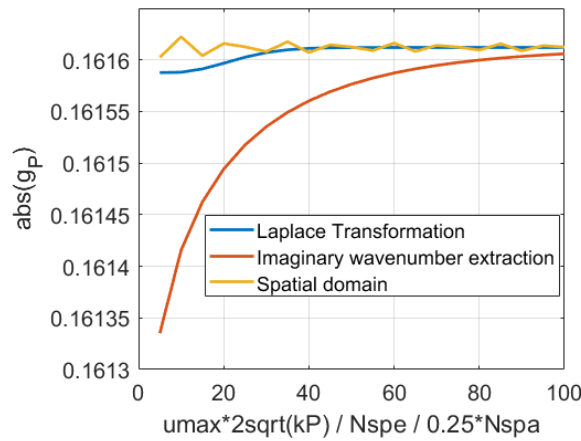
$$g_{P0} = \frac{i}{4} H_0^{(1)}(k \sqrt{(x-x')^2 + (z-z')^2})$$

$$g_{P0+} = \frac{e^{(i(k+k_{ix})P - ik(x-x'))}}{\pi} \int_0^{\infty} du \frac{e^{(-u^2 k P + k(x-x') u^2)}}{1 - e^{(-u^2 k P + i(k+k_{ix})P)}} \frac{\cos(k(z-z')u\sqrt{u^2 - 2i})}{\sqrt{u^2 - 2i}}$$

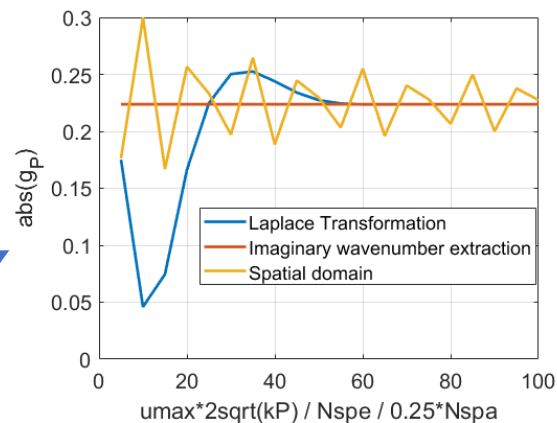
$$g_{P0-} = \frac{e^{(i(k+k_{ix})P + ik(x-x'))}}{\pi} \int_0^{\infty} du \frac{e^{(-u^2 k P - k(x-x') u^2)}}{1 - e^{(-u^2 k P + i(k-k_{ix})P)}} \frac{\cos(k(z-z')u\sqrt{u^2 - 2i})}{\sqrt{u^2 - 2i}}$$

Evaluation of periodic Green's function-Comparing convergence

Case 1 Near



Case 2 Far

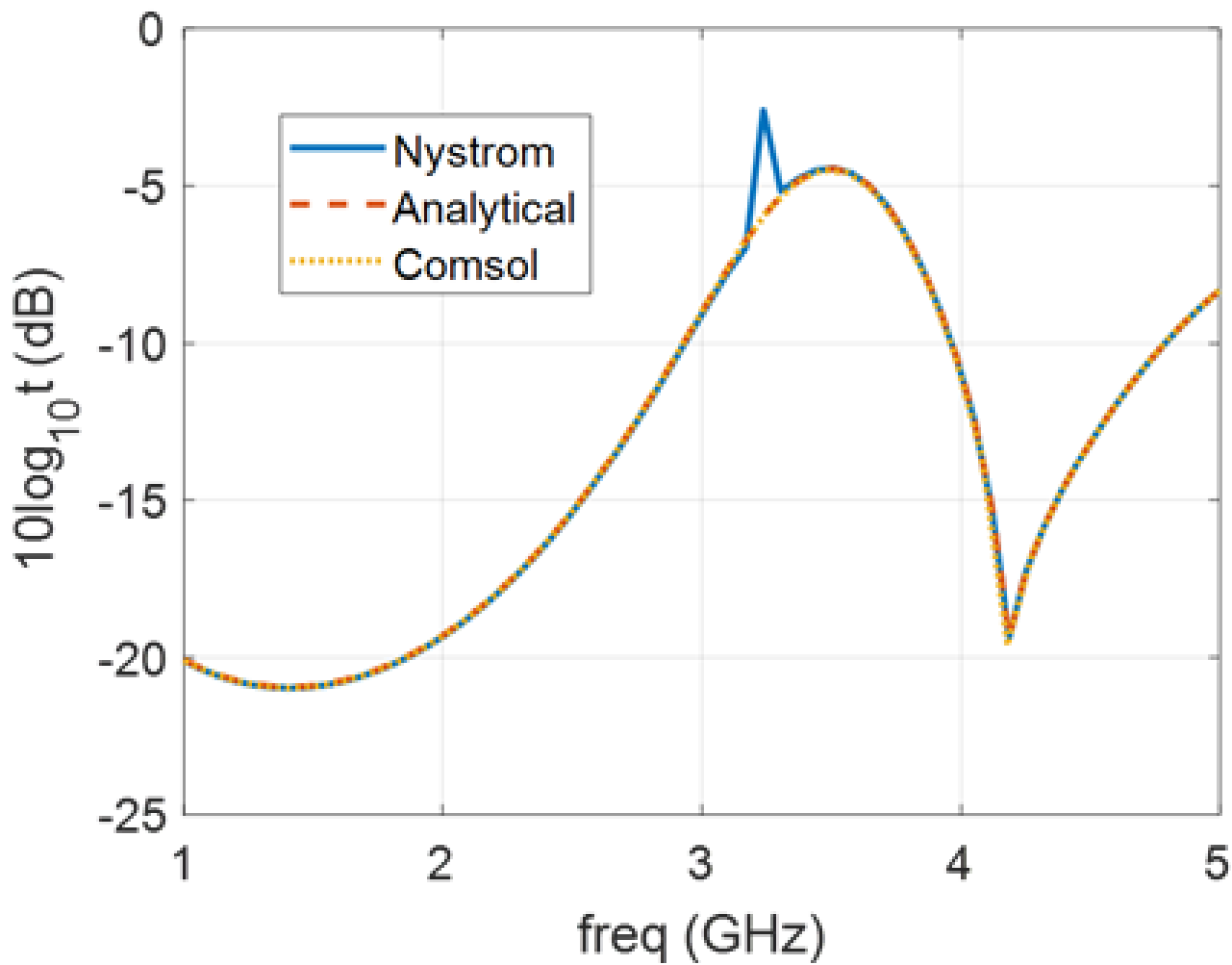


Criterion

$|y - y'| < \text{wavelength}/20$: The transformation method

$|y - y'| \geq \text{wavelength}/20$: The imaginary wavenumber extraction technique

Inaccuracy due to internal resonance



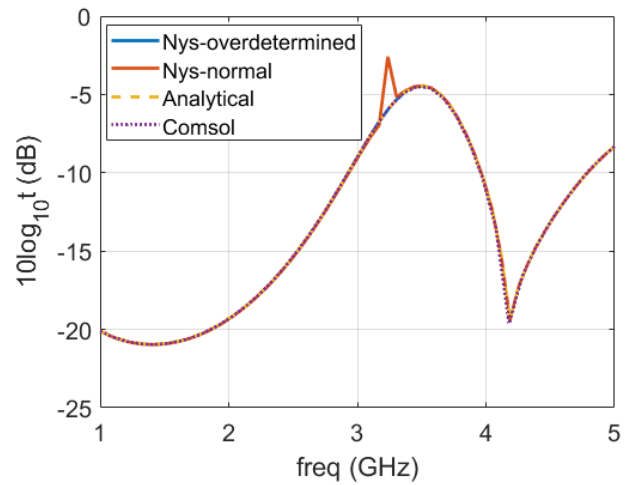
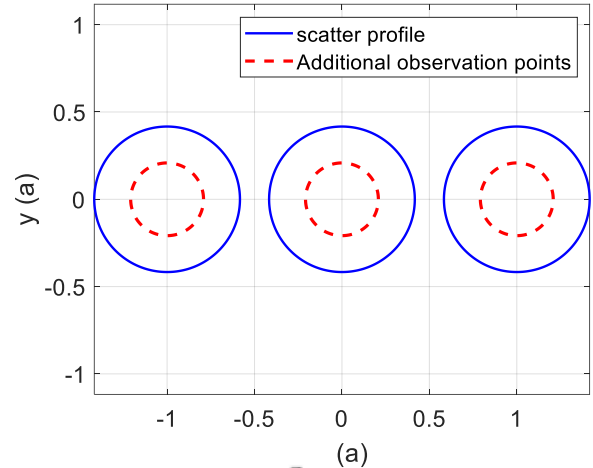
Over-determined testing scheme

$$\overline{\overline{Z}}_{over} \overline{\psi} = -\overline{\psi}_{inc}^{over}$$

$$\overline{\overline{Z}}_{over} = \begin{bmatrix} \overline{\overline{Z}}_{surface} \\ \overline{\overline{Z}}_{inner} \end{bmatrix} \quad \overline{\psi}_{inc}^{over} ((2N_p \times N_q) \times 1) = \begin{bmatrix} \overline{\psi}_{inc} ((N_p \times N_q) \times 1) \\ \overline{\psi}_{inc}^{over} ((N_p \times N_q) \times 1) \end{bmatrix}$$

$$\overline{\overline{Z}}_{over}^\dagger \overline{\overline{Z}}_{over} \overline{\psi} = -\overline{\overline{Z}}_{over}^\dagger \overline{\psi}_{inc}^{over}$$

conjugate transpose



Multiple scattering theorem method

$$\psi^{ex}(\vec{\rho}) = \psi^{inc}(\vec{\rho}) + \int_{S_{00}} dl' \left[\psi^s(\vec{\rho}') \frac{\partial g_R(\vec{\rho}, \vec{\rho}')}{\partial n'} - g_R(\vec{\rho}, \vec{\rho}') \frac{\partial \psi^s(\vec{\rho}')}{\partial n'} \right]$$

$$g_R(\bar{\rho}; \bar{\rho}') = \sum_{p,q \neq (0,0)} g(\bar{\rho}; \bar{\rho}' + \bar{R}_{pq}) \exp(i \bar{k}_b \cdot \bar{R}_{pq})$$

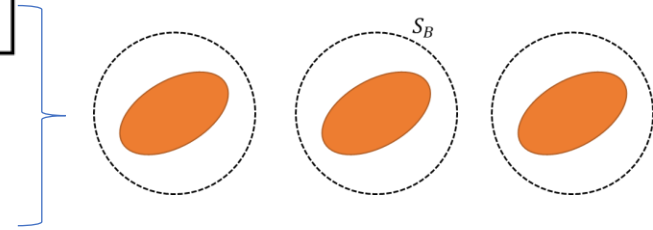
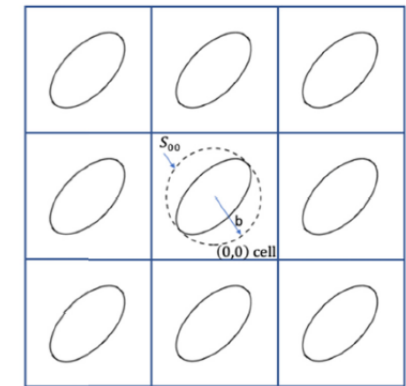
$$\psi^{ex}(\vec{\rho}) = \psi^{inc}(\vec{\rho}) + \int_{S_B} dl' \left[\psi^s(\vec{\rho}') \frac{\partial g_R(\vec{\rho}, \vec{\rho}')}{\partial n'} - g_R(\vec{\rho}, \vec{\rho}') \frac{\partial \psi^s(\vec{\rho}')}{\partial n'} \right]$$

$$g_{R_x}(\bar{\rho}; \bar{\rho}') = \sum_{q \neq 0} g(\bar{\rho}; \bar{\rho}' + \hat{x}qa) \exp(i \bar{k}_i \cdot \hat{x}qa)$$

$$g_R = \sum_{m=-\infty}^{\infty} D_m J_m(k|\vec{\rho}|) e^{im\phi_{\vec{\rho}}}$$

$$\int_0^{2\pi} g_R(\vec{\rho}, \vec{\rho}') e^{-il\phi} d\phi = \int_0^{2\pi} \sum_{m=-\infty}^{\infty} D_m J_m(k|\vec{\rho}|) e^{im\phi_{\vec{\rho}}} e^{-il\phi} d\phi = 2\pi D_m J_m(k|\vec{\rho}|)$$

$$D_m = \frac{\int_0^{2\pi} g_R(\vec{\rho}, \vec{\rho}'=0) e^{-im\phi} d\phi}{2\pi J_m(k|\vec{\rho}|)}$$



Calculation of periodic Green's function coefficient \bar{D}

$$D_m = \frac{\int_0^{2\pi} g_R(\vec{\rho}, \vec{\rho}'=0) e^{-im\phi} d\phi}{2\pi J_m(k|\vec{\rho}|)} \quad g_R(k, k_{ix}; \rho, \phi) = \sum_{l \neq 0} \frac{i}{4} H_0^{(1)}(k_0 |\vec{\rho} - \hat{x}la|) e^{ik_{ix}la}$$

Using addition theorem for periodic Green's function in spatial domain

$$H_0^{(1)}(k_0 |\vec{\rho} - \hat{x}qa|) = \sum_{n=-\infty}^{\infty} J_n(k|\vec{\rho}|) e^{in\phi_{\vec{\rho}}} H_n^{(1)}(k|\hat{x}qa|) e^{-in\phi_{\vec{\rho}}} \quad |\vec{\rho}| < |\hat{x}qa|$$

$$\begin{aligned} D_m(k) &= \frac{\int_0^{2\pi} g_R(k, k_{ix}; \rho, \phi) e^{-im\phi} d\phi}{2\pi J_m(k\rho)} = \frac{\frac{i}{4} \sum_{l \neq 0} \sum_{n=-\infty}^{\infty} J_n(k\rho) H_n^{(1)}(kla) e^{-in\phi_{\vec{\rho}}} e^{ik_{ix}la} \int_0^{2\pi} e^{in\phi_{\vec{\rho}}} e^{-im\phi} d\phi}{2\pi J_m(k\rho)} \\ &= \frac{i}{4} \sum_{l \neq 0} H_m^{(1)}(|kla|) e^{-im\phi_{\vec{\rho}}} e^{ik_{ix}la} \\ &= \frac{i}{4} \sum_{l=1}^{\infty} H_m^{(1)}(kla) e^{ik_{ix}la} + \frac{i}{4} (-1)^l \sum_{l=1}^{\infty} H_m^{(1)}(kla) e^{-ik_{ix}la} \end{aligned}$$

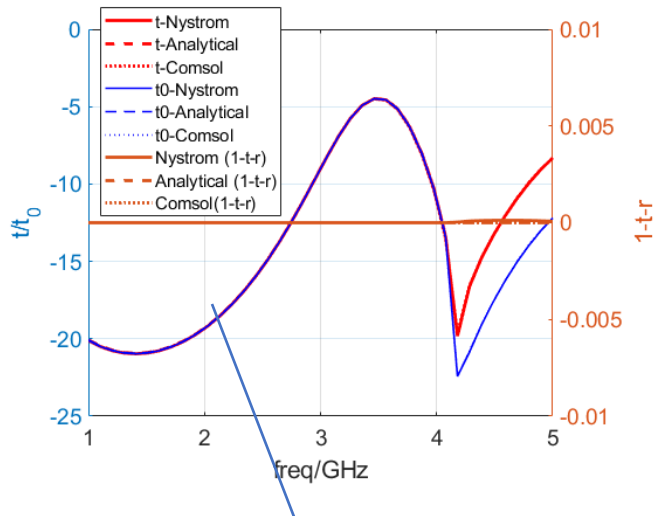
For Lattice Summation:

Yasumoto, Kiyotoshi, and Kuniaki Yoshitomi. "Efficient calculation of lattice sums for free-space periodic Green's function." IEEE Transactions on Antennas and Propagation 47.6 (1999): 1050-1055.

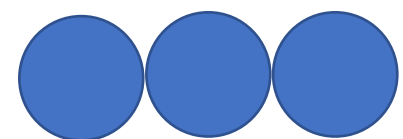
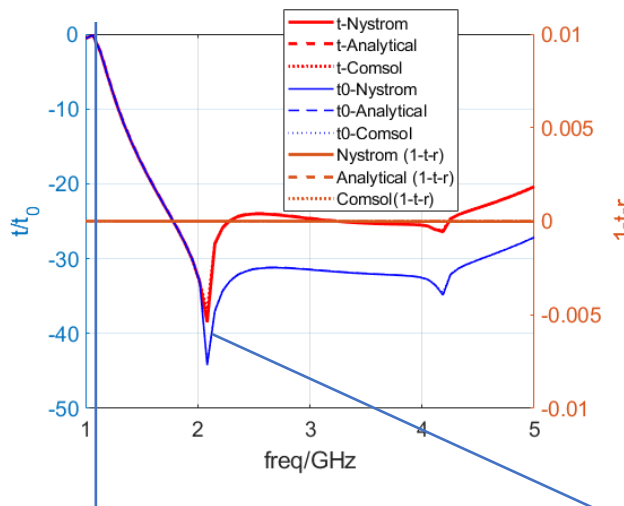
Transmission spectrum and surface field of cylindrical structure

Transmission spectrum

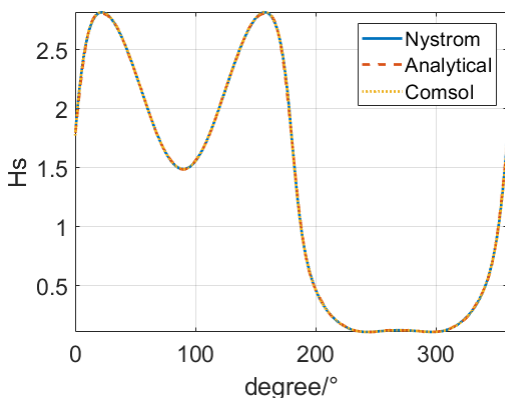
0 degree incidence



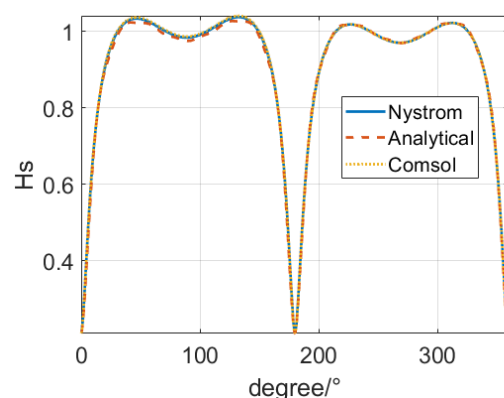
89 degree incidence



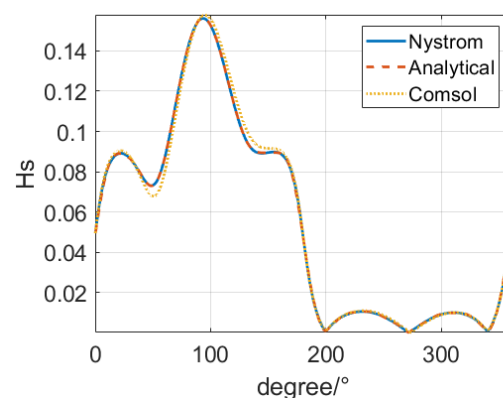
Surface field



0degree 2GHz



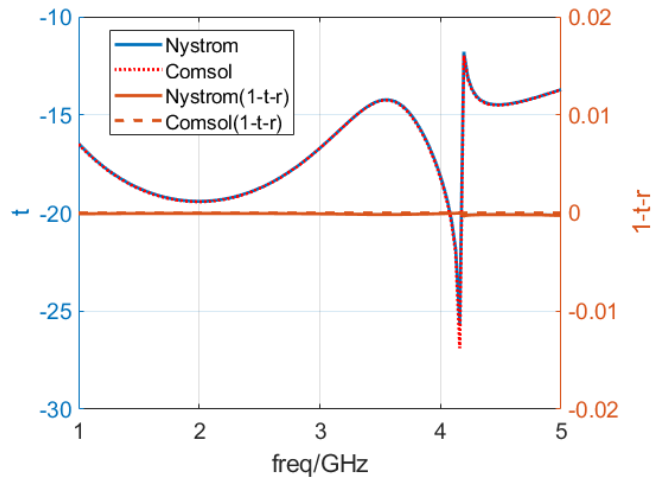
89degree 1.05GHz



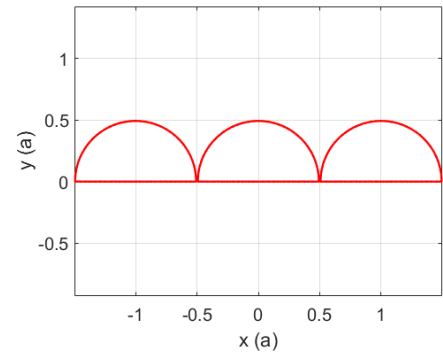
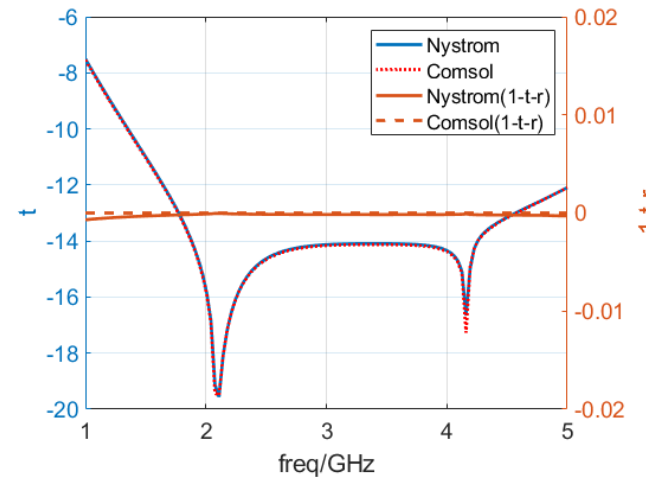
89degree 2.085GHz

Transmission spectrum of semi-cylindrical structure

0 degree

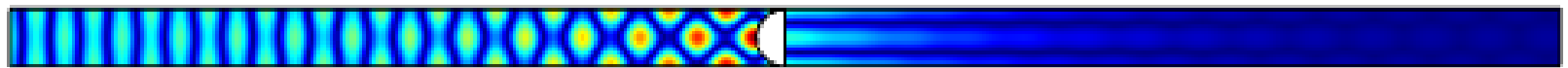


89 degree

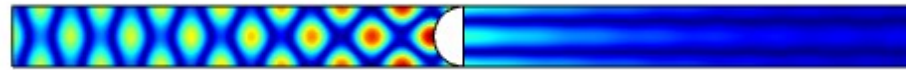


Comsol near fields with port length

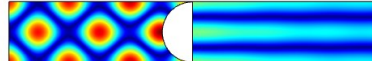
10P



6P

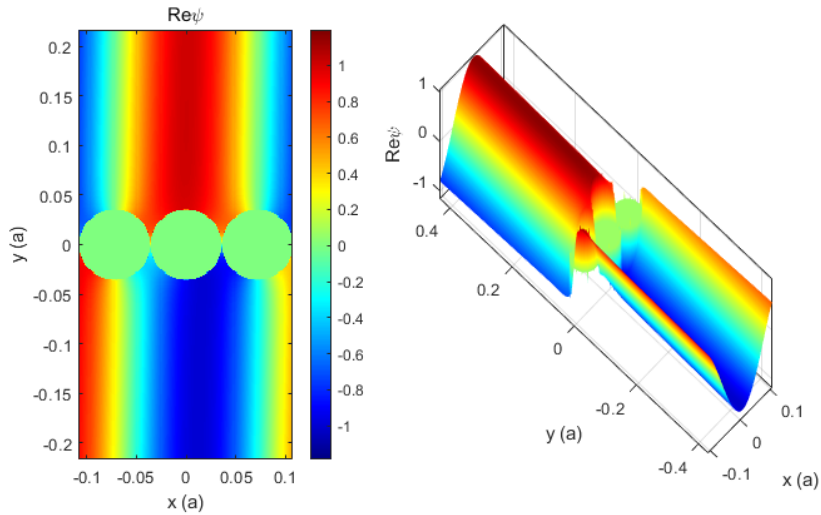


3P



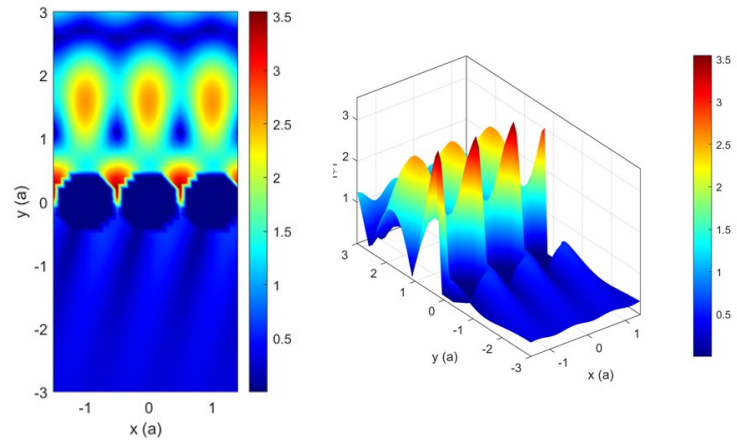
Comsol results change with the ports distance for the influence of evanescent modes.

Near fields distribution

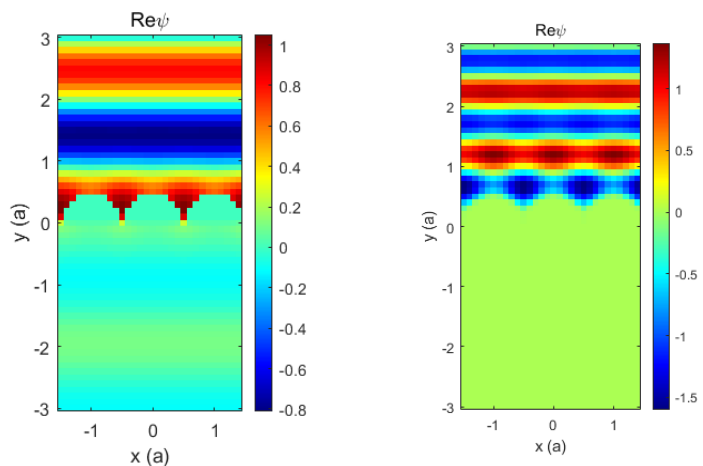


Cylindrical
89degree
1.05GHz

**Extraordinary
transmission**



TE Cylindrical 60dgree 2.5GHz
Field Enhancement



TE Semi-cylindrical
0degree
2GHz

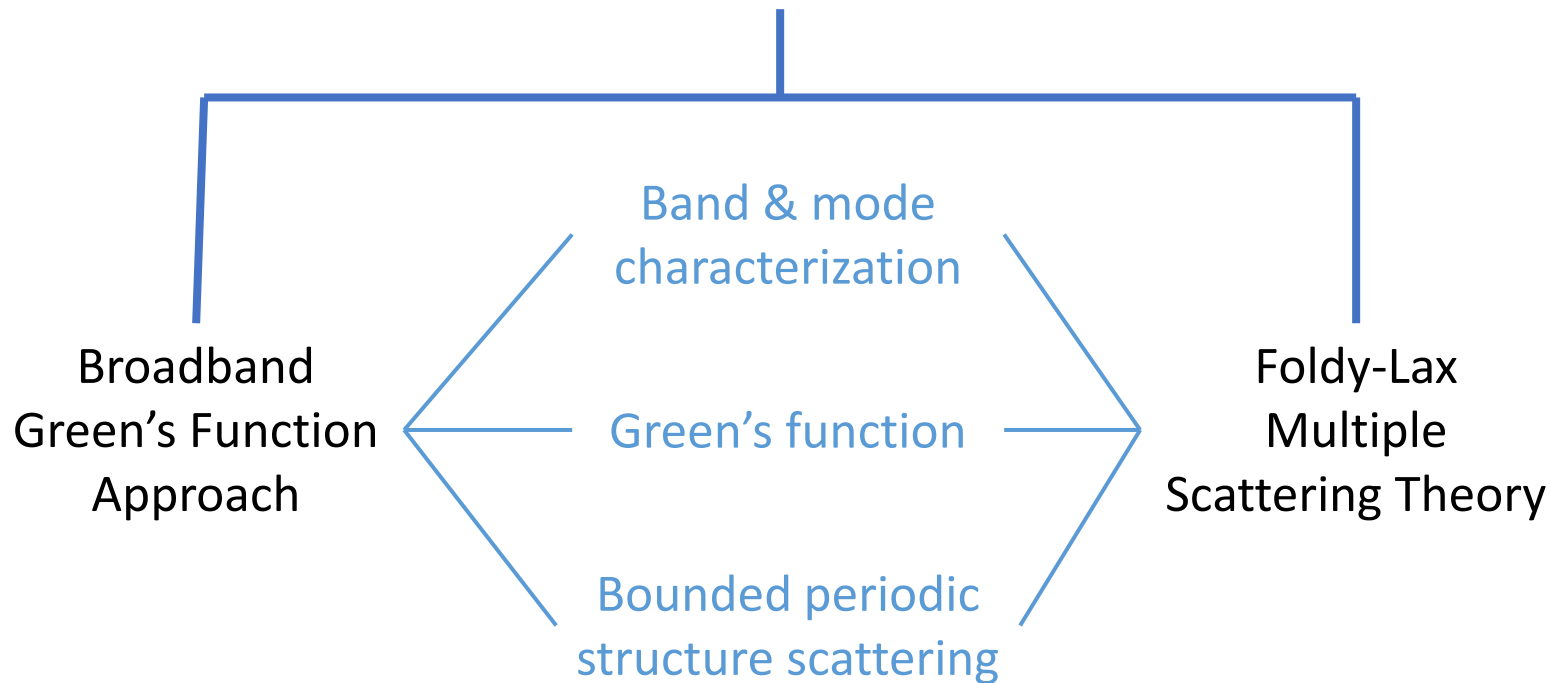
TM Semi-cylindrical
0degree
2GHz

Summary

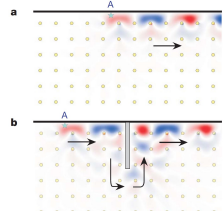


Summary

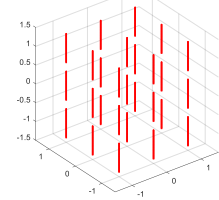
Integral Equation & Extinction Theorem



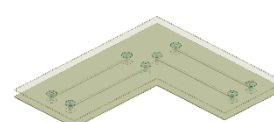
Photonic crystal



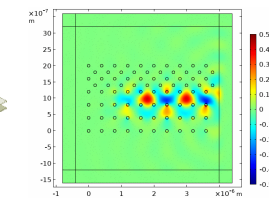
Wire medium



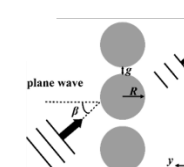
Cavity



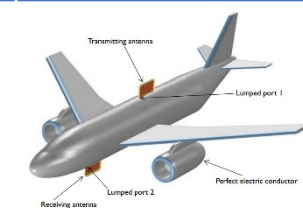
Topological edge states



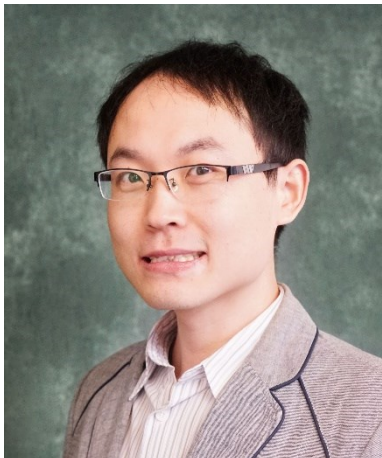
Periodic gratings



Multi-scale structure scattering



Main Contributors



Shurun Tan



Mr. Zhaoyang Feng,
ZJUI, Zhejiang U



Mr. Xuyang Bai,
ZJUI, Zhejiang U



Prof. Leung Tsang,
U of Michigan



Dr. Tien-Hao Liao,
JPL, Caltech



Ms. Ruoxing Gao,
U of Michigan

Thank you & Welcome





ZJU-UIUC INSTITUTE

Zhejiang University/University of Illinois at Urbana-Champaign Institute



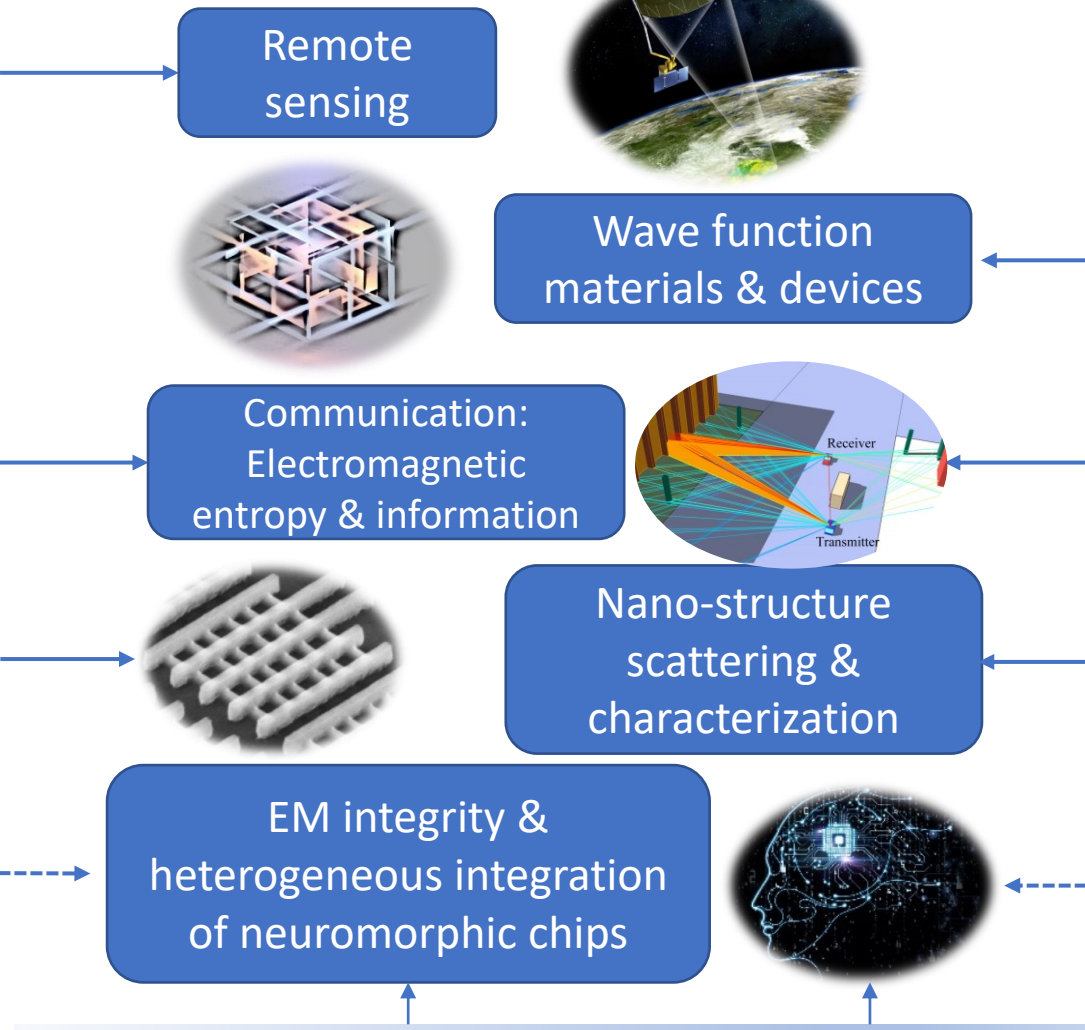
Overview of Our Research Scope

Applied Electromagnetics & Information Science Lab

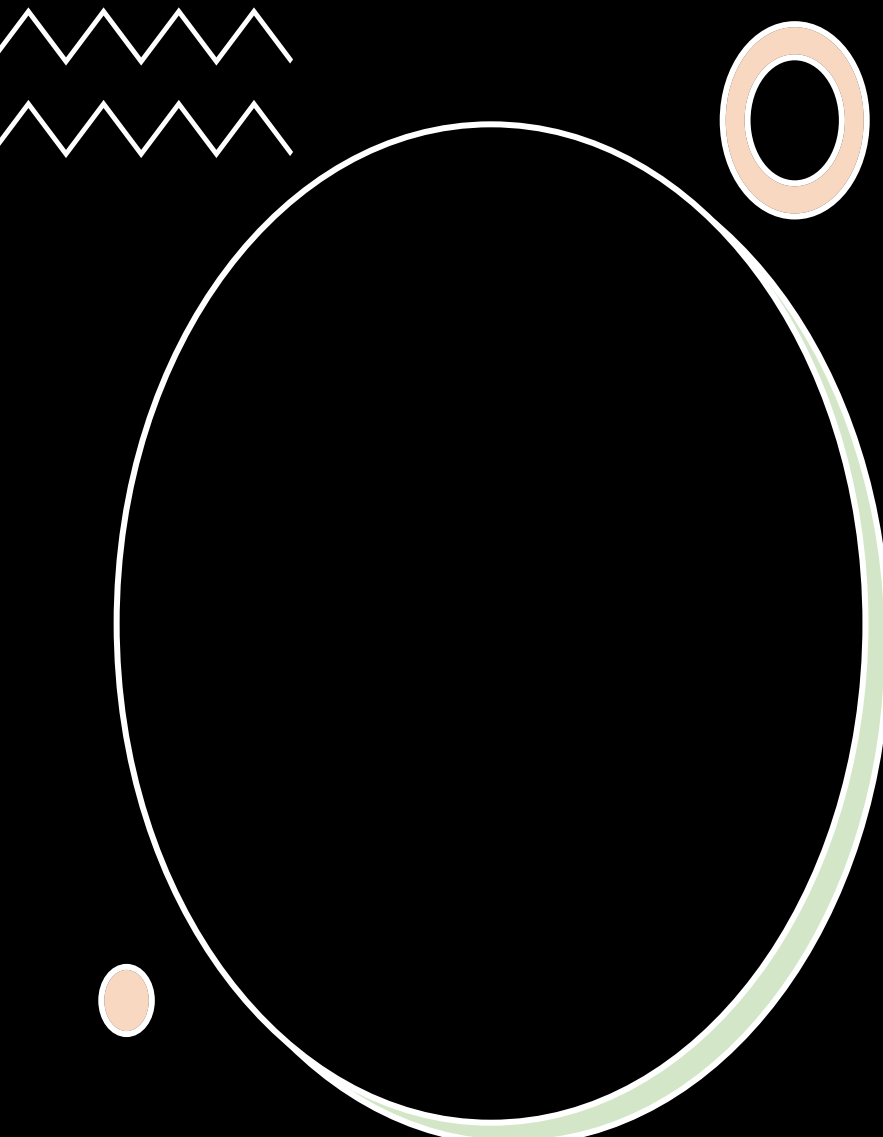
Electromagnetic Scattering Lab (EMSL)

Random media

Periodic structures



High speed circuits & electronic systems



EMSL Identity

Mission: We solve intriguing electromagnetic scattering problems emerged from cutting-edge cross-disciplinary research through theoretical, computational and experimental approaches.

Vision: We explore electromagnetic wave interactions with cross-scale structures and environments and the associated physical and informational effects to develop electromagnetic basis for advanced engineering and science.

Our Research Team

